



Calhoun: The NPS Institutional Archive
DSpace Repository

Theses and Dissertations

1. Thesis and Dissertation Collection, all items

1968

Determination of performance parameters of a dual discharge radial turbine.

Williams, David Daniel; Zucker, Robert D.

Monterey, California. Naval Postgraduate School

<http://hdl.handle.net/10945/11979>

Downloaded from NPS Archive: Calhoun



Calhoun is the Naval Postgraduate School's public access digital repository for research materials and institutional publications created by the NPS community. Calhoun is named for Professor of Mathematics Guy K. Calhoun, NPS's first appointed -- and published -- scholarly author.

Dudley Knox Library / Naval Postgraduate School
411 Dyer Road / 1 University Circle
Monterey, California USA 93943

<http://www.nps.edu/library>

**NPS ARCHIVE
1968
WILLIAMS, D.**

DETERMINATION OF PERFORMANCE PARAMETERS
OF A DUAL DISCHARGE RADIAL TURBINE

by

David Daniel Williams

DUDLEY KNOX LIBRARY
ROYAL POSTGRADUATE SCHOOL
BERKELEY CA 93943-5101

UNITED STATES NAVAL POSTGRADUATE SCHOOL



THESIS

DETERMINATION OF PERFORMANCE PARAMETERS

OF A

DUAL DISCHARGE RADIAL TURBINE

by

David Daniel Williams

December 1968

This document has been approved for public release and sale; its distribution is unlimited.

LIBRARY
NAVAL POSTGRADUATE SCHOOL
MONTEREY, CALIF. 93940

DETERMINATION OF PERFORMANCE PARAMETERS
OF A

DUAL DISCHARGE RADIAL TURBINE

by

David Daniel Williams
Lieutenant, United States Navy
B. S., Naval Academy, 1962

Submitted in partial fulfillment of the
requirements for the degree of

MASTER OF SCIENCE IN AERONAUTICAL ENGINEERING

from the

NAVAL POSTGRADUATE SCHOOL
December 1968

ABSTRACT

This study was conducted to establish the performance parameters of a radial inflow, dual discharge turbine and to determine the effect of variations in axial clearance on these parameters. The representative stream surface is taken at the outer discharge radius instead of at a computed mass-average discharge radius, as was done previously. This technique results in considerably simplified computations and in better correlation of the rotor loss parameters.

Tests were conducted at axial clearances from 0.015 to 0.081 inches and at total-to-static pressure ratios from 1.2 to 1.7 for each clearance. The test installation is located at the Turbo-Propulsion Laboratory of the Naval Postgraduate School, Monterey, California.

TABLE OF CONTENTS

| SECTION | PAGE |
|--|------|
| 1. INTRODUCTION | 17 |
| 2. THE ICP RADIAL TURBINE | 19 |
| 2.1 Description of Turbine Assembly | 19 |
| 2.2 Modifications to Turbine Assembly | 21 |
| 3. ANALYSIS OF SCROLL AND GUIDE VANE PERFORMANCE | 23 |
| 3.1 Instrumentation and Test Procedures | 24 |
| 3.2 Theoretical Analysis | 28 |
| 3.3 Data Reduction: Program SCROLL | 31 |
| 3.4 Discussion of Results | 31 |
| 4. ANALYSIS OF OVERALL TURBINE PERFORMANCE | 36 |
| 4.1 Instrumentation | 36 |
| 4.2 Test Procedures | 39 |
| 4.3 Theoretical Analysis | 43 |
| 4.4 Data Reduction: Programs RADIAL and NOSPD | 52 |
| 4.5 Discussion of Results | 52 |
| 5. CONCLUSIONS | 61 |
| ILLUSTRATIONS | 63 |
| REFERENCES | 101 |
| APPENDIX A: Program SCROLL | 102 |
| A1. Main Program | 102 |
| A2. Subroutine TEMP | 103 |
| A3. Subroutine FLOW | 103 |
| A4. Subroutine PRESS | 105 |
| A5. Method of Assembly of Input Data | 105 |

| | | |
|-------------|--|-----|
| APPENDIX B: | Program PHIAL | 119 |
| | B1. Subroutines TEMP and FLOW | 120 |
| | B2. Subroutine PRESS | 120 |
| | B3. Subroutine EDC | 121 |
| | B4. Subroutines TORQ and DYNA | 122 |
| | B5. Subroutine TURB | 123 |
| | B6. Subroutine PHIAL | 123 |
| | B7. Subroutine REFER | 124 |
| | B8. Method of Assembly of Input Data | 124 |
| APPENDIX C: | Program NOSP | 148 |

LIST OF TABLES

| TABLE | | PAGE |
|-------|---|------|
| A1 | Listing of Program SCROLL | 107 |
| A2 | Results from Program SCROLL Clearance 0.081 In. | 111 |
| A3 | Results from Program SCROLL Clearance 0.072 In. | 112 |
| A4 | Results from Program SCROLL Clearance 0.061 In. | 113 |
| A5 | Results from Program SCROLL Clearance 0.050 In. | 114 |
| A6 | Results from Program SCROLL Clearance 0.041 In. | 115 |
| A7 | Results from Program SCROLL Clearance 0.030 In. | 116 |
| A8 | Results from Program SCROLL Clearance 0.024 In. | 117 |
| A9 | Results from Program SCROLL Clearance 0.015 In. | 118 |
| B1 | Listing of Program RADIAL | 126 |
| B2 | Additional Control Cards Required for Program RADIAL | 136 |
| B3 | Torque Calibration Data | 137 |
| B4 | Program RADIAL Input Data Clearance 0.081 In. | 138 |
| B5 | Results from Program RADIAL Clearance 0.081 In. | 139 |
| B6 | Program RADIAL Input Data Clearance 0.061 In. | 140 |
| B7 | Results from Program RADIAL Clearance 0.061 In. | 141 |
| B8 | Program RADIAL Input Data Clearance 0.041 In. | 142 |
| B9 | Results from Program RADIAL Clearance 0.041 In. | 143 |

| TABLE | | PAGE |
|-------|--|------|
| B10 | Program RADIAL Input Data Clearance 0.024 In. | 144 |
| B11 | Results from Program RADIAL Clearance 0.024 In. | 145 |
| B12 | Program RADIAL Input Data Clearance 0.015 In. | 146 |
| B13 | Results from Program RADIAL Clearance 0.015 In. | 147 |
| C1 | Listing of Program NOSPD | 149 |
| C2 | Results from Program NOSPD | 154 |

LIST OF ILLUSTRATIONS

| FIGURE | | PAGE |
|--------|---|------|
| 1. | Active Rotor Test Installation | 63 |
| 2. | Dummy Rotor Test Installation | 64 |
| 3. | Wooden Scroll Insert | 65 |
| 4. | Turbine Scroll and Guide Vane Assembly | 66 |
| 5. | Cross-Section of Turbine | 67 |
| 6. | Dummy Rotor and Flow Straighteners | 68 |
| 7. | Active Rotor | 69 |
| 8. | Left Turbine Discharge | 70 |
| 9. | Turbine Inlet Piping, Flow Control Valves, and Flow Measuring Orifice | 71 |
| 10. | Remote Control for Flow Regulation, Vortec Remote Throttle Control, and Daytronic Strain Gage Digital Indicator | 72 |
| 11. | Schematic of Radial Turbine Instrumentation | 73 |
| 12. | Meriam Mercury Micromanometers | 74 |
| 13. | Brown Potentiometer | 75 |
| 14. | Temperature-Entropy Diagram for Radial Turbine | 76 |
| 15. | Velocity Diagrams for Radial Turbine | 77 |
| 16. | Velocity Coefficient vs. Mach Number | 78 |
| 17. | Absolute Rotor Inlet Flow Angle vs. Mach Number | 79 |
| 18. | Velocity Coefficient vs. Mach Number from Derived Equation | 80 |
| 19. | Absolute Rotor Inlet Flow Angle vs. Mach Number from Derived Equation | 81 |
| 20. | Dummy Alignment Shaft | 82 |
| 21. | Flux Cutter, Quill Shaft, and Dynamometer Torque Capsule | 83 |

| FIGURE | | PAGE |
|--------|---|------|
| 22. | Electronic Speed Counter and Vibration Analyzer | 84 |
| 23. | Five Inch Inlet Pipe and Bearing Lubrication Unit | 85 |
| 24. | Schematic of Turbine Lubrication System | 86 |
| 25. | Automatic Data Acquisition System | 87 |
| 26. | Torque Capsule Calibration Apparatus | 88 |
| 27. | Degree of Reaction vs. Head Coefficient | 89 |
| 28. | Overall Efficiency (No Bearing Losses) vs. Referred Speed | 90 |
| 29. | Overall Efficiency (No Bearing Losses) vs. Head Coefficient | 91 |
| 30. | Overall Efficiency (with Bearing Losses) vs. Referred Speed | 92 |
| 31. | Overall Efficiency (with Bearing Losses) vs. Head Coefficient | 93 |
| 32. | Rotor Velocity Coefficient (No Bearing Losses) vs. Head Coefficient | 94 |
| 33. | Rotor Velocity Coefficient (with Bearing Losses) vs. Head Coefficient, Clearance 0.081 In. | 95 |
| 34. | Rotor Velocity Coefficient (with Bearing Losses) vs. Head Coefficient, Clearance 0.061 In. | 96 |
| 35. | Rotor Velocity Coefficient (with Bearing Losses) vs. Head Coefficient, Clearance 0.041 In. | 97 |
| 36. | Rotor Velocity Coefficient (with Bearing Losses) vs. Head Coefficient, Clearance 0.024 In. | 98 |
| 37. | Rotor Velocity Coefficient (with Bearing Losses) vs. Head Coefficient, Clearance 0.015 In. | 99 |
| 38. | Referred Moment (with Bearing Losses) vs. Referred Speed | 100 |

TABLE OF SYMBOLS

| Symbol | FORTTRAN | Definition | Units |
|-------------|----------|---|--|
| A_1 | - - - - | Meridional cross-sectional area of rotor inlet | ft ² |
| A_5 | - - - - | Cross-sectional area of five inch inlet pipe | ft ² |
| B_1 | B1 | Perpendicular distance between shroud inner extremities | in |
| C | - - - - | Flow measurement factor dependent on units, orifice diameter, and type of pressure taps | - - - |
| C_{f1} | CF1 | Pressure conversion factor | lb/ft ² /in Hg |
| Clnc | CLNC | Rotor axial tip clearance, on one side of blade only | in |
| C_0 | C0 | Velocity corresponding to the isentropic enthalpy drop through the turbine | ft/sec |
| C_p | CP5 | Constant pressure specific heat, based on total inlet temperature | BTU/lb _m -°F |
| C_p (avg) | CP | Constant pressure specific heat, based on average temperature t | BTU/lb _m -°F |
| D_1 | D1 | Rotor diameter at inlet, 9.40 in. | in |
| D_{20} | - - - - | Rotor outer discharge diameter, 5.88 in. | in |
| F | SR | Scale reading | lb |
| Fr | - - - - | Reynolds number correction factor | - - - - |
| G_{Hg} | GHG | Specific gravity of mercury at t_{rm} | - - - - |
| G_{H2O} | GWR | Specific gravity of water at t_{rm} | - - - - |
| g | 32.174 | Unit Conversion Factor | ft-lb _m ^t /lb-sec ² |
| H_E | - - - - | Total enthalpy at equivalent state point E | BTU/lb _m |

| Symbol | FORTTRAN | Definition | Units |
|-------------------|----------|--|--------------------------|
| HP_f | HPF | Power required to overcome bearing friction | hp |
| H_R | - - - - | Relative total enthalpy at rotor inlet | BTU/lb _m |
| H_{refl} | HREF1 | Measured reference pressure applied to water manometer board | in Hg gage |
| h_1 | - - - - | Static enthalpy at rotor inlet | BTU/lb _m |
| h_2 | - - - - | Static enthalpy at rotor discharge | BTU/lb _m |
| $h_1(\text{avg})$ | H1 | Average static pressure ahead of rotor | in H ₂ O gage |
| ΔH_{is} | DHIS | Isentropic total enthalpy drop across turbine | BTU/lb _m |
| ΔH_w | - - - - | Enthalpy drop representing work output of turbine | BTU/lb _m |
| Δh_{lvc} | DPVC | Measured pressure differential across flow orifice, from vena contracta taps | in Hg |
| J | 778.16 | Joule's constant | ft-lb/BTU |
| k_{is} | HEAD | Isentropic head coefficient | - - - - |
| M | TNET | Net torque output of turbine | ft-lb |
| M_f | BFM | Bearing friction moment | ft-lb |
| M_{ref} | TNETR | Referred net torque output of turbine | ft-lb |
| M_1 | ACH1 | Mach number at rotor inlet | - - - - |
| N | RPM | Measured turbine speed | rpm |
| N_{ref} | RPMR | Referred turbine speed | rpm |
| P_{atm} | PATM | Barometric pressure | in Hg |
| P_{t0} | PTO | Absolute total pressure ahead of turbine | in Hg abs |

| Symbol | FORTTRAN | Definition | Units |
|--------------|----------|---|---------------------------|
| P_{t0}/p_1 | PR1 | Pressure ratio across scroll and guide vanes | - - - - |
| P_{t0}/p_2 | PR2 | Pressure ratio across turbine | - - - - |
| P_E | - - - - | Equivalent rotor inlet static pressure | in Hg abs |
| p_0 | PS5 | Absolute static pressure at turbine inlet | in Hg abs |
| p_1 | P1 | Average absolute static pressure at rotor inlet | in Hg abs |
| p_{1VC}' | PUVC | Measured pressure upstream of flow orifice, from vena contracta tap | in Hg gage |
| p_{1VC} | PVC | Absolute pressure upstream of flow orifice from vena contracta taps | in Hg abs |
| p_2 | P2 | Static discharge pressure | in Hg abs |
| p_5' | P5P | Measured static pressure at turbine inlet | in Hg gage |
| R_g | 53.3448 | Gas constant for air | ft-lb/lb _m -°R |
| R_1 | R1 | Rotor inlet radius, 4.70 in. | in |
| R_{20} | R20 | Rotor outer discharge radius, 2.94 in | in |
| r | DR | Isentropic degree of reaction | - - - - |
| T | T | Torque measured by dynamometer | ft-lb |
| TCD | TCD | Torque calibration data | counts |
| TQ | TQ | Torque indicator reading | counts |
| T_E | - - - - | Equivalent rotor inlet temperature | °R |
| T_{ref} | TR | Referred torque output for no-loss case | ft-lb |
| T_{to} | T5 | Total temperature ahead of turbine | °R |
| T_0 | T0 | Static temperature ahead of turbine | °R |

| <u>Symbol</u> | <u>FORTTRAN</u> | <u>Definition</u> | <u>Units</u> |
|-----------------|-----------------|--|--------------------|
| T_1 | T1 | Static temperature ahead of rotor | $^{\circ}\text{R}$ |
| T_1' | - - - - | Static temperature at rotor inlet for isentropic expansion from P_{t0} to p_1 | $^{\circ}\text{R}$ |
| T_1^* | - - - - | Static temperature at rotor inlet resulting from rotor incidence losses | $^{\circ}\text{R}$ |
| T_2' | - - - - | Static discharge temperature resulting from isentropic expansion from p_E to p_2 | $^{\circ}\text{R}$ |
| T_2'' | - - - - | Static temperature at discharge resulting from isentropic expansion from P_{t0} to p_2 | $^{\circ}\text{R}$ |
| T_4 | T4 | Total temperature ahead of flow orifice | $^{\circ}\text{R}$ |
| T_{20} | T20 | Lubricating oil inlet temperature | $^{\circ}\text{F}$ |
| T_{21} | T21 | Lubricating oil temperature at discharge from right bearing | $^{\circ}\text{F}$ |
| T_{22} | T22 | Lubricating oil temperature at discharge from left bearing | $^{\circ}\text{F}$ |
| ΔT_{is} | DTIS | Isentropic temperature drop from P_{t0} to p_2 | $^{\circ}\text{R}$ |
| ΔT_W | DTW | Temperature drop corresponding to actual work output of turbine | $^{\circ}\text{R}$ |
| t | A | Average temperature through turbine | $^{\circ}\text{F}$ |
| tare | STARE | Tare of precision scales | lb |
| t_{cj} | TCJ | Thermocouple reference cold junction temperature | $^{\circ}\text{F}$ |
| t_{rm} | TRM | Control room temperature | $^{\circ}\text{F}$ |
| U_1 | U1 | Peripheral speed of rotor at inlet | ft/sec |
| U_{20} | U20 | Peripheral speed of rotor at outer discharge radius | ft/sec |

| Symbol | FORTTRAN | Definition | Units |
|-------------------|----------|--|--------|
| V | - - - - | Thermocouple reading | mv |
| V ₀ | VO | Velocity at turbine inlet | ft/sec |
| V ₁ | V1 | Absolute flow velocity at rotor inlet | ft/sec |
| V _{u1} | VUL | Peripheral component of V ₁ | ft/sec |
| V _{m1} | VM1 | Meridional component of V ₁ | ft/sec |
| V _{ith} | VITH | Theoretical absolute rotor inlet velocity for no losses | ft/sec |
| V ₂₀ | V20 | Absolute discharge flow velocity at outer radius of rotor | ft/sec |
| V _{u20} | VU20 | Peripheral component of V ₂₀ | ft/sec |
| V _{m20} | VM20 | Meridional component of V ₂₀ | ft/sec |
| V ₄ | V4 | Thermocouple reading ahead of flow orifice | mv |
| V ₅ | V5 | Thermocouple reading at turbine inlet | mv |
| V ₂₀ | V20 | Thermocouple reading at lube oil inlet | mv |
| V ₂₁ | V21 | Thermocouple reading at lube oil discharge from right bearing | mv |
| V ₂₂ | V22 | Thermocouple reading at lube oil discharge from left bearing | mv |
| W ₁ | W1 | Relative flow velocity at rotor inlet | ft/sec |
| W _{u1} | WU1 | Peripheral component of W ₁ | ft/sec |
| W ₂₀ | W20 | Relative flow velocity at rotor discharge outer radius | ft/sec |
| W _{u20} | WU20 | Peripheral component of W ₂₀ | ft/sec |
| W _{20th} | W20TH | Theoretical relative flow velocity at outer discharge radius, for isentropic expansion from p _E to p ₂ | ft/sec |

| <u>Symbol</u> | <u>FORTTRAN</u> | <u>Definition</u> | <u>Units</u> |
|-----------------|-----------------|---|----------------------|
| \dot{W} | WVC | Mass flow rate, for vena contracta taps | lb _m /sec |
| \dot{W}_{ref} | WVCR | Referred mass flow rate | lb _m /sec |
| \dot{W}_{oil} | - - - - | Mass flow rate of lubricating oil | lb _m /sec |
| Y_1 | Y | Factor accounting for compressibility effects in flow measuring orifice | - - - - |

| Symbol | FORTTRAN | Definition | Units |
|-------------------------|----------|--|----------|
| <u>GREEK SYMBOLS</u> | | | |
| α | A | Area multiplier accounting for thermal expansion of flow orifice | - - - - |
| α_1 | ALPH1 | Absolute rotor inlet flow angle | degrees |
| α_{20} | ALF2 | Absolute rotor discharge flow angle at outer radius, for no bearing loss case | degrees |
| α_{20L} | ALF2L | Absolute rotor discharge flow angle at outer radius, bearing losses considered | degrees |
| β_1 | BETA1 | Relative rotor inlet flow angle | degrees |
| β_{20} | BET20 | Relative rotor discharge flow angle at outer radius | degrees |
| γ | GAMMA | Ratio of specific heats based on T_{t0} | - - - - |
| $\gamma_{(avg)}$ | GAM | Ratio of specific heats based on t | - - - - |
| $(\gamma - 1) / \gamma$ | EXP | Exponent | - - - - |
| δ | DEL | Referred pressure ratio, $P_{t0} / 14.7$ | - - - - |
| ϵ | EPS | Factor which corrects flow rate through the turbine for varying values of γ | - - - - |
| η | ETA | Total-to-static turbine efficiency, bearing losses not considered | per cent |
| η_L | ETAL | Total-to-static turbine efficiency, including bearing losses | per cent |
| ϕ | PHI | velocity coefficient for scroll and guide vanes | - - - - |
| ψ | PSI | Velocity coefficient for rotor, based on ratio of actual to theoretical relative discharge velocities, bearing losses not considered | - - - - |

| <u>Symbol</u> | <u>FORTTRAN</u> | <u>Definition</u> | <u>Units</u> |
|---------------|-----------------|---|----------------------------------|
| Ψ_L | PSIL | Velocity coefficient for rotor, bearing losses included | - - - - |
| ρ_0 | RHO | Density at turbine inlet | lb _m /ft ³ |
| ρ_1 | RHO | Density at rotor inlet | lb _m /ft ³ |
| Θ | THETA | Referred temperature ratio, $T_{to}/518.7$ | - - - - |
| ω | ROSP | Rotational speed of rotor | radians/sec |
| ζ_N | ZETAN | Loss coefficient for scroll and guide vanes | - - - - |
| ζ_R | ZETR | Rotor loss coefficient, bearing losses not considered | - - - - |
| ζ_{RL} | ZETRL | Rotor loss coefficient, with bearing losses | - - - - |

SECTION I

INTRODUCTION

As requirements for smaller more powerful turbines increase, to keep pace with the needs of the rapidly expanding aerospace industry, more and more attention is given to radial turbines. Since the radial turbine can extract more energy per stage than an axial turbine, it is more useful in applications where space limitations preclude the use of a staged axial turbine. Currently, it is therefore used extensively for aircraft electric power generation, in aircraft cockpit and equipment cooling systems, in cryogenic systems, and in missile auxiliary power systems.

As a consequence of the increasingly widespread use of the radial turbine, the establishment of performance parameters as an aid to the design of these turbines is of fundamental importance. It is the objective of this report to establish some of the performance parameters for a particular radial inflow, dual discharge turbine using air as an operating fluid and relating these parameters in such a way that they may be applied to geometrically similar turbines operating with different fluids and in different environments.

Although similar studies have previously been conducted on this machine, this investigation differs in two important aspects. First, several significant and necessary changes in the internal dimensions of the turbine were made, thus resulting in a somewhat different machine than that previously tested. Also, the method of analysis used is a considerably simplified one, which yields more significant results with less computational effort than those methods previously employed by referring all losses to the outer discharge radius rather than a computed average radius.

Additionally, this project had as an objective a significant expansion of the operating ranges examined beyond those previously considered.

Because the evaluation of turbine performance parameters involves a formidable computation requirement, the data obtained in the experiments were reduced by means of the computer programs described herein, which are written in FORTRAN IV language for the IBM 360 computer system used at the Naval Postgraduate School.

The author gratefully acknowledges the guidance and counsel of Professor Robert D. Zucker, of the Department of Aeronautics, Naval Postgraduate School, and of Professor Michael H. Vavra of the same department. Thanks are due also to Mr. James E. Hammer and his coworkers on the technical staff of the Turbopropulsion Laboratory for their many hours of hard work in modifying, repairing, and operating the turbine test rig.

SECTION 2

THE I.C.P. RADIAL TURBINE

The turbine used in this investigation is a dual discharge, radial inflow turbine installed at the Turbopropulsion Laboratory of the Department of Aeronautics, Naval Postgraduate School. It was originally designed and built by the Aerojet General Corporation, for application as the power supply for a missile propulsion combustion cycle. The original performance evaluation was conducted by Vavra (1), with subsequent investigations by Finn (2), Riley (3), and Boshoven (4).

2.1 Description of Turbine Assembly

The basic turbine test installations used are shown in Figures 1 and 2. The turbine assembly consists of: the wooden inlet casing, with its inner contour in the shape of a varying diameter torus, or scroll; a circular stainless steel guide vane assembly consisting of seven circular-arc blades and the rings themselves; the rotor assembly; and two plexi-glass shrouds.

The inner contour of the inlet casing was formed by casing plaster of paris around a wooden insert of the desired scroll dimensions. The inner surface of the scroll was varnished to prevent erosion. The wooden insert used in this process is shown in Figure 3, and Figure 4 presents a cross-section of the wooden casing, showing the shape of the scroll and the locations of the various scroll pressure taps. It is worthy of note that the flow entry is not tangential, as is customarily the case in radial turbine installations. This characteristic is a result of design requirements in the originally proposed missile installation.

A cross-section of the turbine is shown in Figure 5. In this view are indicated the turbine dimensions and minimum clearance as they existed for the test runs. The clearance, or axial distance between the rotor and the shrouds, was increased during the tests by means of circular metal shims inserted between the shroud flanges and the aluminum rings on which they rest.

The series of tests conducted utilized two different rotors. The "dummy" rotor, so called because it does not rotate, is a special device designed to permit measurement of the torque generated by the incoming flow and thus provides a measure of scroll and guide vane performance. This rotor is shown in Figure 6. It has a diameter of 9.50 inches, an axial length of 8.50 inches, and 36 meridional blades. This diameter places the blade leading edges at the radius which corresponds to that of the annulus containing the static pressure taps ahead of the rotor, and the axial length extends the blade trailing edges beyond the shrouds.

The "active" rotor, or the power-producing rotating element, is shown in Figure 7. It is 9.40 inches in diameter and has an axial length of 5.00 inches. The rotor discharge radius is 1.76 inches at the hub and 2.94 inches at the tip. The fifteen blades have a spacing at the discharge varying from 0.737 to 1.232 inches, hub to tip respectively. The actual rotor discharge area on one side of the rotor is 6.43 square inches, including an effective flow area through the radial gap between the blades and the shroud taken at the discharge plane (1). A view of the left rotor discharge, showing the plexiglass shroud and several of the eight shroud pressure taps which measure static pressure at the rotor inlet, is given in Figure 8.

2.2 Modifications to Turbine Assembly

When the turbine assembly was dismantled in preparation for this series of tests, it was discovered that one of the plexiglass shrouds was deeply gouged. Since removal of enough material to eliminate this fault would have destroyed the contour of the shroud, it was decided to cut the contours of both shrouds so that they would exactly fit the rotor contour. Additionally, it was decided to correct several dimensional discrepancies noted in earlier reports.

Riley (3) indicates a distance of 0.943 inch between the inner extremities of the shrouds. Since the axial width of the blade tips is 0.894 inch, this indicates a basic (unshimmed) axial tip clearance of 0.025 inch on each side of the blade. Boshoven (4), however, determined the distance between shrouds to be 0.966 inch, with a resulting unshimmed clearance of 0.036 inch. Additionally, Boshoven discovered that the inside extremity of the left shroud (as viewed from the turbine inlet) was offset 0.016 inch more from the guide vane ring than the right shroud.

In order to correct these discrepancies, an extensive series of measurements was undertaken. The guide vane rings, which were found to be warped, were lapped until they were flat, and all rough edges, burrs, and high spots on the inner surfaces of the casing halves were carefully removed. This resulted in a consistency to within 0.0025 inch in the dimension between the shroud support rings, at all points around the periphery. Initial measurements showed a maximum variation of 0.01 inch in this dimension.

Measurements with the reworked shrouds installed then showed a minimum clearance of 0.0477 inch, with the left shroud offset axially outward 0.0056 inch more than the right. The shroud flange thicknesses were then reduced so as to compensate for this dissymmetry and to yield

a final unshimmed clearance of 0.015 inch. Subsequent measurement of the axial travel of the active rotor, from contact at one shroud face to contact at the other, verified that all calculated clearances used in these tests were correct to within ± 0.002 inch.

Additional modifications were made to the dummy rotor in order to correct the axial stagger and unequal widths of the blades and to correct as much as possible the large gaps which were found to exist between the rotor blade contours and the shroud contours. By careful machining, the blade contours were made uniform, and a much closer fit was made to the shroud contours, even though it was not possible to completely correct this condition and still maintain the blade width.

It is thus apparent that the results obtained from the turbine after this series of modifications could differ to a marked degree from those previously obtained under identical operating conditions. It also seems to this author that both Riley (3) and Boshoven (4) were operating at clearances somewhat greater than stated in their respective studies. Based only on these modifications, the distance between the shroud inner extremities for their tests would have been approximately 0.989 inch, yielding a minimum clearance of 0.048 inch. This may be compared with the minimum clearance of 0.0245 inch reported by Riley and 0.036 inch reported by Boshoven.

Other modifications to the components of the test rig were made and are covered in the sections to which they apply. In this section only those modifications basic to the radial turbine itself are discussed.

SECTION 3

ANALYSIS OF SCROLL AND GUIDE VANE PERFORMANCE

In order to evaluate the performance parameters of a turbine, it is necessary to divide the losses into those which occur in the inlet guide vanes and those which occur in the rotor itself. Riley (3) and Boshoven (4) have used the special dummy rotor installation previously described (Figure 2) to determine the losses in the stator, or scroll and guide vane assembly. The installation determines the average conditions at the rotor inlet and thus provides an indication of scroll and guide vane efficiency as well as the absolute velocity (in both magnitude and direction) at the rotor inlet.

Riley (3) concluded that the velocity coefficient, which is a measure of the losses occurring in the inlet manifold and guide vanes, as well as the absolute inlet flow angle, was essentially constant in the range of turbine pressure ratios and axial clearances examined. The results obtained by Boshoven (4) indicate that this assumption is invalid; in fact, the velocity coefficients were found to increase with pressure ratio for a given clearance, and the absolute rotor inlet flow angles were found to decrease linearly with pressure ratio. Specific results of these earlier tests are discussed in detail in Section 3.3.

It was originally intended to utilize the dummy rotor test data of Boshoven (4) in this experiment. However, because of the extensive modifications previously discussed, it was necessary to repeat these tests. This repetition yielded the additional advantage of permitting testing over a wider range of clearances.

3.1 Instrumentation and Test Procedures

The dummy rotor shown in Figure 6 is mounted on self-aligning ball bearings and replaces the turbine rotor. Its purpose is to turn the flow from the guide vanes into the axial direction and to discharge it with no peripheral velocity component. If this condition is met, the losses in the scroll and guide vanes may be determined by measuring the torque exerted on the static dummy rotor, the flow rate, the conditions at the manifold inlet, and the static pressure at the dummy rotor inlet.

As was previously mentioned, the dummy rotor has an axial length of 8.50 inches, which extends the blade trailing edges beyond the shrouds. To insure that the discharge flow had no whirl components, flow straighteners, also shown in Figure 6, were used. These devices consist of aluminum caps containing a 1.00 inch depth of 0.125 by 0.0015 inch honeycomb material. The caps slide over the rotor shaft and cover the rotor blade trailing edges. The entire dummy rotor assembly is supported by brackets attached to the manifold casing, as shown by Figure 2.

Air for turbine operation was supplied by an Allis-Chalmers 12-stage axial compressor. Air from the main supply line passes through a four-inch pipe, a settling tank, a five-inch pipe, and then into the turbine. The flow rate was regulated by remotely controlled butterfly valves in the inlet line to the turbine and in the outside discharge line of the Allis-Chalmers compressor. (See Figure 9.) The controls for operating these valves are located in the control room (Figure 10).

The flow rate of the incoming air was measured with a sharp-edged orifice located in the four-inch inlet pipe. This orifice is also shown in Figure 9. The pressure ahead of the orifice and the pressure differential across the orifice were measured with standard vena contracta taps. The total temperature ahead of the orifice was measured with an

iron-constantan thermocouple installed in a Kiel temperature probe. The orifice installation conforms to standards set forth by Stearns, et al. (5).

The total inlet conditions in the five-inch pipe just upstream of the turbine were measured with a Kiel probe, also incorporating an iron-constantan thermocouple. The static pressure at the same location was measured by two static pressure taps in the line. The static pressure at the rotor inlet was measured by pressure taps located at eight peripheral stations in each shroud. The axial location of these taps is depicted in Figure 5, and their peripheral locations are shown in Figure 4. These taps were moved to the positions shown from their original locations near the shroud inner extremities by Boshoven (4) in order to reduce the effects of local pressure perturbations experienced in previous tests.

The torque exerted on the dummy rotor by the flow was measured on a 25-pound capacity Toledo precision scale, shown in Figure 2. A twelve-inch lever arm was attached to the rotor shaft and incorporated a simple provision for leveling, so that the force was exerted on the scale through an exactly vertical link. This was done to preserve the direct relationship between scale reading and moment. A counter balance was added to the lever arm in order to extend the capacity of the scales to accommodate higher mass flow rates.

A general schematic of the instrumentation used in this and the subsequent active rotor tests is shown in Figure 11. From this schematic it may be seen that the pressure upstream of the flow measuring orifice, the total and static pressures at the turbine inlet, and the reference pressures 1 and 2 were read from an eleven column, 40-inch mercury manometer board located in the control room. This board was referenced to

atmospheric pressure. Additionally, one arbitrarily selected scroll pressure tap was connected to the mercury board, and this pressure, together with the total inlet pressure, was used to set the pressure ratio across the scroll and guide vanes. The total inlet pressure displayed on the mercury board was used only for setting this pressure ratio since a more representative total pressure was computed in the data reduction.

The sixteen shroud pressure taps that measure the static pressure at the rotor inlet were read on a fifty-column, 96-inch water manometer board. Also displayed on this board were the pressures at various stations in the scroll itself, although these pressures were not used in the tests. These pressures were measured against atmospheric pressure for the entire series of dummy rotor runs. However, additional, controlled, pressures could have been imposed on the water board reservoirs by means of regulated house air if this had become necessary in order to avoid exceeding the limits of the manometer board. These pressures (the reference pressures 1 and 2 mentioned above) were displayed on the mercury manometer board. The first of these pressures, displayed on column 10 of the mercury board, was recorded as a test datum since it applied to the sixteen columns which indicated the rotor inlet pressures. The value of this pressure was thus zero for all dummy rotor runs.

The pressure differential across the flow orifice was measured on a 20-inch Meriam model 34FB2 mercury micro-manometer, which has a measuring accuracy of ± 0.001 inch. A pair of these instruments is shown in Figure 12.

The potentials generated by the iron-constantan thermocouples were measured on a 48-channel Brown potentiometer, manufactured by Minneapolis-Honeywell. This potentiometer, shown in Figure 13, was located in the control room and used an ice bath in the test cell as a cold junction reference.

A series of eighteen test runs were made on the dummy rotor installation, of which eight are documented in this report. These eight runs represent clearances of 0.015, 0.024, 0.030, 0.041, 0.051, 0.061, 0.072, and 0.081 inches, respectively. For each clearance ten pressure ratios were sampled, ranging in value from 1.05 to 1.65. These pressure ratios represent the ratio of total turbine inlet pressure to the static pressure at the rotor inlet.

This large number of runs was necessitated by several factors. Data from the initial runs possessed an unacceptable degree of scatter. This was attributed to an unstable supply of source air from the Allis-Chalmers compressor. When this unsatisfactory trend was discovered, the speed control system was overhauled, and the subsequent test results were significantly improved.

Additionally, the stability of the system was improved by judicious use of the aforementioned butterfly control valve. Experimentation showed that if less of the excess air from the compressor were discharged to the outside, the compressor would be operating at a higher pressure ratio, (with a greater pressure drop across the valve feeding the turbine), and the pressurized air in the house plumbing would act as an additional plenum. The system fluctuations would then be substantially reduced. These improvements in equipment and operating technique, as well as the inevitable improvement in data taking technique, led to such improved results that many runs were repeated in order to obtain the best possible test data.

As first observed by Boshoven (4), it was noted that the pressure distribution around the shroud was very sensitive to the relative positions of the rotor blade leading edges. To eliminate this factor as a possible variable, it was arranged to permit the return of the rotor to

the same location each time a new pressure ratio was set. This was accomplished by means of a wing nut on the end of the rod connecting the moment arm to the scale.

It was also observed that the pressures seemed to be higher by about 4 to 5 inches of water at the right side of the rotor inlet than at the left. This condition could be eliminated by moving the rotor approximately 0.001 inch axially to the left; but since the condition was also present in the scroll itself, it was attributed to scroll pressure distribution rather than to misalignment. The rotor was centered for all runs.

3.2 Theoretical Analysis

From the law of moment of momentum (6), the moment M exerted on the dummy rotor by the flow is given by

$$M = (\dot{W}/g) R_1 V_{u1} \quad (1)$$

where \dot{W} is the mass flow rate, R_1 is the inlet radius of the dummy rotor, and V_{u1} is the peripheral velocity component at R_1 . Equation (1) is valid for the case of steady flow in the dummy rotor because the pressures acting over the inlet and discharge areas cannot produce a moment about the axis, and because the flow straighteners insure an axial discharge velocity.

A measure of the performance of the scroll and guide vanes is given in the form of the velocity coefficient, ϕ , which is defined by

$$\phi \equiv V_1 / V_{1th} \quad (2)$$

where V_1 is the average velocity at the dummy rotor inlet and V_{1th} is the theoretical velocity at the dummy rotor inlet which would result from an isentropic expansion from the manifold inlet total conditions P_{t0} , T_{t0} ,

to the static pressure p_1 at the dummy rotor inlet. This process is shown on the T-s diagram of Figure 14. The component velocities may be seen on Figure 15.

From the energy equation for an adiabatic, no work process, the velocity V_1 at the dummy rotor inlet is

$$V_1 = \sqrt{2gJc_p(T_{t0} - T_1)} \quad (3)$$

If use is made of the isentropic pressure-temperature relation for a perfect gas and of Equation (2), V_1 may be alternately expressed as

$$V_1 = \phi \sqrt{2gJc_p T_{t0} \left[1 - (P_1/P_{t0})^{\frac{\gamma-1}{\gamma}} \right]} \quad (4)$$

Application of the equation of continuity at the dummy rotor inlet yields the following expression for the average meridional velocity component:

$$V_{m1} = \dot{W} / \rho_1 A_1 \quad (5)$$

where ρ_1 is the density at the dummy rotor inlet, and A_1 is the cross-sectional area normal to the flow (meridional cross-section). The area A_1 is given by

$$A_1 = 2\pi R_1 B_1 \quad (6)$$

where B_1 is the distance between the shrouds at the rotor inlet. Using the equation of state for a perfect gas, ρ_1 may be expressed as

$$\rho_1 = P_1 / R_g T_1 \quad (7)$$

Substitution of this relation and Equation (6) into Equation (5) yields the resultant expression for V_{m1} :

$$V_{m1} = \frac{\dot{W} R_g T_1}{2\pi R_1 B_1 P_1} \quad (8)$$

From Equation (1), the peripheral velocity may be expressed as

$$V_{u1} = \frac{M g}{R_1 \dot{W}} \quad (9)$$

and V_1 may additionally be given by

$$V_1 = \sqrt{V_{u1}^2 + V_{m1}^2} \quad (10)$$

Thus, three equations expressing the velocity V_1 are established, these being Equations (3), (4), and (10). Upon substitution of Equations (8) and (9) into Equation (10), it may be seen that this set of three equations contains three unknowns. The unknown quantities to be determined are the velocity V_1 , the velocity coefficient ϕ , and the temperature T_1 , all other quantities being either constants or determined directly from measured data. Solution of this system of equations establishes the velocity components, which may then be used to calculate the absolute flow angle at the dummy rotor inlet, according to the relation

$$\alpha_1 = \tan^{-1} (V_{u1} / V_{m1}) \quad (11)$$

A nozzle loss coefficient, ζ_N , may be obtained from the relation

$$\zeta_N = 1 - \phi^2 = 1 - \eta \quad (12)$$

where η is an efficiency based on the ratio of the actual-to-isentropic temperature drop across the scroll and guide vanes. It is introduced here only to illustrate the significance of ζ_N and ϕ .

3.3 Reduction of Data: Program SCROLL

The computer program SCROLL, listed in Appendix A, determines the unknown quantities, V_1 , ϕ , and T_1 , and the absolute inlet angle, α_1 , from the test data using an iterative procedure. The program makes temperature corrections to the physical properties of air and to the specific gravities of the water and mercury used as manometer fluids. It converts the manometer readings and thermocouple voltages into pressures and temperatures, as required, and then establishes the mass flow rate. The average conditions at the dummy rotor inlet are then calculated from the measured torque in accordance with the previously given relations.

Program SCROLL has been described in detail by Riley (3) and Boshoven (4). Except for conversion to the FORTRAN IV language, the program used in this experiment remains essentially the same; therefore, the details of the computational processes will not be repeated. However, certain minor changes were incorporated in the temperature corrections applied to the manometer fluids, in the thermocouple equations used, and in the pressure and flow rate solutions. These changes are briefly described in Appendix A, although they become evident if the program used in this report is compared with either of the two above-listed references.

3.4 Discussion of Results

The results of program SCROLL consist primarily of values of the velocity coefficient, ϕ , and the absolute flow angle at the rotor inlet, α_1 . These values are plotted versus M_1 , the Mach number at the rotor inlet, as opposed to the pressure ratio, P_{t0}/P_1 , because the Mach number is a more significant parameter in the application of test results to geometrically similar machines. Figure 16 shows ϕ as a function of

M_1 for each of the eight clearances tested, and Figure 17 is a similar plot for α_1 as a function of M_1 . Each of the curves was fitted to the data obtained for that run by the least squares method. The tabulated results for each of the eight runs are given in Appendix A.

It may be seen from Figure 16 that the velocity coefficient increases with Mach number, the average increase being approximately 4.75 per cent over a Mach number range of 0.2 to about 0.8. This percentage increase is practically the same regardless of clearance. This increase is due, at least in part, to the decreasing coefficient of friction in the scroll and guide vanes, which results from the increasing Reynolds number.

The coefficient ϕ generally increases with decreasing clearance for a given pressure ratio with the maximum values of ϕ occurring at the minimum clearance of 0.015 inches. As clearance is increased beyond a value of about 0.070 inches, the incremental drop in ϕ per increment of clearance increase appears to become much larger. An explanation for this occurrence is that as clearance is increased, an increasing amount of flow escapes around the blade tips. This flow loses angular momentum by wall friction and subsequently strikes the dummy rotor blades at some lesser radius, thus imparting a reduced amount of torque to the rotor. The cumulative effect of this energy loss would logically become more pronounced at increased clearances. The overlapping of certain of the curves in Figure 16 at the lower Mach numbers occurred because of the relative insensitivity of the instrumentation at low pressures.

Figure 17 shows that the absolute rotor inlet flow angle, α_1 , increases with increasing Mach number up to a Mach number of approximately 0.4. Beyond that point, α_1 decreases with increasing Mach number. These changes are small, although they appear to be significant because of the

highly expanded scale of Figure 17. In fact, the average maximum change in α_1 over the range of Mach numbers is approximately 0.52 degrees. In general, increasing the mass flow rate will increase V_1 and, of course, the components V_{u1} and V_{m1} . The variations in the magnitudes of these two quantities as the Mach number is increased determine the variations of α_1 , as shown by Equation (11).

It is also shown on Figure 17 that the angle α_1 increases as clearance increases. This is primarily because V_{m1} is inversely proportional to the meridional cross section, which increases with clearance since it depends on the distance between the shrouds. By Equation (11), the smaller values of V_{m1} result in larger inlet flow angles.

It was concluded by Riley (3) that the velocity coefficient ϕ was essentially independent of the pressure ratio P_{t0}/P_1 , and that a constant representative value of 0.889 was sufficiently accurate. Although he determined that α_1 decreases with increasing pressure ration, he also assumed a representative value of 80.0 degrees for α_1 .

Boshoven (4) subsequently investigated the scroll and guide vane performance in greater detail and obtained results that agree in a qualitative sense with those described above. Because of the many modifications made to the machine components, both in preparation for this experiment and during the course of Boshoven's, a more precise comparison is not warranted. It is worthy of note, however, that Boshoven did not obtain the continuous decrease in ϕ with increasing clearance which is apparent from Figure 16. Further, the increase in ϕ with Mach number found in the present tests is more pronounced than Boshoven's, his increase being on the order of 2 per cent for a given clearance, over the range of Mach numbers. It is felt that these changes have occurred because of the machining of the rotor so that it more closely fits the shroud contours,

thus minimizing flow loss around the blades and permitting closer minimum clearances.

An examination of the data points given in Figure 16 for \emptyset as a function of Mach number shows that some scatter exists. This scatter may be attributed to fluctuations in the air supply from the Allis-Chalmers compressor. The presence of this problem and methods undertaken to alleviate it have been discussed previously in Section 3.1. This scatter of data is also present in the curves of α_1 as a function of Mach number given in Figure 17, but to a lesser extent.

In order to use the results of the dummy rotor tests in later data reduction programs, it was necessary to obtain equations representing \emptyset and α_1 in the form

$$\alpha_1 = \text{Constant} [f_1 (\text{clearance})][f_2 (\text{Mach number})]$$

The function f_1 was obtained by first taking the ratio of α_1 to α_1 maximum at each Mach number, for each clearance. The values of this ratio were then plotted versus clearance. From this plot an average curve was obtained, and its equation was computed by the least squares technique. The resulting equation expressed $\alpha_1 / \alpha_{1\text{max}}$ as a dimensionless function of clearance.

The function f_2 was obtained by computing the ratio of α_1 to the value of α_1 at a Mach number of 0.5, and plotting this ratio versus Mach number for each clearance. Again, an average curve was determined, and its equation was computed. This equation, again dimensionless, expresses $\alpha_1 / \alpha_{1(M=.5)}$ as a function of Mach number.

The appropriate scaling factor was determined for each test point. An average of all of these factors, which did not differ greatly in value, was taken as the constant in the above expression. The equation for \emptyset was determined in the same manner.

The final equations resulting from this procedure were

$$\alpha_1 = (81.762) [.98267 + .26958 (Clnc) - .65080 (Clnc)^2] \quad (13)$$

$$[.99624 + .02223 (M_1) - .02940 (M_1)^2]$$

$$\phi = (.92473) [1.01433 - 1.24601 (Clnc) + 24.06839 (Clnc)^2 \quad (14)$$

$$- 180.36258 (Clnc)^3]$$

$$[.93149 + .18292 (M_1) - .09202 (M_1)^2]$$

Families of curves produced by these equations are given in Figures 18 and 19, for ϕ and α_1 respectively. These curves agree well with those of Figures 16 and 17 when consideration is given to the approximations introduced in the derivations of Equations (13) and (14). For the velocity coefficient, ϕ , the maximum difference which exists at any point between the curves of Figure 16 and those of Figure 18 is 0.0052. A similar comparison for α_1 yields a maximum difference of 0.06 degrees. Because of the manner in which Equations (13) and (14) were derived, the most significant discrepancies occur near the extremes of the Mach number range.

SECTION 4

ANALYSIS OF OVERALL TURBINE PERFORMANCE

The turbine overall performance tests, when combined with the results of the dummy rotor tests, provided data from which detailed performance parameters of the turbine could be evaluated. The specific parameters evaluated were: the total-to-static overall efficiency; velocity and loss coefficients for the rotor and guide vanes; rotor inlet and outlet flow angles; referred speed, moments, and flow rates; the head coefficient; and the degree of reaction. Calculations were made assuming no bearing losses and also for the case of "maximum" bearing losses. Bearing loss values were determined from equations given by Vavra (1), which were established from coast-down tests. The analysis was made using a "mean" streamline approach, which is defined as utilizing a representative streamline along which the measured flow conditions are assumed to exist. This streamline was taken as that at the outer discharge radius of the turbine for this analysis, and thus all losses are referred to that outer radius.

4.1 Instrumentation

The "active" rotor shown in Figure 7 was installed for this series of tests, and the rotor and wooden casing were placed in an aluminum test stand. Figure 1 shows the test installation. Alignment of the scroll with respect to the rotor was accomplished by the use of the dummy alignment shaft and dial micrometers shown in Figure 20. Precise alignment was found to be quite difficult because the massive wooden casing and scroll assembly had to be positioned relative to the rotor. Positioning was accomplished by means of four adjusting bolts located at the bottom

of the casing and by four angle-irons attached to the casing and resting on the bearing supports. In spite of the difficulty involved, alignment of the concentric aluminum rings which serve as supports for the shrouds was obtained to within ± 0.001 inch in the radial direction from the dummy alignment shaft. These rings were found to deviate from a plane perpendicular to the rotor axis by less than 0.002 inch at a radius of 4.7 inches.

The power developed by the turbine was absorbed by a Vortec Products Company air dynamometer, model 20.075, shown in Figure 1. Lubrication of the dynamometer was accomplished by an oil mist generated by air pressure. The torque output was measured with a torque capsule having a maximum rated capacity of 400 inch-pounds. This capsule utilized strain gages arranged on an internal flexure and was additionally instrumented with an iron-constantan thermocouple to provide a means of monitoring the capsule temperature. The signal generated by the strain gages was read on a Daytronic model 700 digital indicator located in the control room (Figure 10).

The dynamometer shroud was modified from the configuration used by Riley (3) so as to discharge the hot exhaust air radially outward, rather than back onto the torque capsule and housing, in order to minimize thermal effects on the torque capsule. The circular aluminum ring visible in Figure 1 was used to accomplish this modification. Additionally, a wooden baffle, not shown on Figure 1, was used to protect the capsule from the cold turbine discharge air, and to prevent any interference between the dynamometer discharge and the right rotor discharge.

Figure 21 shows the inner face of the torque capsule, the steel quill shaft used to connect the dynamometer to the turbine, and the magnetic pick-up and six-lobe flux cutter used to measure turbine speed. The turbine speed was read from a Hewlett-Packard electronic counter located in the

control room (Figure 22). Speed was regulated by means of a remotely controlled motor on the dynamometer itself, which changes the load capacity of the dynamometer. The remote control unit is shown in Figure 10, and the drive motor is shown in Figure 1.

Lubrication of the turbine bearings was provided by a dry-sump system utilizing a gear-driven oil pump and an upper and a lower oil mist injector for each bearing. The lubricating fluid used was 1010 jet engine oil. The cart containing the pump, oil reservoir, heat exchanger, and system pressure gages is shown in Figure 23, and the lubrication system is shown schematically in Figure 24. For these tests the previously existing system was changed to that shown in Figure 24 to permit measurement of the oil temperature into the bearings and at the point of discharge from both bearings. This was accomplished with iron-constantan thermocouples installed as shown on the schematic.

Figure 24 also shows the iron-constantan thermocouples used to measure the bearing outer race temperatures. Vibration signals from the bearings were detected by a piezo-quartz accelerometer mounted on the upper left bearing cap and monitored on a Panoramic vibration analyzer manufactured by the Singer Metrics Company. The accelerometer is visible in Figure 8, and the analyzer is shown in Figure 22.

The pressures and flow rates were measured in the same manner as for the dummy rotor test previously described. The signals from the thermocouples were initially read from the Brown potentiometer shown in Figure 13. During the latter part of the testing period, however, they were read from a new automatic data acquisition system manufactured by B & F Instruments, Inc. This system is shown in Figure 25.

4.2 Test Procedures

Test runs were conducted at five different axial clearances: 0.081, 0.061, 0.041, 0.024, and 0.015 inches. For each clearance, runs were made at total inlet to static discharge pressure ratios of 1.2, 1.3, 1.4, 1.5, 1.6, and 1.7. At each pressure ratio, turbine speed was varied from the minimum speed (maximum load condition) for that pressure, to the highest speed attainable, in increments of about 1,500 rpm. Maximum speed was restricted to 18,000 rpm for reasons of safety.

Measurement of the torque at zero speed was also made for each pressure ratio at each clearance. This was accomplished by engaging the dynamometer rotor lock and measuring the resulting torque.

As turbine speed was increased during the first run, a point was reached at which the bearings overheated and started to seize, causing a rapid drop in speed. The turbine was dismantled and carefully examined. No apparent damage had been incurred by the ball bearings. The oil system was flushed and refilled, and the unit was reassembled. This condition repeated itself in several subsequent runs, occurring whenever the bearing temperature reached approximately 135°F. Additionally, considerable amounts of oil were being lost from around the shaft and bearing caps at higher speeds. Apparently neither of these conditions had existed in previous tests.

Since the bearings themselves did not appear to be at fault, extensive tests were made to determine whether changing the amount of lubricating oil flow would alleviate these problems. It was found that varying the oil system pressure from 10 pounds per square inch to 50 pounds per square inch would reduce the bearing temperature a maximum of six degrees, but this variation did not significantly reduce leakage. A solution was ultimately found to both problems by carefully positioning

the oil injectors so that they discharged directly into the balls of the bearing and did not strike the race and by slightly enlarging the injector orifices so as to increase the mass flow rate of the oil. The bearing temperatures could then be kept below a maximum of about 125°F at 18,000 rpm, and oil leakage was negligible.

The fact that the bearings experienced a maximum temperature increase of about 50° over the range of speeds tested, whereas in previous tests the increase had been only about half as much (7), created a question as to the applicability of the bearing loss information obtained from the coast-down tests conducted by Vavra (1). It was therefore decided to attempt to evaluate the bearing losses by measuring the oil flow rate and the amount of heat absorbed by the oil as it flowed across the bearings. If the constant pressure specific heat, C_p , of the oil were known, the energy lost in the bearings could be obtained from the relation

$$\text{BFM} = \frac{\dot{W}_{\text{oil}} C_{p\text{oil}} \Delta T_{\text{bearings}}}{\omega} \quad (15)$$

where BFM is the bearing friction moment in foot-pounds and ω is the turbine rotational speed.

Numerous tests were made in order to calibrate the mass flow rate of the oil with the system pressure, and the lubrication system was modified to include the previously discussed thermocouples ahead of and after the bearings. Flow rate calibration was accomplished by weighing the amount of oil discharged by the injectors on each side in a given time interval.

In attempting to evaluate bearing losses by this technique, the results obtained from several test points indicated losses on the order of 20 per cent of the minimum losses predicted by Vavra (1). In fact, it was discovered that the exposure of the inlet lines, the bearing block itself, and the sumps to the cold discharge air sometimes produced cooler

temperatures on the discharge side of the bearings than existed ahead of the injectors. Since insulation of the oil lines and the bearing blocks to the extent necessary to overcome this deficit was not feasible, this attempt to determine the bearing losses was abandoned. The oil temperatures were recorded as data for future use, however, and appear in Appendix B.

The dynamometer torque capsule was calibrated both before and after each day's runs in order to permit consideration of any variations during the course of the runs. Calibration was accomplished by use of the device shown in Figure 26. An aluminum plug was fabricated to fit into the torque ring of the capsule. Torque was applied by loading the weight pans on the moment arm, which was attached to the plug. Riley (3) attached the moment arm directly to the inlet side of the dynamometer; thus, a moment was introduced due to the axial distance between the capsule and the point of application of the load. The apparatus used in these tests reduced this potential source of error almost entirely.

Loads of 0 to 400 inch-pounds were applied to the capsule in 100 inch-pound increments. The span of the digital readout was set at 0 to 1000 counts, the latter approximately corresponding to 400 inch-pounds. Calibration readings were taken for both increasing and decreasing loads in order to evaluate the amount of hysteresis present in the readout. As each load was applied, the capsule housing was tapped gently with a mallet to overcome any drag in the capsule itself and to eliminate errors caused by lag in the servomechanism of the digital counter. This procedure is valid, because a like amount of vibration was observed to exist under the dynamic load conditions of an actual test run. Using this technique, the amount of hysteresis present between the loading and unloading cycles was found to be negligible.

The torque readouts for calibrations performed both before and after the test runs were found to vary linearly with applied torque. However, the data obtained after the run were generally higher, by 2 to 3 counts at zero load, to 13 to 15 counts at 400 inch-pounds, than the original calibration. This was felt to be due to the thermal effects of the higher capsule temperatures which existed during the run. A thermocouple was installed in the capsule in an attempt to establish some correlation between this temperature rise and the torque count increase. Tests in which the capsule was heated from the outside with a strip heater were inconclusive, because similar increase in torque counts for given torque loadings could not be produced, even though the temperatures indicated by the thermocouple were considerably higher than those recorded during the actual test runs.

When the turbine is in operation, the capsule is heated from within by heat from the dynamometer bearings. This is modified by the dynamometer water cooling system and by the cold turbine discharge air. A method of reproducing the interaction of all of these conditions in static calibration tests was not found, and so the torque calibration data ultimately used represented an average of the data obtained before and after the test runs. This accounts for some increase due to thermal effects and is felt to be a reasonable representation. In some instances, the capsule temperature was observed to increase immediately following shut-down, while at other times the reverse effect occurred. It is felt that more representative temperature data could be obtained by relocating the thermocouple on the flexure closer to the strain gages.

The compressor which provides house air failed after two clearances, 0.081 and 0.061 inches, had been tested. This compressor provides air to the speed controls of the Allis-Chalmers compressor and also provides the

air which is used as a reference pressure for the water manometer board. The remaining three clearances were tested using a smaller auxiliary compressor, which introduced considerable fluctuations into the house air system.

4.3 Theoretical Analysis

The known quantities necessary for the turbine analysis as performed in this project are: mass flow rate; total inlet temperature and pressure; static inlet pressure; turbine speed and torque output; atmospheric pressure and temperature; and the absolute rotor inlet flow angle and velocity coefficient based on the results of the scroll and guide vane analysis.

The working fluid is assumed to undergo an adiabatic process, since the quantity of heat passing through the casing is negligible compared to the enthalpy change undergone by the fluid as it passes through the turbine. It is additionally assumed that the fluid behaves as a perfect gas.

The flow is assumed to have axisymmetric stream surfaces; thus, in effect, the analysis is one-dimensional, based on the determination of the flow properties along a particular streamline lying on a chosen surface of revolution. Vavra (8) states that the major portion of the rotor losses is due to secondary flow phenomena, tip leakage losses, and the loss that occurs because of the motion of the blade tips in the wall boundary layers. Thus it would appear that the majority of the losses occur near the shrouds, and the representative streamline was accordingly chosen as that existing at the outer radius of the rotor discharge. It was felt that this approach would yield a better correlation of results than that obtained from use of a calculated mass-averaged mean radius at the rotor discharge (7).

It is assumed that the relative flow angle β_{20} , calculated from the blade dimensions, is very nearly equal to the actual relative flow angle at the outer discharge radius (where β_{20} assumes its maximum value). This implies that the so-called slip factor may be neglected. Verification of the validity of this assumption is given by the flow surveys taken at the rotor discharge by Riley (3). Accordingly, β_{20} was calculated from Equation A2(4) of (1) and found to be equal to -69.85 degrees at the outer radius. This value was used in all calculations.

The thermodynamic process of a fluid passing through a turbine is given in Figure 14. The resulting flow velocities are shown in Figure 15. The derivations which follow are based on these two diagrams.

Referring to Figure 14, for a reversible, adiabatic process,

$$\frac{T_2''}{T_{t0}} = \left(\frac{P_2}{P_{t0}} \right)^{\frac{\gamma-1}{\gamma}} \quad (16)$$

where T_2'' represents the static temperature at the rotor discharge for an isentropic expansion through the turbine to P_2 . The isentropic temperature drop which would occur for such an expansion is

$$\Delta T_{is} \equiv T_{t0} - T_2'' \quad (17)$$

and may therefore be expressed as

$$\Delta T_{is} = T_{t0} \left[1 - \left(P_2 / P_{t0} \right)^{\frac{\gamma-1}{\gamma}} \right] \quad (18)$$

Similarly, for an isentropic expansion across the inlet guide vanes

$$\frac{T_1'}{T_{t0}} = \left(\frac{P_1}{P_{t0}} \right)^{\frac{\gamma-1}{\gamma}} \quad (19)$$

and

$$(\Delta T_{is})_{\text{guide vanes}} \equiv T_{t0} - T_1' = T_{t0} \left[1 - \left(P_1 / P_{t0} \right)^{\frac{\gamma-1}{\gamma}} \right] \quad (20)$$

The isentropic, or theoretical degree of reaction, r , represents that portion of the overall isentropic enthalpy drop which occurs in the rotor, or

$$r \equiv \frac{T_1' - T_2''}{\Delta T_{is}} \quad (21)$$

Therefore,

$$r = 1 - \frac{(\Delta T_{is})_{\text{guide vanes}}}{\Delta T_{is}} \quad (22)$$

and, from Equations (18) and (20),

$$r = 1 - \frac{\left[1 - (P_1/P_{t0})^{\frac{\gamma-1}{\gamma}} \right]}{\left[1 - (P_2/P_{t0})^{\frac{\gamma-1}{\gamma}} \right]} \quad (23)$$

The total-to-static efficiency of the turbine is defined as the ratio of the work actually produced by the turbine to that work which could ideally be accomplished by isentropic expansion from total inlet to static outlet conditions. For this case, the efficiency may be expressed by the ratio of the corresponding temperature drops,

$$\eta = \Delta T_w / \Delta T_{is} \quad (24)$$

The change in total enthalpy across the turbine is

$$\Delta H_w = c_p \Delta T_w = \frac{M \omega}{J \dot{W}} \quad (25)$$

where M is the net torque produced, ω is the rotational speed, and \dot{W} is the mass flow rate. Therefore, ΔT_w may be expressed as:

$$\Delta T_w = \frac{M \omega}{J c_p \dot{W}} \quad (26)$$

The efficiency given by Equation (24) was computed both for the case where bearing friction was considered and for the case where it was not. Bearing friction was calculated based on the results of coast-down

tests performed by Vavra (1). The friction horsepower is expressed by

$$HP_f = -0.6 + (N/1000)(.17143) \quad (27)$$

for $N \leq 10,500$ rpm, and by

$$HP_f = -0.6 + (N/1000)(.17143) - (4.898 \times 10^{-3})(N/1000 - 10.5)^2 \quad (28)$$

for $N > 10,500$ rpm. The bearing friction moment is then given by

$$M_f = \frac{HP_f \times 550}{\omega} \quad (29)$$

The net moment is then the sum of T , the moment measured by the dynamometer, and the bearing friction moment:

$$M = T + M_f \quad (30)$$

The velocity C_o corresponding to the isentropic enthalpy drop through the turbine is given by the expression

$$C_o^2 \equiv 2gJc_p \Delta T_{is} \quad (31)$$

and the peripheral speed of the rotor at the rotor inlet is

$$U_1 = \frac{\pi N D_1}{720} \quad (32)$$

where D_1 is the rotor inlet diameter in inches. By Equations (31) and (32), the isentropic head coefficient is given by

$$K_{is} \equiv (C_o / U_1)^2 \quad (33)$$

The absolute velocity V_1 is expressed by Equation (4). An alternate expression, obtained by substitution of Equation (23) into Equation (4), is

$$V_1 = \phi \sqrt{2gJc_p (1-r) \Delta T_{is}} \quad (34)$$

The temperature T_1 may then be obtained from

$$T_1 = T_{to} - \frac{V_1^2}{2gJc_p} \quad (35)$$

and M_1 , the Mach number at the rotor inlet, is

$$M_1 = \frac{V_1}{\sqrt{2gJc_p T_1}} \quad (36)$$

The results of the dummy rotor tests can now be used by introducing Equation (14) to obtain ϕ by an iterative procedure which is discussed in Appendix B. Equation (12) gives the nozzle loss coefficient as

$$\zeta_N = 1 - \phi^2 \quad (37)$$

Values for α_1 can now be taken from Equation (13) to determine the peripheral and meridional velocity components of V_1 .

$$V_{u1} = V_1 \sin \alpha_1 \quad (38)$$

$$V_{m1} = V_1 \cos \alpha_1 \quad (39)$$

From Figure 15 it is apparent that the peripheral component of the relative rotor inlet velocity W_1 is

$$W_{u1} = V_{u1} - U_1 \quad (40)$$

and W_1 is then found from

$$W_1 = \sqrt{V_{m1}^2 + W_{u1}^2} \quad (41)$$

The relative inlet flow angle β_1 is

$$\beta_1 = \sin^{-1} (W_{u1} / W_1) \quad (42)$$

At this point all conditions at the entrance to the rotor are known.

It is assumed that only the kinetic energy $V_{m1}^2 / 2gJC_p$ is useful in the rotor (since it has radial blades), and that the incidence loss at the rotor inlet is taken as $W_{u1}^2 / 2gJC_p$ (8). Thus, the effective relative velocity head is reduced, and static conditions at the rotor inlet are really those at T_1^* on Figure 14.

The equivalent state point E shown on Figure 14 is established from the energy equation for a rotating system in the following manner (6):

$$H_R = \text{constant} = h_1 + \frac{W_1^2}{2gJ} - \frac{\omega^2 R_1^2}{2gJ} = h_2 + \frac{W_2^2}{2gJ} - \frac{\omega^2 R_2^2}{2gJ} \quad (43)$$

where H_R is the relative total enthalpy. This equation may be rearranged in the form

$$H_E \equiv h_1 + \frac{W_1^2}{2gJ} - \left(\frac{U_1^2 - U_2^2}{2gJ} \right) = h_2 + \frac{W_2^2}{2gJ} \quad (44)$$

where the left side is equal to H_E , the total enthalpy at the state point E. Equation (44) clearly shows that state point E is the proper reference point from which to view the expansion process through the rotor in an analogous manner to that of the stator. The peripheral speed at the outer discharge radius, U_{20} , is given by Equation (32) with D_1 replaced by D_{20} , the outer diameter of the rotor discharge.

The work output of the turbine, represented by the change in total enthalpy, may be represented by Euler's turbine equation (6):

$$\Delta H_W = C_p \Delta T_W = \frac{U_1 V_{u1} - U_{20} V_{u20}}{gJ} \quad (45)$$

where U_{20} and V_{U20} occur at the outer discharge radius. Manipulating this equation and Equations (24) and (31), an expression for the peripheral component of the absolute discharge velocity, V_{U20} , is

$$\frac{V_{u20}}{U_1} = \frac{R_1}{R_{20}} \left[\frac{V_{u1}}{U_1} - \frac{\eta}{2} \left(\frac{C_o}{U_1} \right)^2 \right] \quad (46)$$

Using the velocity diagram of Figure 15, it can be shown that the relative velocity at the outer discharge radius, W_{20} , may be expressed by

$$\frac{W_{20}}{U_1} = \frac{(V_{u20}/U_1) - (R_{20}/R_1)}{\sin \beta_{20}} \quad (47)$$

where, in keeping with the stated assumptions,

$$\beta_{20} = -69.85^\circ \quad (48)$$

If the divergence of the pressure lines on the entropy diagram of Figure 14, in the direction of increasing entropy, is neglected, there is

$$T_1^* - T_2' = T_1' - T_2'' \quad (49)$$

By Equations (21) and (31), the right side of the expression is equivalent to

$$T_1' - T_2'' = r \frac{C_o^2}{2gJc_p} \quad (50)$$

From Figure 14, the left side may be expressed in terms of the velocities:

$$T_1^* - T_2' = \frac{W_{20th}^2}{2gJc_p} + \frac{U_1^2 - U_{20}^2}{2gJc_p} - \frac{V_{m1}^2}{2gJc_p} \quad (51)$$

Manipulation of Equations (50), (51), and (32) yields a relation for W_{20th} , the theoretical relative velocity at the rotor discharge:

$$\frac{W_{20th}}{U_1} = \left[\frac{r}{(U_1/C_o)^2} + \left(\frac{R_{20}}{R_1} \right)^2 + \left(\frac{V_{m1}}{U_1} \right)^2 - 1 \right] \quad (52)$$

Using Equations (47) and (52) it is now possible to define a velocity coefficient Ψ for the rotor, which is analogous to the velocity coefficient ϕ for the scroll and guide vanes given by Equation (2).

$$\Psi \equiv W_{20} / W_{20th} \quad (53)$$

The rotor loss coefficient, which is a measure of the kinetic energy loss through the rotor, is, then

$$\phi_R \equiv 1 - \Psi^2 \quad (54)$$

The meridional velocity component of the absolute discharge velocity can be expressed by

$$V_{m20} = W_{20} \cos \beta_{20} \quad (55)$$

from Figure 15. The absolute discharge flow angle is then

$$\alpha_{20} = \tan^{-1} (V_{u20} / V_{m20}) \quad (56)$$

If consideration is given to the case where bearing losses are assumed to exist, the resulting efficiency will obviously be different from that for no bearing losses. Examination of the foregoing analysis shows that, correspondingly, different values for V_{u20} , V_{m20} , W_{20} , Ψ and ϕ_R will result.

Thus, from the measured items of test data specified at the beginning of this section, the following performance parameters are obtained by the analysis technique: flow rate, head coefficient, degree of reaction, absolute and relative rotor inlet flow angles, velocity and loss coefficients for the scroll and guide vanes, the net torque produced, the absolute discharge flow angle, the rotor velocity and loss coefficients, and the total-to-static efficiency.

In this experiment the above parameters are referred to standard air in accordance with the NASA method, as described in (1). This method utilizes a total inlet pressure of 14.7 pounds per square inch absolute, a total inlet temperature of 518.7 degrees Rankine, a specific heat ratio of 1.4, and a constant pressure specific heat of 0.24 BTU per pound mass-degree Fahrenheit. The referral parameters are

$$\delta \equiv P_{t0} / 14.7 \quad (57)$$

$$\theta \equiv T_{t0} / 518.7 \quad (58)$$

and

$$\epsilon = \frac{0.810}{\gamma} \left(\frac{\gamma+1}{2} \right)^{\frac{\gamma+1}{2(\gamma-1)}} \quad (59)$$

The factor ϵ , which corrects the flow rate through the turbine for varying values of γ , is that given by Vavra (1) and is supposed to give a better correlation than the expression for ϵ used by NASA.

The referred speed is then given by

$$N_{ref.} \equiv N / \sqrt{\theta} \quad (60)$$

The referred flow rate is

$$\dot{W}_{ref.} \equiv \dot{W} \left(\sqrt{\theta} \frac{\epsilon}{\delta} \right) \quad (61)$$

Finally,, the referred moment is

$$M_{ref} \equiv M \left(\frac{\epsilon}{\delta} \right) \quad (62)$$

4.4 Data Reduction: Programs RADIAL and NOSP

The computer program RADIAL, listed in Appendix B, determines the turbine performance parameters described in Section 4.3 from the test data. In general, the specific techniques used by the computer in these computations are apparent from the program itself. However, Appendix B describes each subroutine briefly and elaborates on specific computational procedures which are not immediately obvious.

Program NOSP, listed in Appendix C, was written to compute the desired performance parameters from the locked rotor test data.

4.5 Discussion of Results

The input data and results of program RADIAL are listed in Tables B4 through B13, with input and output for a given clearance appearing in adjacent tables. The input data and results of program NOSP appear in Table C2.

Figure 27 shows the degree of reaction, r , as a function of head coefficient, k_{is} , for the clearances tested in this analysis as well as those of Riley (3) and Vavra (1). For each clearance, the degree of reaction was found to be a unique function of head coefficient, independent of turbine pressure ratio. This is in agreement with the findings of both Riley and Vavra. Riley further concluded that the degree of reaction is independent of axial clearance. The results of the present tests verify this for all clearances except for 0.081 inch. At this clearance, the values of r obtained were found to be approximately 1 to 1.5 per cent lower than those for the other clearances. This is shown on Figure 27, where the resulting curves for all clearances except 0.081 inch are represented by that for 0.061 inch, and the curve for 0.081 inch is plotted separately. This discrepancy implies that, for a given overall pressure

ratio, the pressure p_1 can no longer be maintained at a clearance of 0.081 inch.

It may be seen from the representative curve of Figure 27 that r decreases with increasing k_{is} (decreasing speed), from a value of approximately 0.75 at a k_{is} of 1.05 to 0.30 at a k_{is} of 6. This drop occurs because, with decreasing speed, a smaller pressure drop is required to pass the flow through the rotor.

The degree of reaction curves obtained in earlier tests by Vavra (1) and Riley (3) are superimposed on the curve of Figure 27. Vavra states that the value of r at design k_{is} of 2.3 should be approximately 0.486, as compared with the value of 0.395 obtained by him and with Riley's value of 0.402. The current tests yielded a value of 0.440 at design k_{is} , except for a clearance of 0.081 inch, for which the corresponding value of r was 0.434. This apparent increase in degree of reaction is due primarily to a more accurate determination of p_1 than was used by either Vavra or Riley. Boshoven (4) relocated the shroud pressure taps, which measure the pressure p_1 , to a position axially outward in the annulus around the periphery of the shroud. This was done to reduce the effects of local perturbations on the pressure readings and greatly improved the uniformity of the pressure distribution around the shrouds. This improvement in the accuracy of p_1 yields a more accurate value of r since degree of reaction is directly dependent on p_1 .

The degree of reaction remains lower than the design value because the guide vane exit area is too small to permit discharge of the design mass flow (1).

Significant plots resulting from the overall turbine efficiency calculations are given in Figures 28 through 31. Figure 28 depicts turbine efficiency as a function of referred speed for the case of no bearing

losses and a clearance of 0.081 inch. Figure 29 is a corresponding plot of efficiency versus head coefficient. Figures 30 and 31 represent these same respective parameters, also at a clearance of 0.081 inch, for the case where bearing losses are considered.

Efficiency was found to be essentially independent of clearance over the range of clearances tested. Figures 28 through 31 are therefore representative of the results for all clearances between 0.015 and 0.081 inch.

Values of turbine efficiency were obtained from measurements of the torque at the turbine shaft made with the air dynamometer and from the bearing loss values as determined from the results of coast-down tests conducted by Vavra (1). Because of the previously discussed problem of excessive bearing temperatures and seizing experienced during these tests, the bearing losses are probably greater than the maximum losses determined by Vavra. However, since time did not permit a repetition of the coast-down tests, Vavra's equations for maximum bearing losses [Equations (27) and (28)] were used.

A comparison of Figures 28 and 29 and of Figures 30 and 31 shows the advantage derived from representing efficiency as a function of head coefficient instead of referred speed. Use of the head coefficient effectively reduces a family of curves to a single curve. However, if the bearing losses are ignored, as in Figure 29, the resulting plot depends significantly on pressure ratio. In this figure only those curves representing the pressure ratios for maximum and minimum efficiencies are shown to avoid clutter.

Figure 31 shows that the efficiencies are nearly independent of pressure ratio in the case where allowance is made for bearing losses. If these bearing losses were accurately known, it would appear that the influence of pressure ratio would be completely eliminated from a plot of efficiency versus head coefficient.

In general, if bearing losses are not considered, a pressure ratio of 1.7 yields a maximum efficiency of 81.1 per cent at a k_{is} of 2.35 and an axial clearance of 0.015 inch. Minimum efficiencies are obtained for a pressure ratio of 1.2 and are in most cases 10 to 12 per cent lower than maximum efficiencies in the vicinity of the design k_{is} of 2.3. Vavra (1) reported a maximum efficiency of 81 per cent for the case of no bearing losses at a pressure ratio of 1.616, k_{is} of 2.37, and clearance of 0.062 inch. Riley (3) obtained a corresponding maximum efficiency of 82.52 per cent at a k_{is} of 2.26, pressure ratio of 1.678, and clearance of 0.027 inch.

For the case where bearing losses are taken into account, the maximum efficiency, η_L , was found to be 84.6 per cent at a pressure ratio of 1.7, head coefficient of 2.28, and clearance of 0.081 inch. This compares favorably with the design efficiency of 85.5 per cent at a pressure ratio of 1.7 and head coefficient of 2.3, as given by Vavra (1). Riley (3) obtained a maximum efficiency of 86.04 per cent at a pressure ratio of 1.678, head coefficient of 2.259, and clearance of 0.027 inch, based on the maximum values of bearing losses.

At minimum speed (maximum k_{is}) for a given pressure ratio and clearance, the efficiency in general is about 65 per cent. As speed is increased (k_{is} decreased), the efficiency increases to a maximum of about 84 per cent in the vicinity of a k_{is} of 2.3 and then falls off rapidly to 30 to 40 per cent at a k_{is} of about 1.05. Initially, then, the efficiency increases with speed because, by Equation (26), an increase in ω and decrease in \dot{W} offset the decrease in torque, resulting in increased turbine work and efficiency. As speed is further increased, the decreasing torque begins to predominate, causing the efficiency curve to peak and then rapidly decrease.

It was expected that, as the clearance was varied over the range encompassed by these tests, a "critical" clearance would be reached beyond which turbine efficiency would deteriorate rapidly. Riley (3) observed this to occur at a clearance of 0.052 inch. Such an occurrence was not observed in these tests over the range of clearances from 0.015 to 0.081 inch. Thus, it appears that axial clearance has no appreciable effect on turbine efficiency over this range of clearances.

It has been previously stated that Riley (3) was in all likelihood operating at a considerably greater clearance than he believed himself to be. This is substantiated to a degree by the fact that Vavra (1) did not experience this efficiency drop at a clearance of 0.062 inch. Since gaps also existed between the rotor and shrouds during Riley's tests, the blades would have left the wall boundary layer at a lesser axial clearance than in these tests where the blade and shroud contours were matched. Thus, it is reasonable to assume that the critical clearance is at some value greater than 0.081 inch.

That such a drop in efficiency should occur as clearance is increased to some critical value is explained in part by Csanady (9). The rotating blades "scrape up" the shroud boundary layer and produce vortices in the vicinity of the tips of the blades which, in turbines, tend to nullify the tip vortices themselves. At a particular tip clearance, then, these two vortices would neutralize each other, leaving only the passage vortex which causes secondary flow losses. This neutralization should produce a pronounced increase in efficiency at that clearance at which it occurs. For the subject turbine, it would appear that if this condition does exist, it occurs at a clearance less than 0.015 inch.

The efficiency is essentially independent of clearance because, although the tip vortices become more predominant as clearance increases,

there is also a buildup of the boundary layer. This buildup maintains a reasonably even relative balance between the tip vortices and the "scraped up" vortices. As clearance is extended beyond some critical value, however, the blades begin to operate near the edge of the wall boundary layer, and the countering vortices quickly cease to be effective in neutralizing the increasing tip vortices. The result is a pronounced increase in rotor loss and a corresponding decrease in turbine efficiency. It is also worthy of note that, for the test turbine, although the axial tip clearance is increased, the radial clearance between the shrouds and the rotor blades in the vicinity of the discharge remains essentially unchanged.

The rotor velocity coefficient, Ψ , is plotted as a function of the head coefficient in Figure 32, for the case where bearing losses are neglected. The clearance represented is 0.024 inch. Figures 33 through 37 show the curves of Ψ_L versus k_{is} , with bearing losses considered, for each of the five clearances tested. Again, it may be seen that if bearing losses are ignored, there is considerably more variation of the curves with pressure ratio than in the case where bearing losses are considered.

The only variation in rotor velocity coefficient with axial clearance which can be established is that values of Ψ for a clearance of 0.081 inch seem to be generally higher than for all other clearances. This variation is evident for both bearing loss cases, with values of Ψ_L being generally 10 to 15 per cent higher at a clearance of 0.081 inch. Because of the negligible effect of axial clearance and the doubtful significance of the case where bearing losses are neglected, Figure 32, for a clearance of 0.024 inch, is the only curve included for the case where bearing losses are not considered.

Figures 33 through 37 show that maximum values of ψ_L do not always occur at the higher pressure ratios, although ψ_L is more nearly constant over the range of k_{is} values for the higher pressure ratios.

At the design k_{is} of 2.3, a value for ψ_L of 0.960 was produced at a pressure ratio of 1.2 and clearance of 0.081 inch. The maximum value of ψ_L was found to occur at the same pressure ratio and clearance and at a k_{is} of 3.35. Its value is 0.990.

It can be seen from the curves for ψ_L given in Figures 33 through 37 that ψ_L remains relatively constant over a range of k_{is} between about 2.3 and the maximum value. As k_{is} is decreased below 2.3, ψ_L first decreases, with a minimum occurring at a k_{is} of 1.7 to 1.9. It then increases to a peak at a k_{is} of about 1.5, and falls off sharply as the head coefficient is further decreased. Examination of the tabulated performance data in Appendix B shows that the relative rotor inlet flow angle β_1 is positive at values of k_{is} greater than about 2.3, so that the relative flow strikes the pressure side of the blades. This produces the accompanying incidence losses, and further losses occur as the flow is turned through a relatively large angle to follow the flow channel.

As U_1 is increased (k_{is} decreased), β_1 becomes negative, so that impingement of the flow on the blades acts opposite to the direction of rotation. The incidence losses are not significantly changed; however, the flow must now be turned by a considerably smaller amount in order to follow the flow channel. Thus, the resultant sum of these three losses appears to be less, and an increase in ψ_L occurs at a k_{is} of about 1.5. Below this point, as β_1 becomes increasingly negative, the relative flow becomes almost perpendicular to the blades. Thus, the advantage is lost, and the rotor efficiency deteriorates rapidly.

A plot of referred moment with bearing losses included, as a function of referred speed, is shown in Figure 38 for data obtained at a clearance of 0.081 inch. The values of the torque at zero speed resulting from the locked rotor tests are also shown. The effects of clearance on this parameter were also found to be negligible over the range of clearances from 0.015 to 0.081 inch, there being only slight random variations present in the resulting data. Therefore, Figure 38 is a representative plot for all clearances.

As expected, the maximum moment of about 16.1 foot-pounds was found to occur at zero speed and at a pressure ratio of 1.7. For the maximum speed of about 18,000 rpm, this pressure ratio yielded 6.3 foot-pounds for zero bearing losses and 6.8 foot-pounds for maximum bearing losses. The lowest pressure ratio, 1.2, consistently yielded the lowest values of moment. The moment curves of Vavra (1) and Riley (3) are almost identical to those obtained in these tests, except for the results obtained by Riley beyond the "critical" clearance.

In general, the torque produced by the flow energy at a given pressure ratio is a maximum at zero speed and decreases with increasing turbine speed. This may be explained by the law of angular momentum, which, by reference to the velocity diagram of Figure 15, can be written as

$$M = \dot{W} R_{20} \left[\left(\frac{R_1}{R_{20}} \right) V_{u1} - V_{u2} \right] \quad (63)$$

For a given pressure ratio, V_{u1} is nearly constant with speed, and the mass flow rate \dot{W} decreases with increasing speed. From Figure 15, V_{u2} also increases with speed. Thus, it is seen that the torque produced, M , decreases with increasing turbine speed.

After completion of the test runs previously described, an informal trial run was made at a clearance of 0.100 inch in an attempt to determine the critical clearance. Although not conclusive, the results indicated no significant change in the values of the performance parameters. This implies that a reasonable overall efficiency may be maintained at clearances which might considerably exceed those tested in this analysis. Since these additional tests were not complete, the resulting data are not included in this report.

SECTION 5

CONCLUSIONS AND RECOMMENDATIONS

At a pressure ratio of 1.7, a clearance of 0.081 inch, and a head coefficient of 2.28, a maximum total-to-static overall efficiency of 84.6 per cent was obtained for the case where bearing losses were considered. The efficiency, referred moment, and degree of reaction were found to be independent of clearance over the range of clearances between 0.015 and 0.081 inch. A clearance tolerance of this sort is very important in small turbines and in turbines where thermal expansion must be considered. It is recommended that additional testing be performed in order to determine the precise clearance beyond which turbine performance deteriorates. Tests might also be conducted in which the clearance at the rotor discharge is varied in addition to the tip clearance, although this would require cutting the shrouds or the manufacture of additional shrouds with various annular openings.

The results of this investigation show that computations based on flow conditions at the outer discharge radius are simpler and more straightforward than those obtained by referring the losses to a calculated mass-average radius, and that this simplicity does not compromise the quality of the results. On the contrary, a correlation of the rotor velocity coefficient is obtained by this method, whereas previous efforts to obtain meaningful loss parameters were not successful (7).

There is strong evidence that the bearing loss data used in this investigation are no longer applicable. Correct data should be obtained either through new coast-down tests or through some implementation of the lubricating oil temperature differential across the bearings, as previously described. The latter method would be highly preferable since it

would provide accurate loss information on a current basis and would correctly reflect any change in the mechanical condition of the bearings. Successful implementation of such a method would probably be contingent on a complete redesigning of the test rig, so that the oil lines are routed outside of the discharge flow as much as possible and are thoroughly insulated.

Since any inaccuracies in torque measurement introduce considerable error into the calculations as performed herein, additional effort is required in order to determine how to properly compensate the torque capsule output for thermal effects. An alternative solution would be to utilize a force (reluctance) capsule and a moment arm arrangement. This capsule could be remotely located and shielded so as to be free of the effects of the dynamometer bearing heat and the cold turbine discharge air.

It is recommended that the modifications described by Vavra (1) be performed in order to improve the component matching of the turbine and that further tests be carried out in order to determine the effects of these modifications on the performance parameters. Specifically, the enlarging of the guide vane discharge area or the reduction of the rotor discharge area would ultimately increase the relative rotor discharge velocity W_2 , which would reduce the peripheral velocity V_{u2} . Greater turbine work, and thus higher efficiencies, should result.

It is felt that the turbine test rig is now in much better operating condition than for any previous tests. The instrumentation has been proven; and, for the first time, the axial clearances may be accurately set. Accordingly, further testing to verify and expand on the performance parameters obtained in this investigation is recommended.

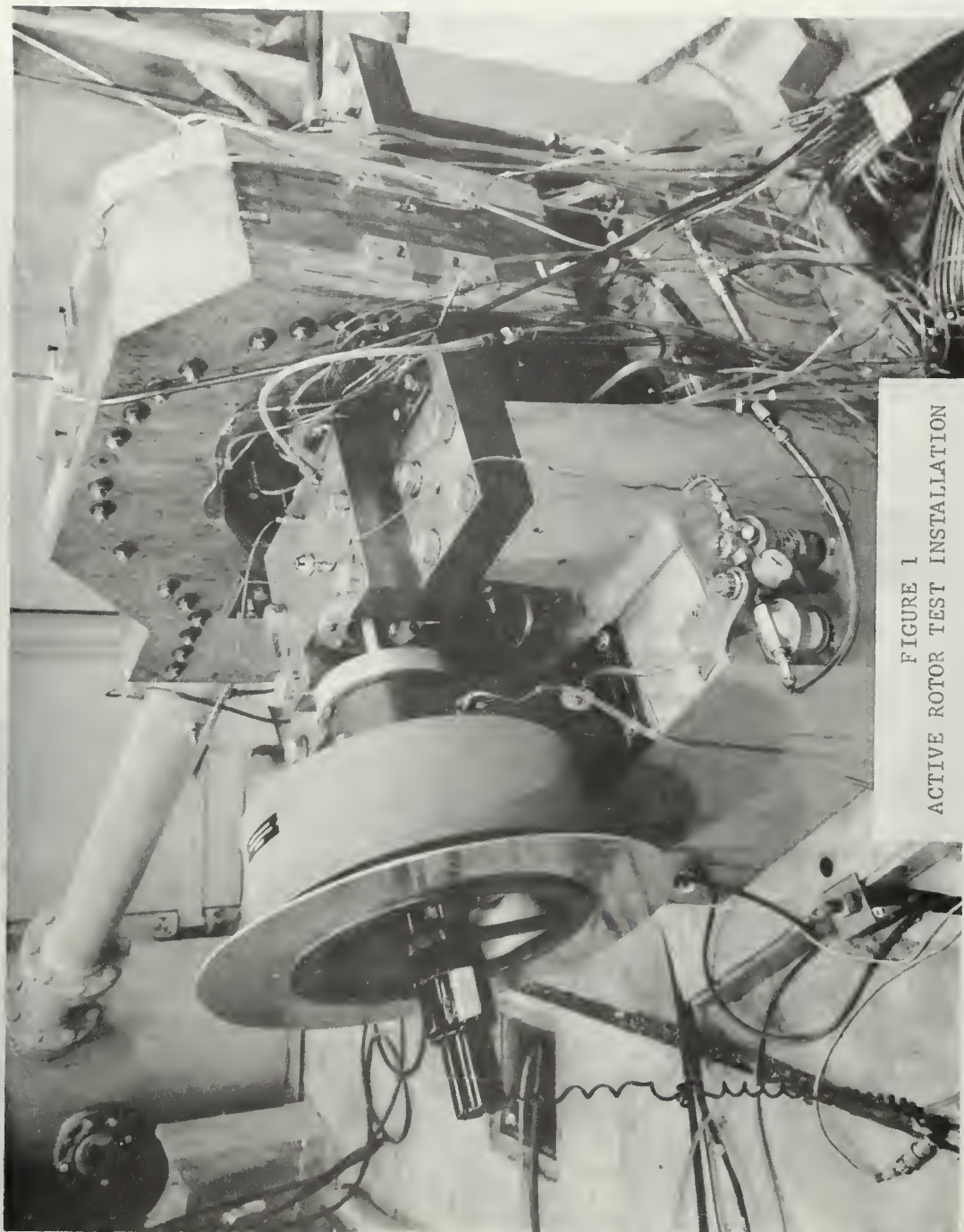


FIGURE 1
ACTIVE ROTOR TEST INSTALLATION

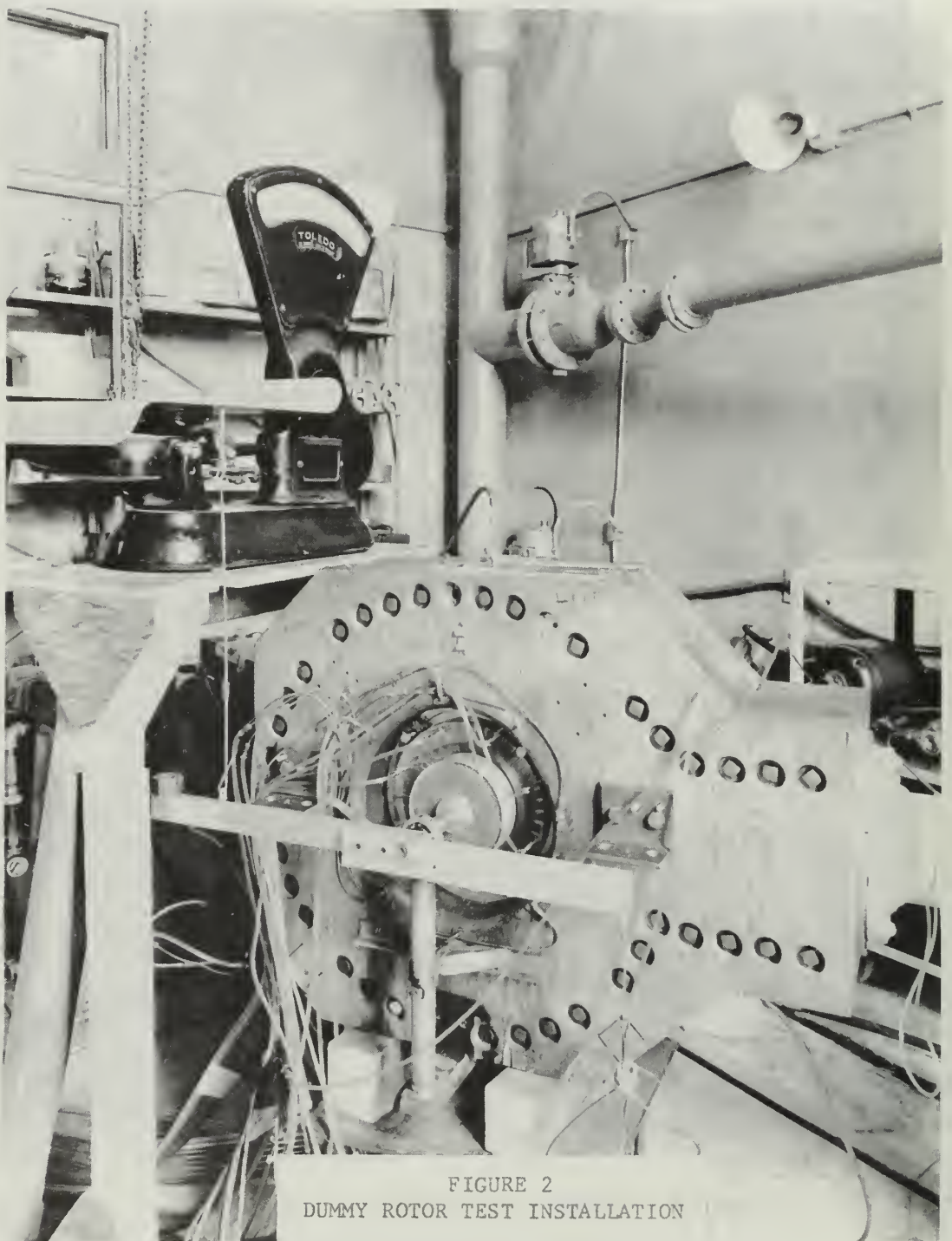


FIGURE 2
DUMMY ROTOR TEST INSTALLATION



FIGURE 3
WOODEN SCROLL INSERT

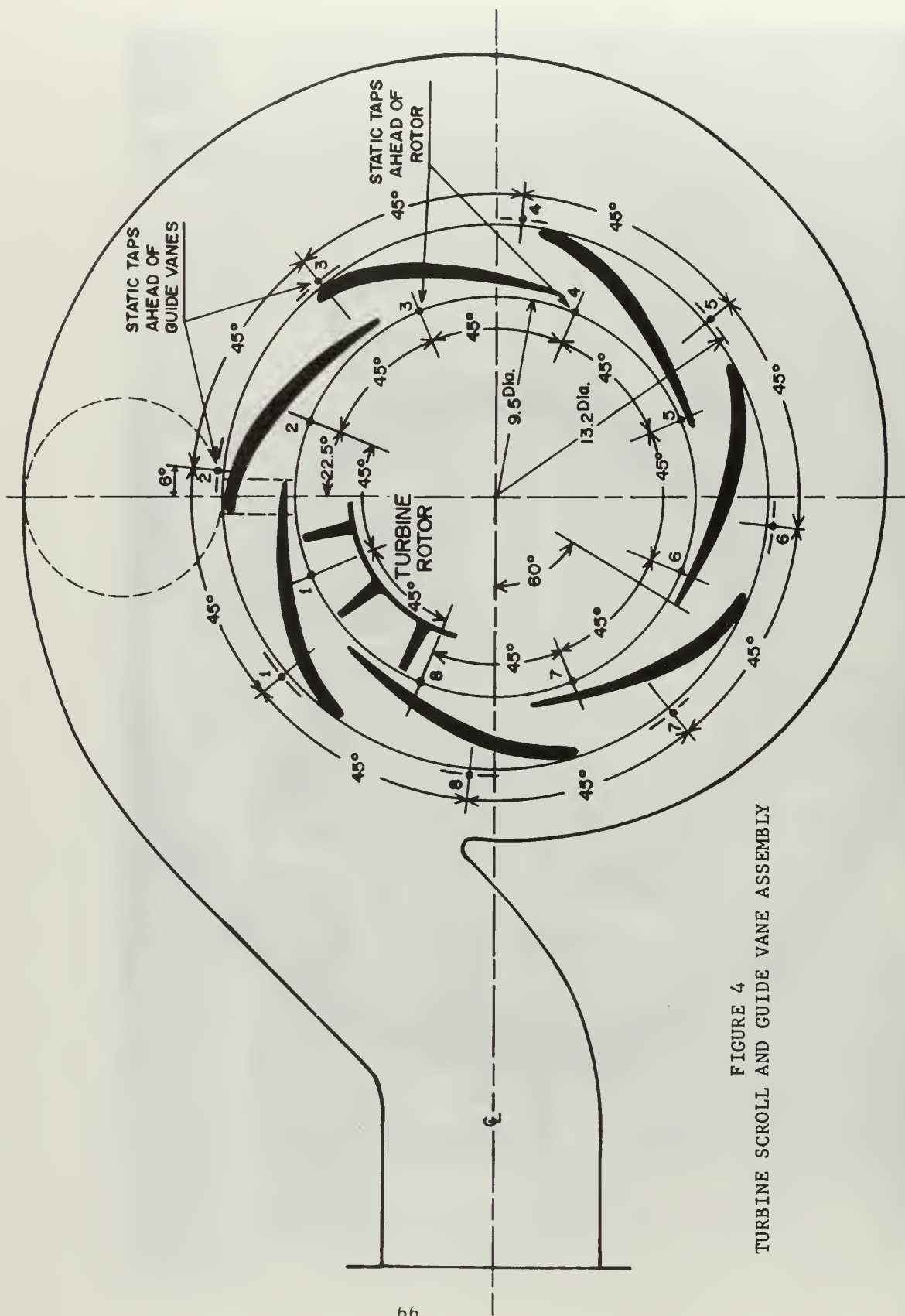


FIGURE 4
 TURBINE SCROLL AND GUIDE VANE ASSEMBLY

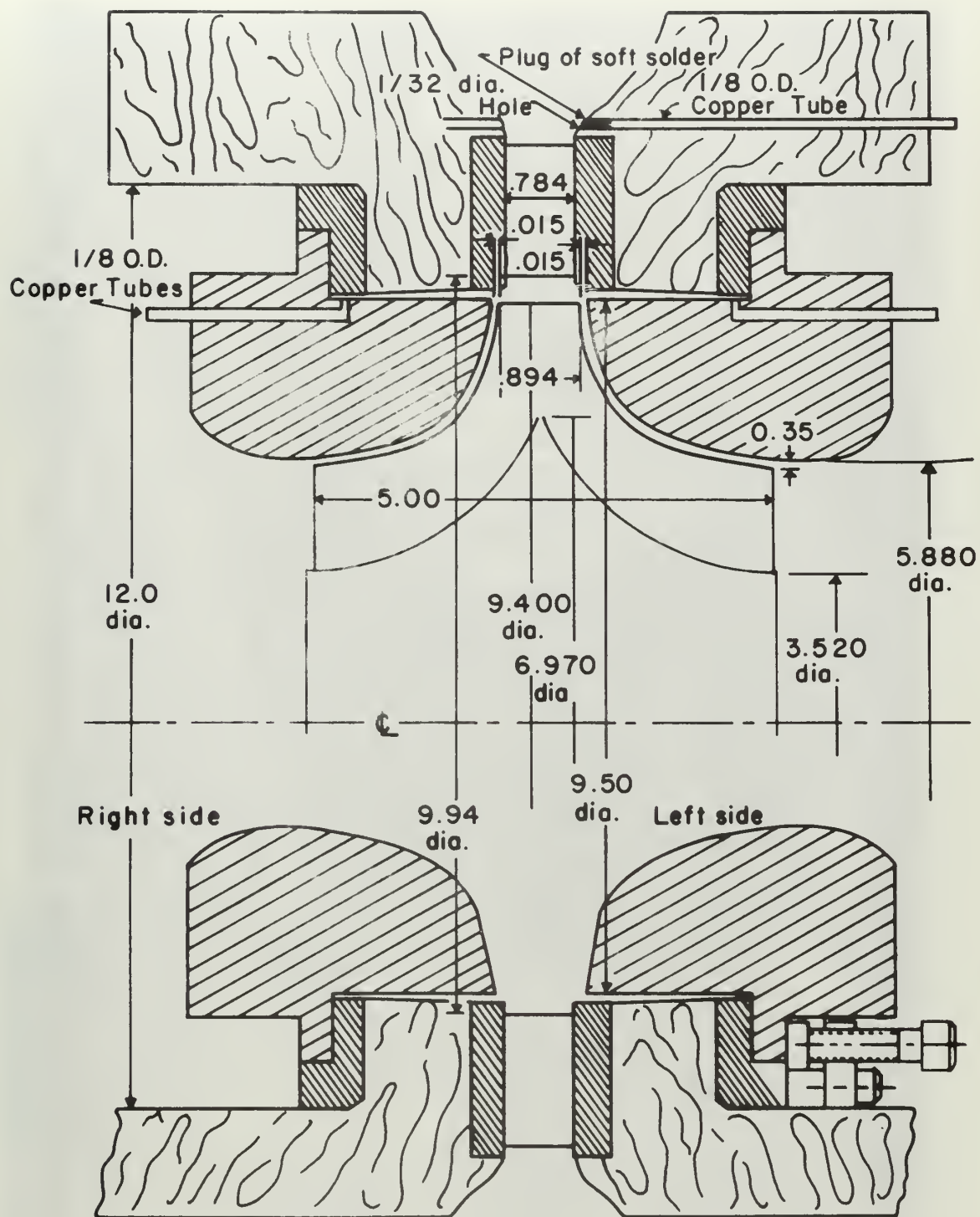


FIGURE 5
CROSS-SECTION OF TURBINE

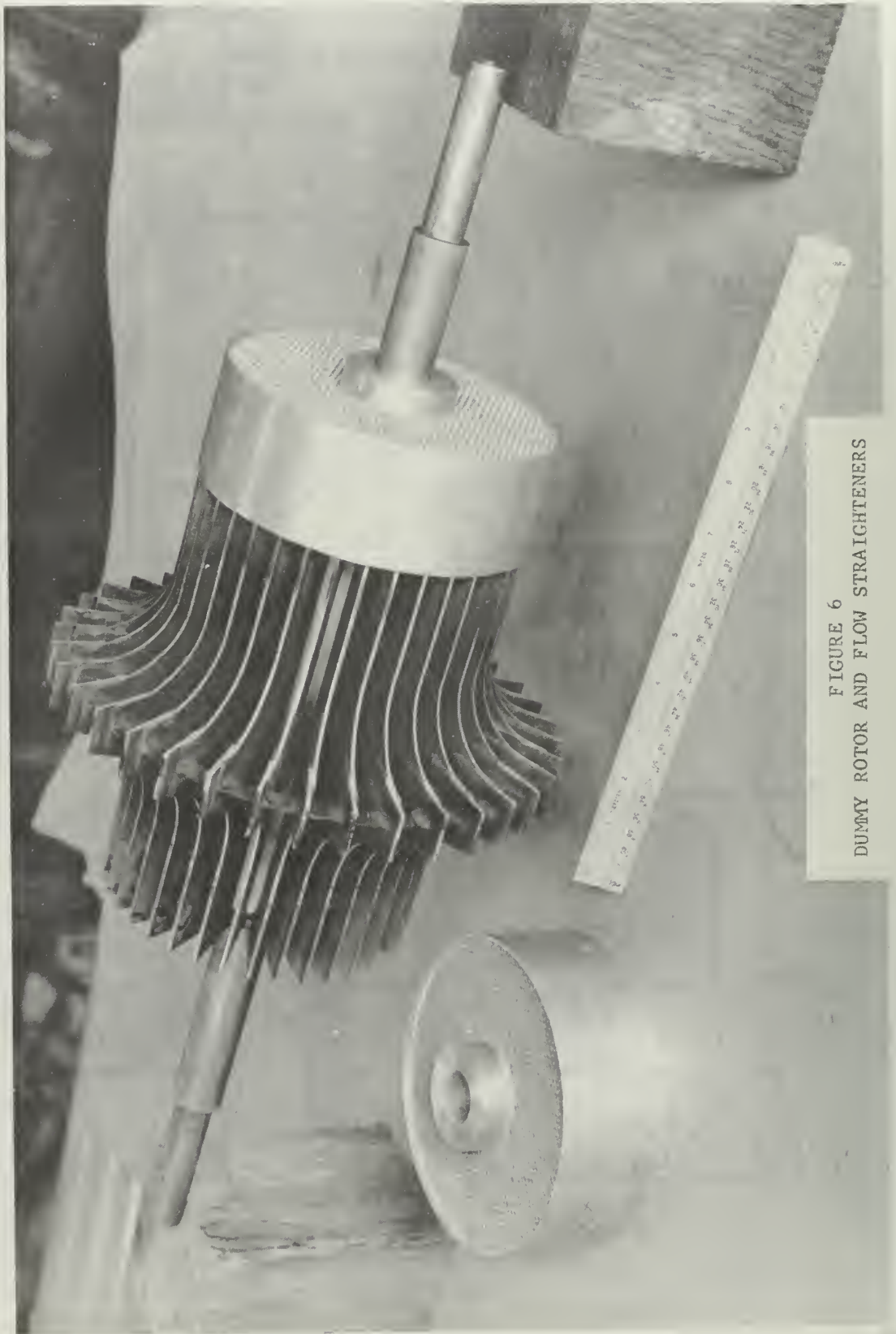


FIGURE 6
DUMMY ROTOR AND FLOW STRAIGHTENERS

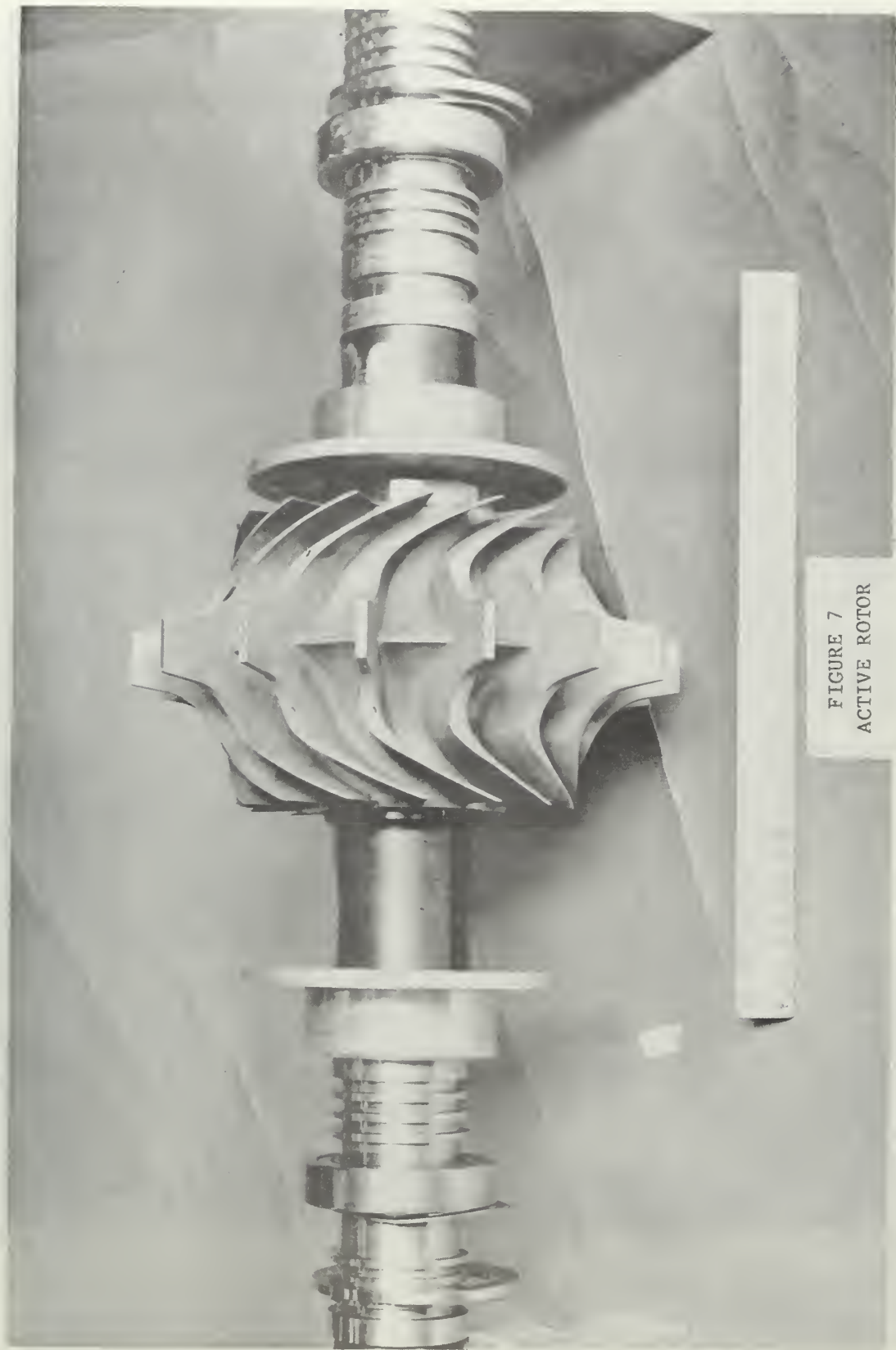


FIGURE 7
ACTIVE ROTOR



FIGURE 8
LEFT TURBINE DISCHARGE

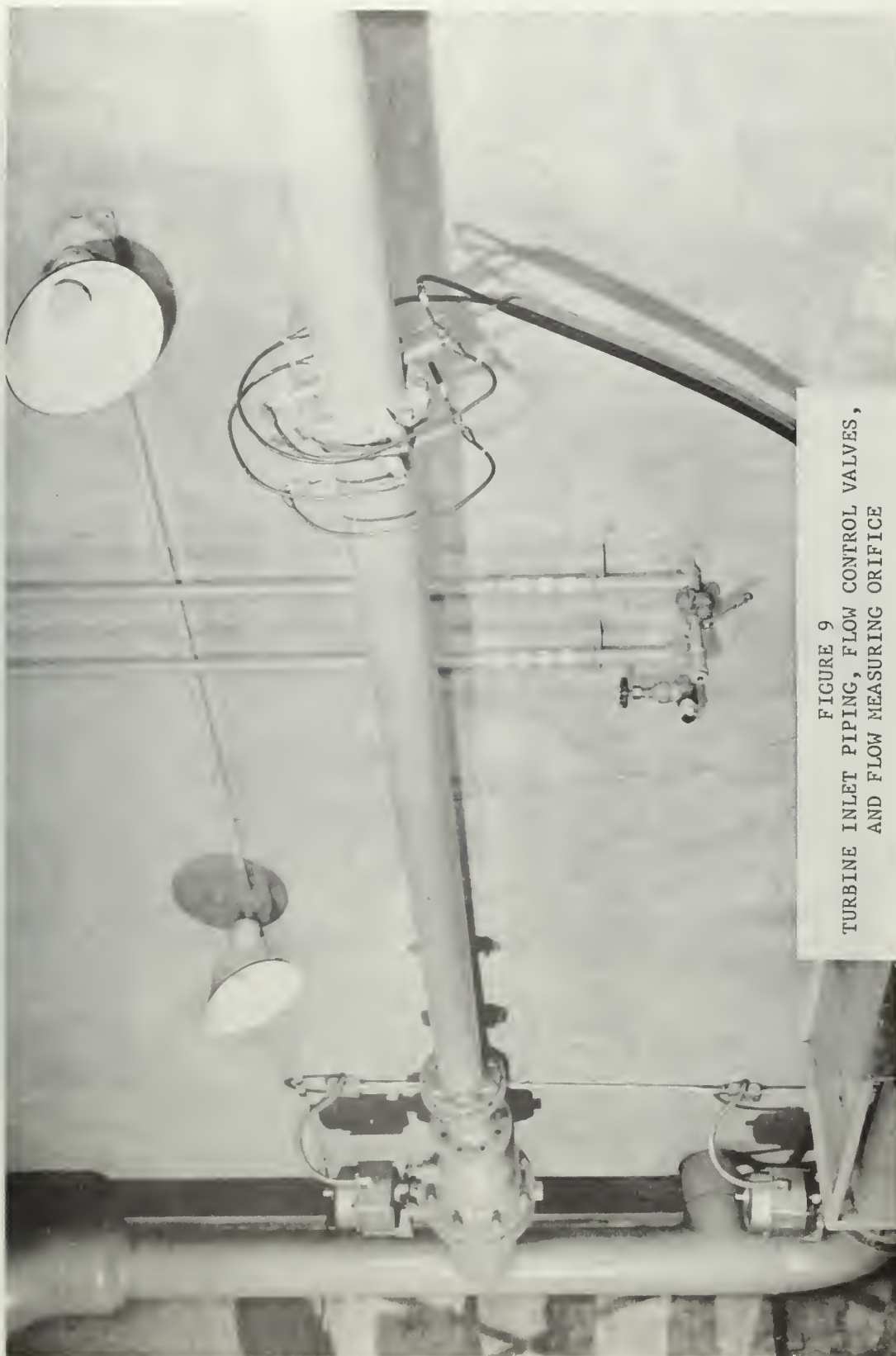


FIGURE 9
TURBINE INLET PIPING, FLOW CONTROL VALVES,
AND FLOW MEASURING ORIFICE

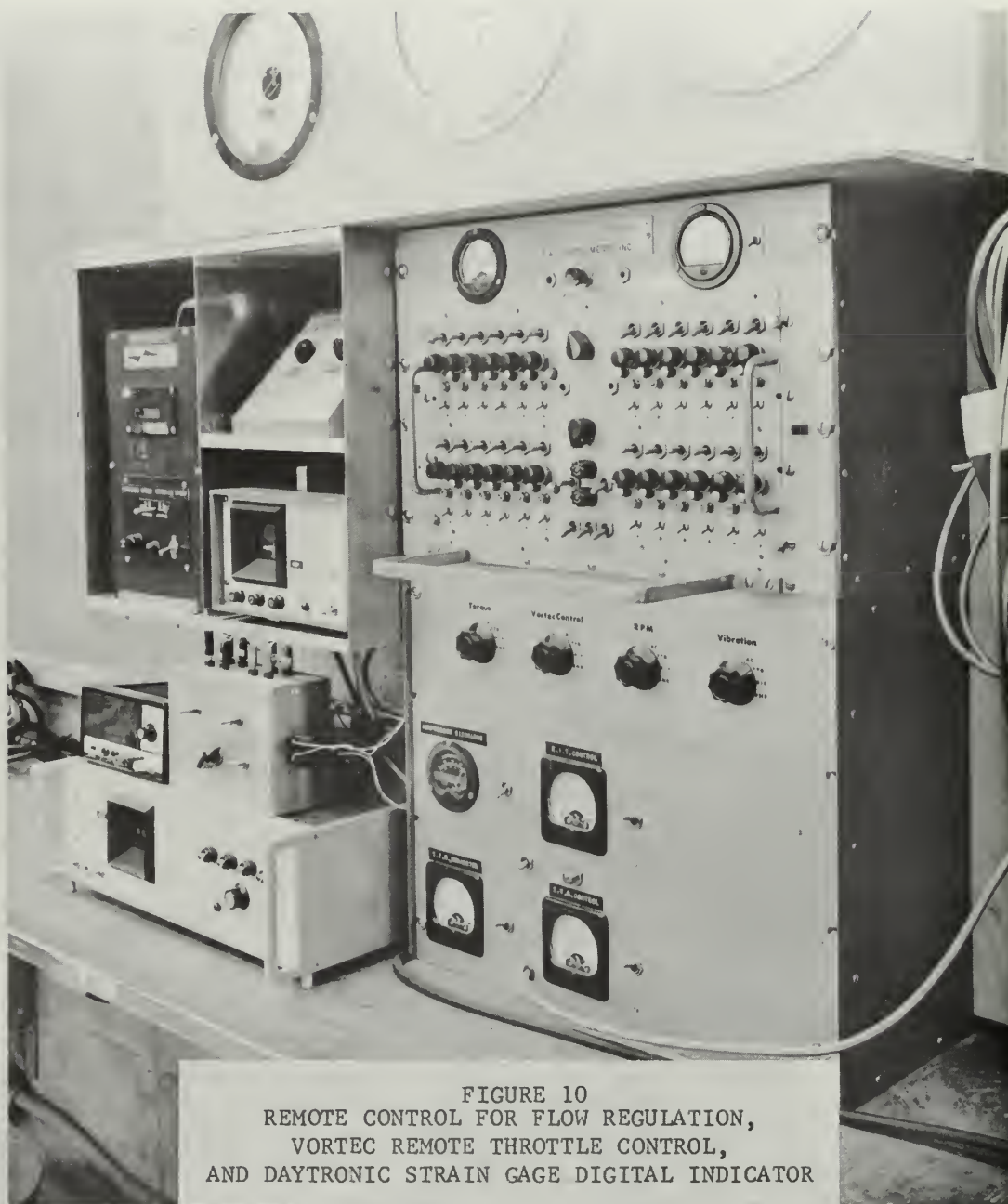


FIGURE 10
 REMOTE CONTROL FOR FLOW REGULATION,
 VORTEC REMOTE THROTTLE CONTROL,
 AND DAYTRONIC STRAIN GAGE DIGITAL INDICATOR

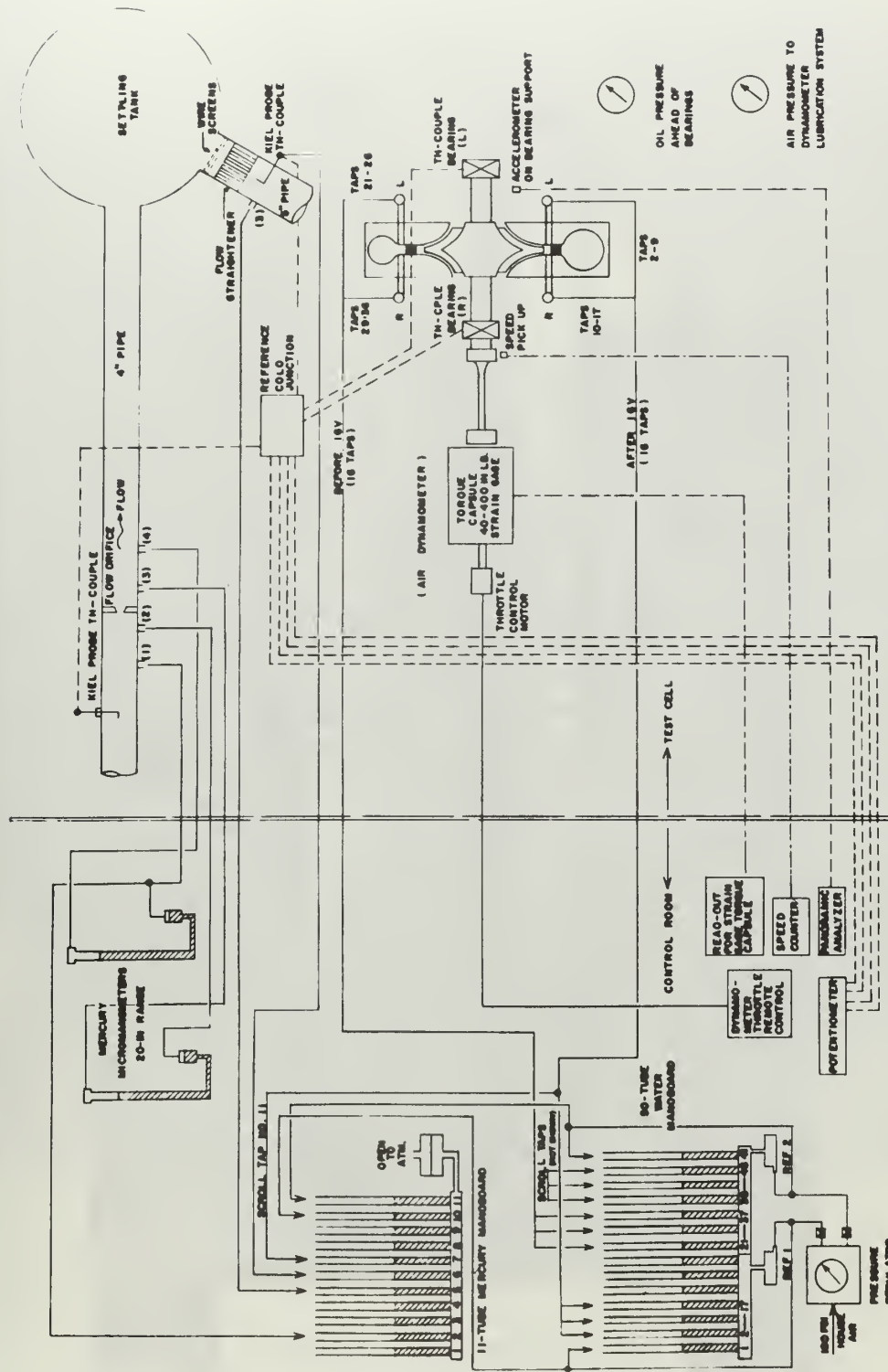


FIGURE 11
SCHEMATIC OF RADIAL TURBINE INSTRUMENTATION

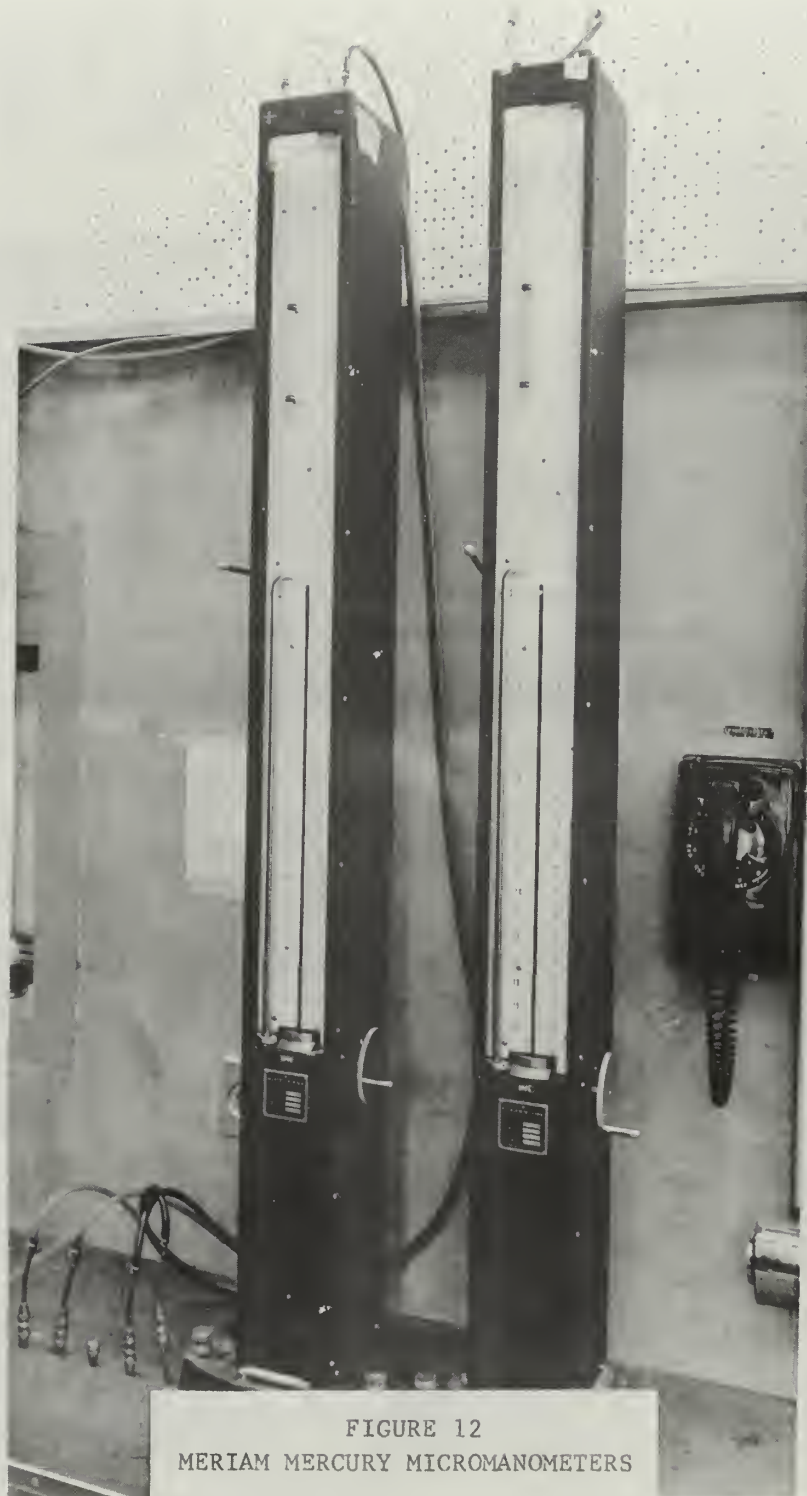


FIGURE 12
MERIAM MERCURY MICROMANOMETERS



FIGURE 13
BROWN POTENTIOMETER

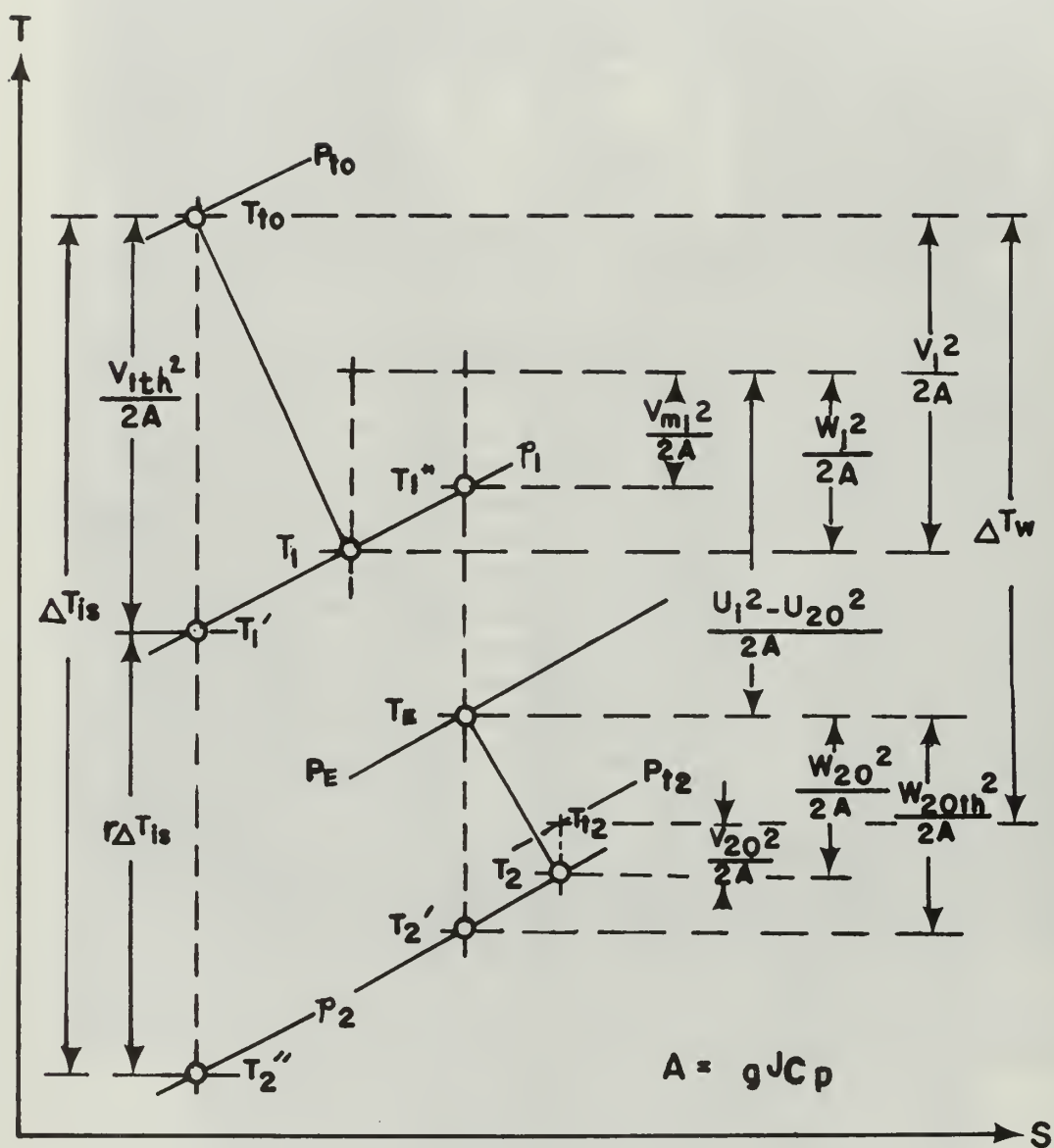


FIGURE 14
TEMPERATURE-ENTROPY DIAGRAM FOR RADIAL TURBINE

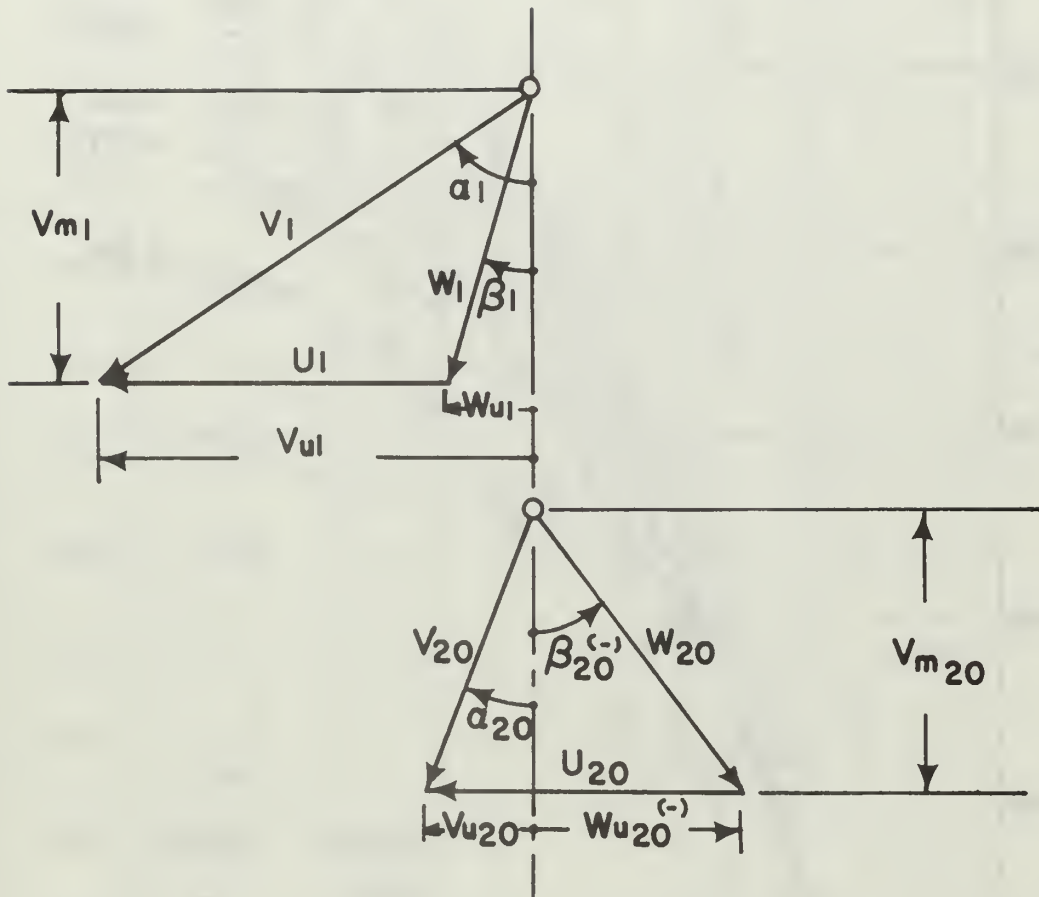


FIGURE 15
VELOCITY DIAGRAMS FOR RADIAL TURBINE

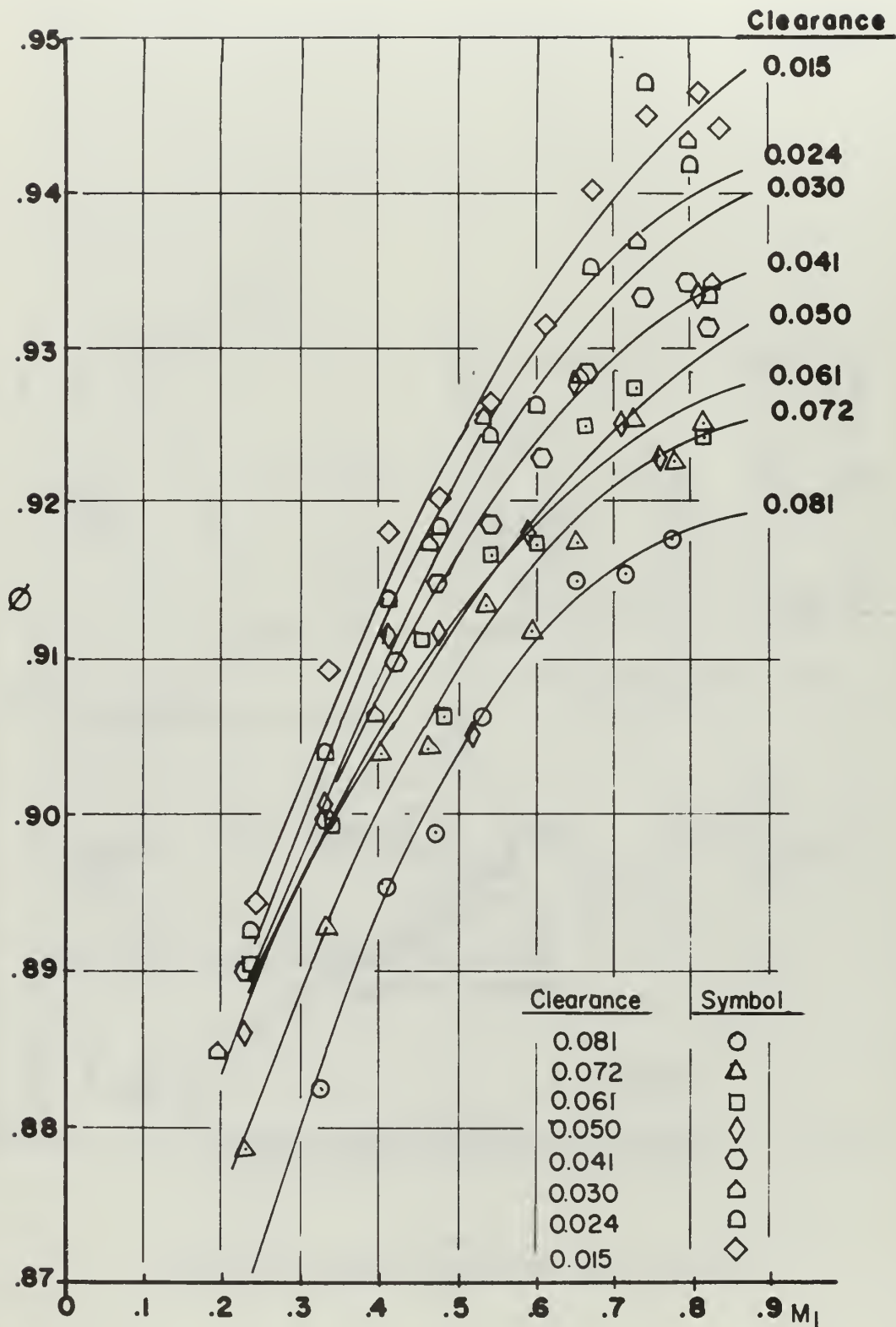


FIGURE 16
VELOCITY COEFFICIENT VS. MACH NUMBER

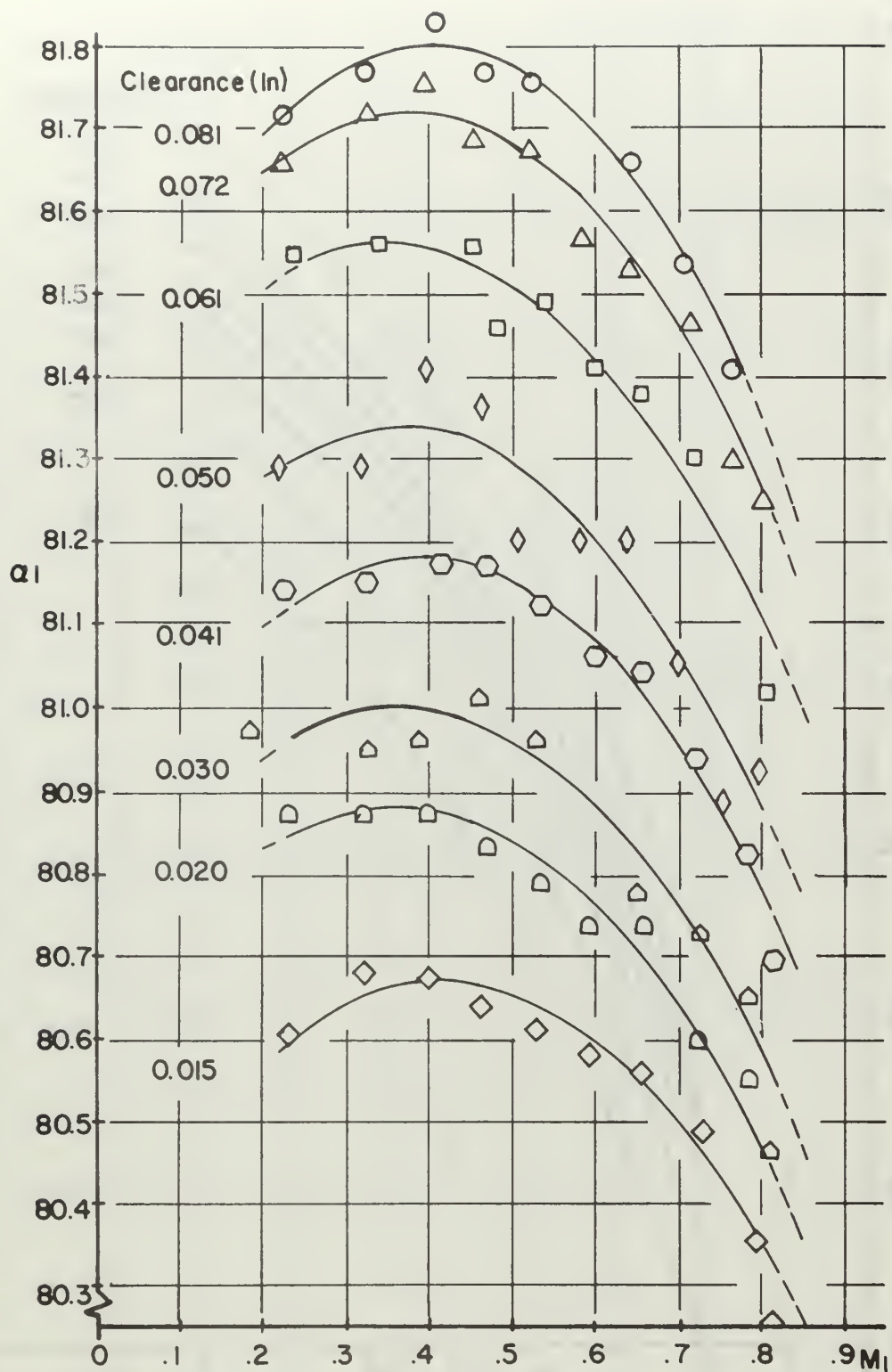


FIGURE 17
ABSOLUTE ROTOR INLET FLOW ANGLE VS. MACH NUMBER

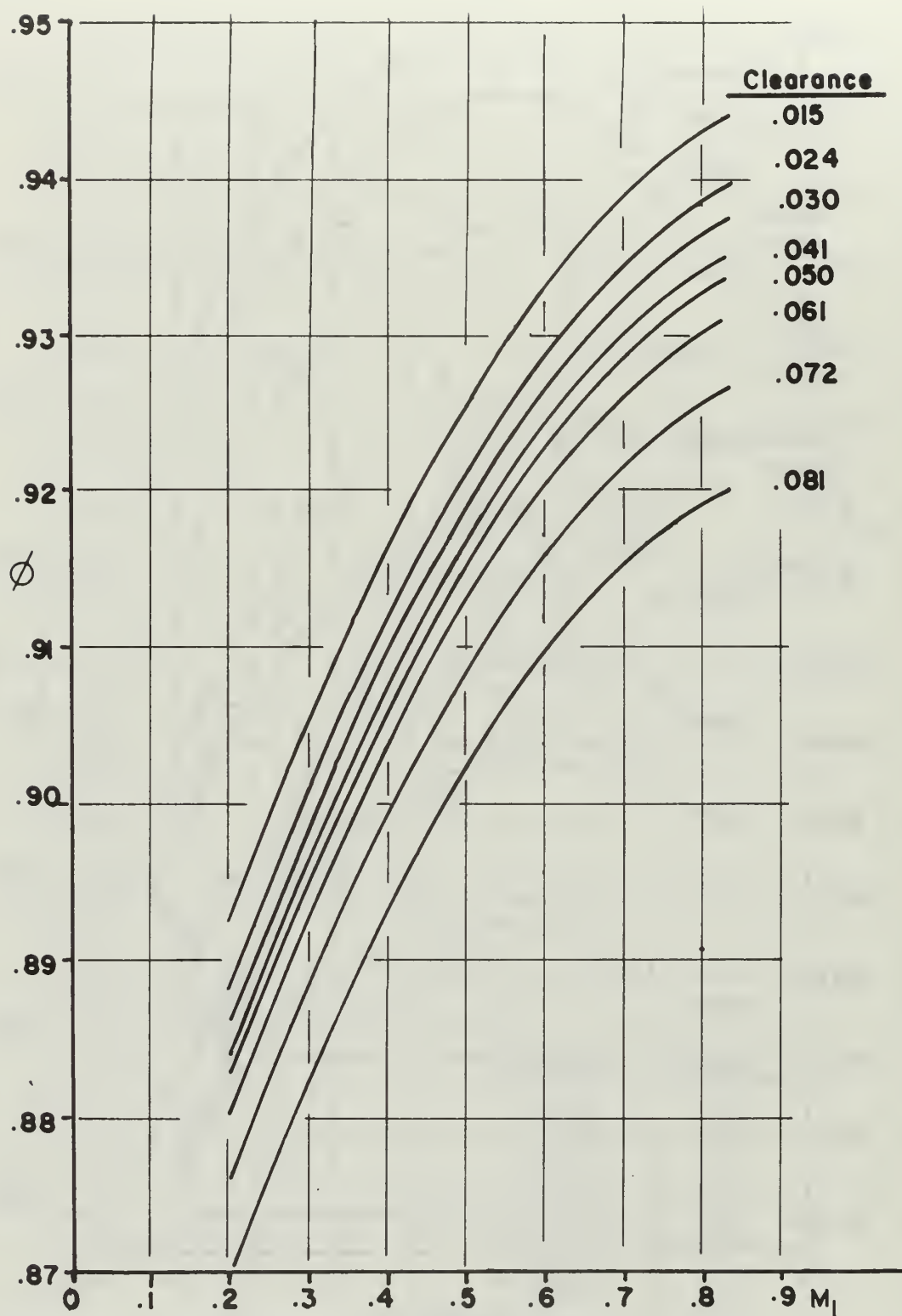


FIGURE 18
VELOCITY COEFFICIENT VS. MACH NUMBER
FROM DERIVED EQUATION

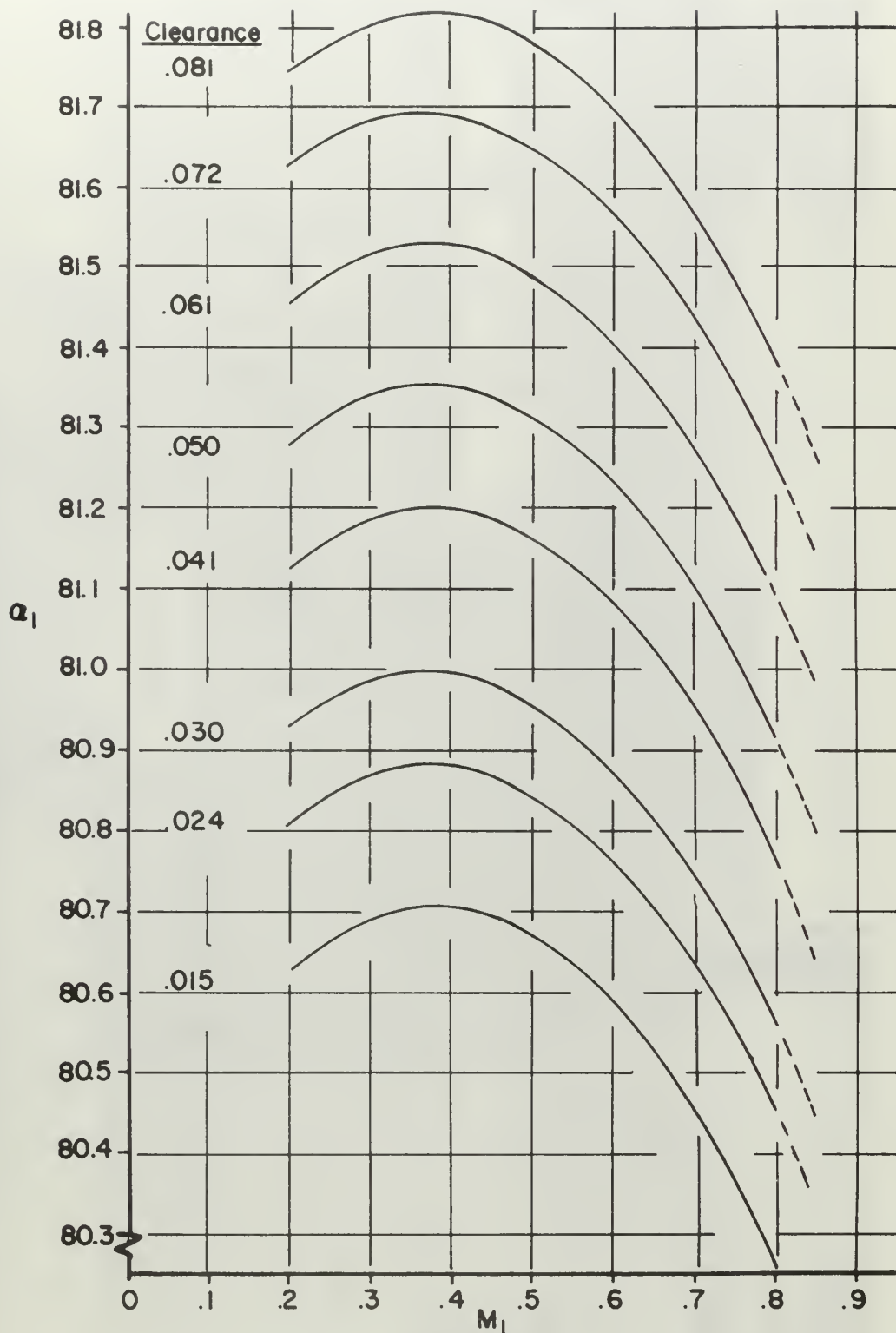


FIGURE 19
ABSOLUTE ROTOR INLET FLOW ANGLE VS. MACH NUMBER
FROM DERIVED EQUATION

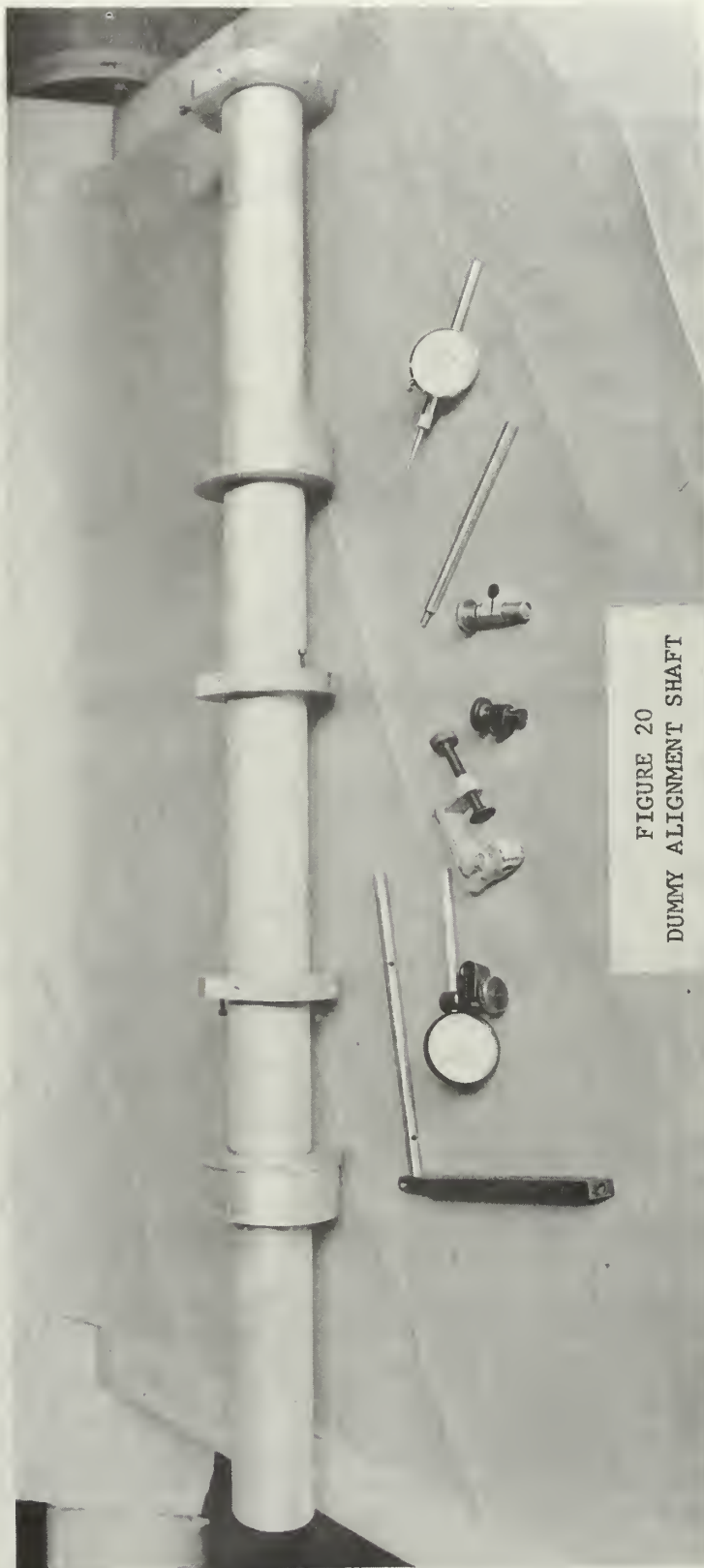


FIGURE 20
DUMMY ALIGNMENT SHAFT



FIGURE 21
FLUX CUTTER, QUILL SHAFT,
AND DYNAMOMETER TORQUE CAPSULE

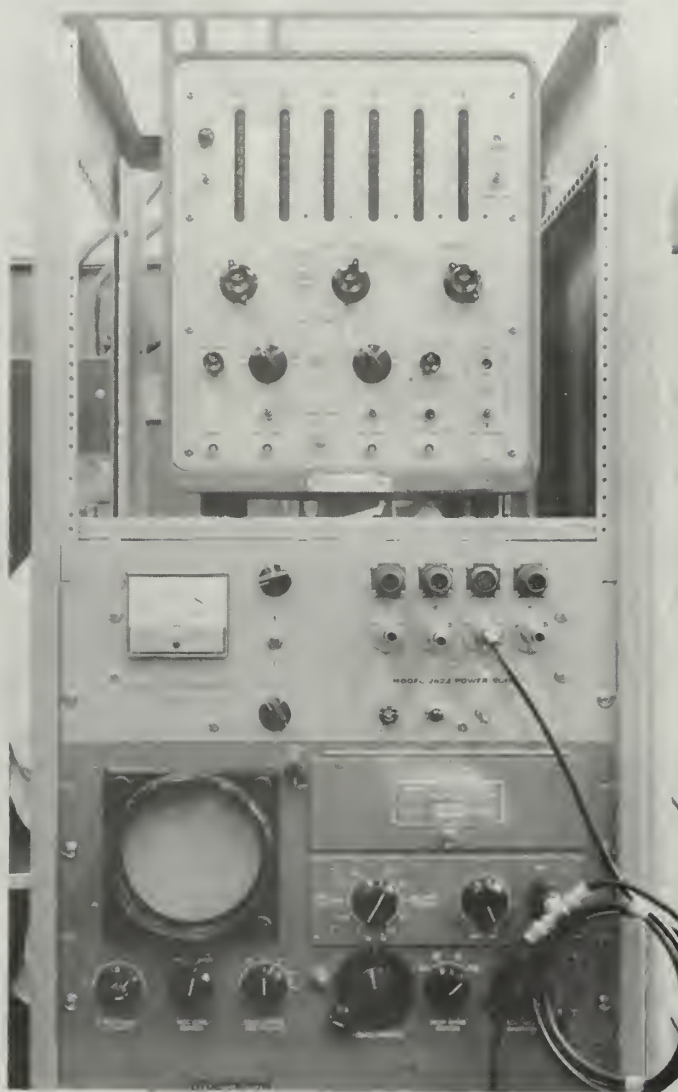


FIGURE 22
ELECTRONIC SPEED COUNTER
AND VIBRATION ANALYZER

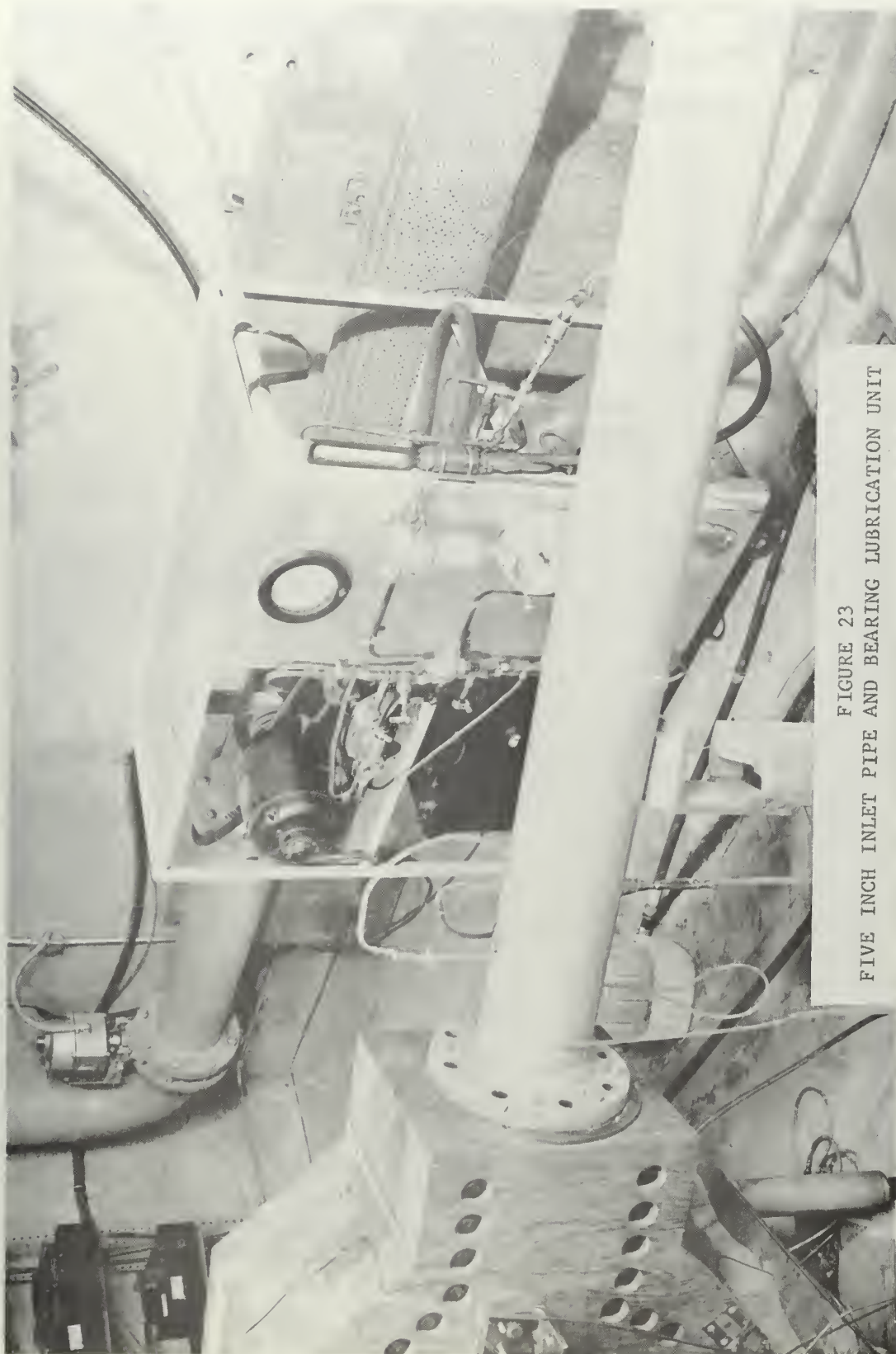


FIGURE 23
FIVE INCH INLET PIPE AND BEARING LUBRICATION UNIT

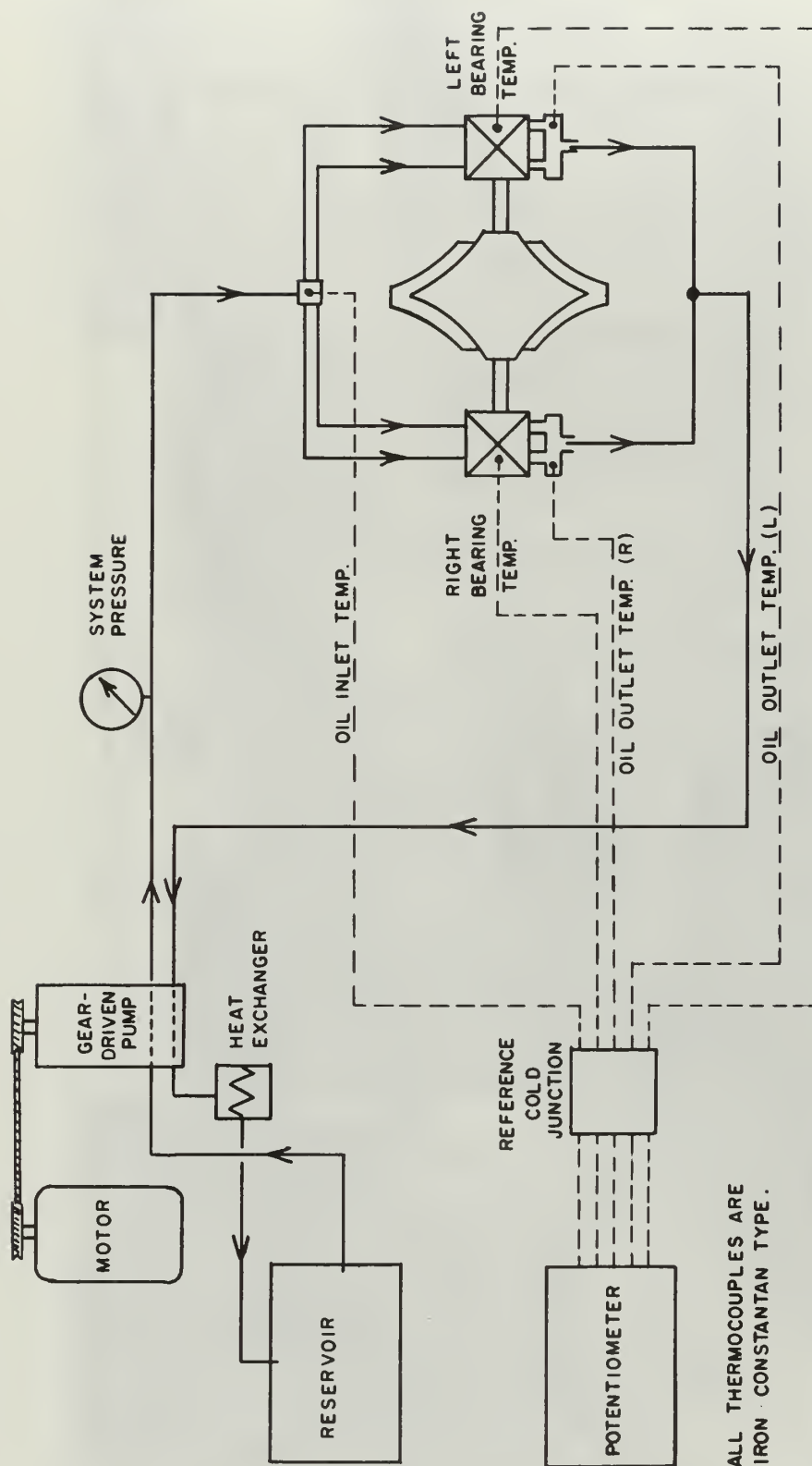


FIGURE 24
SCHEMATIC OF TURBINE LUBRICATION SYSTEM

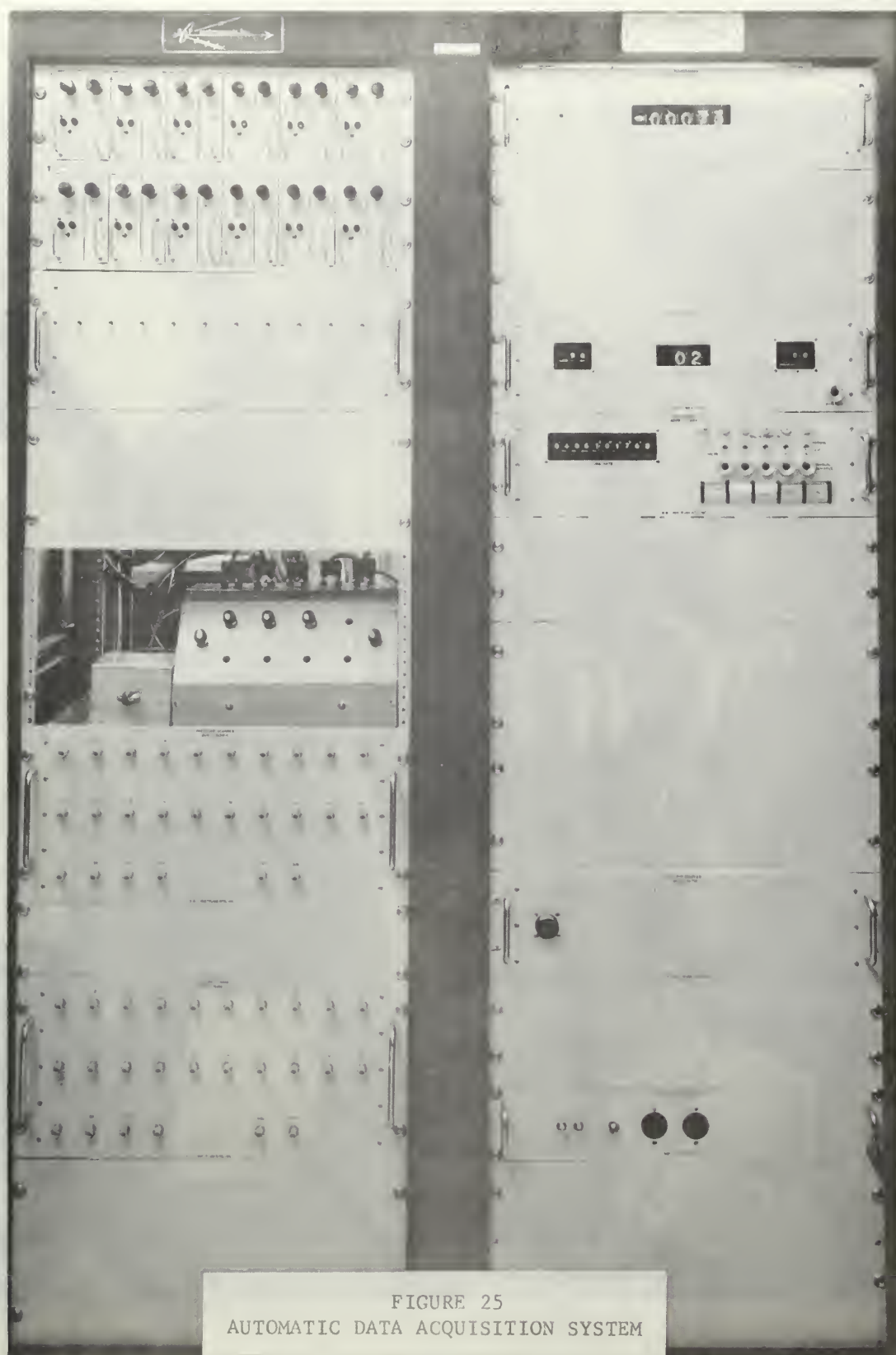


FIGURE 25
AUTOMATIC DATA ACQUISITION SYSTEM

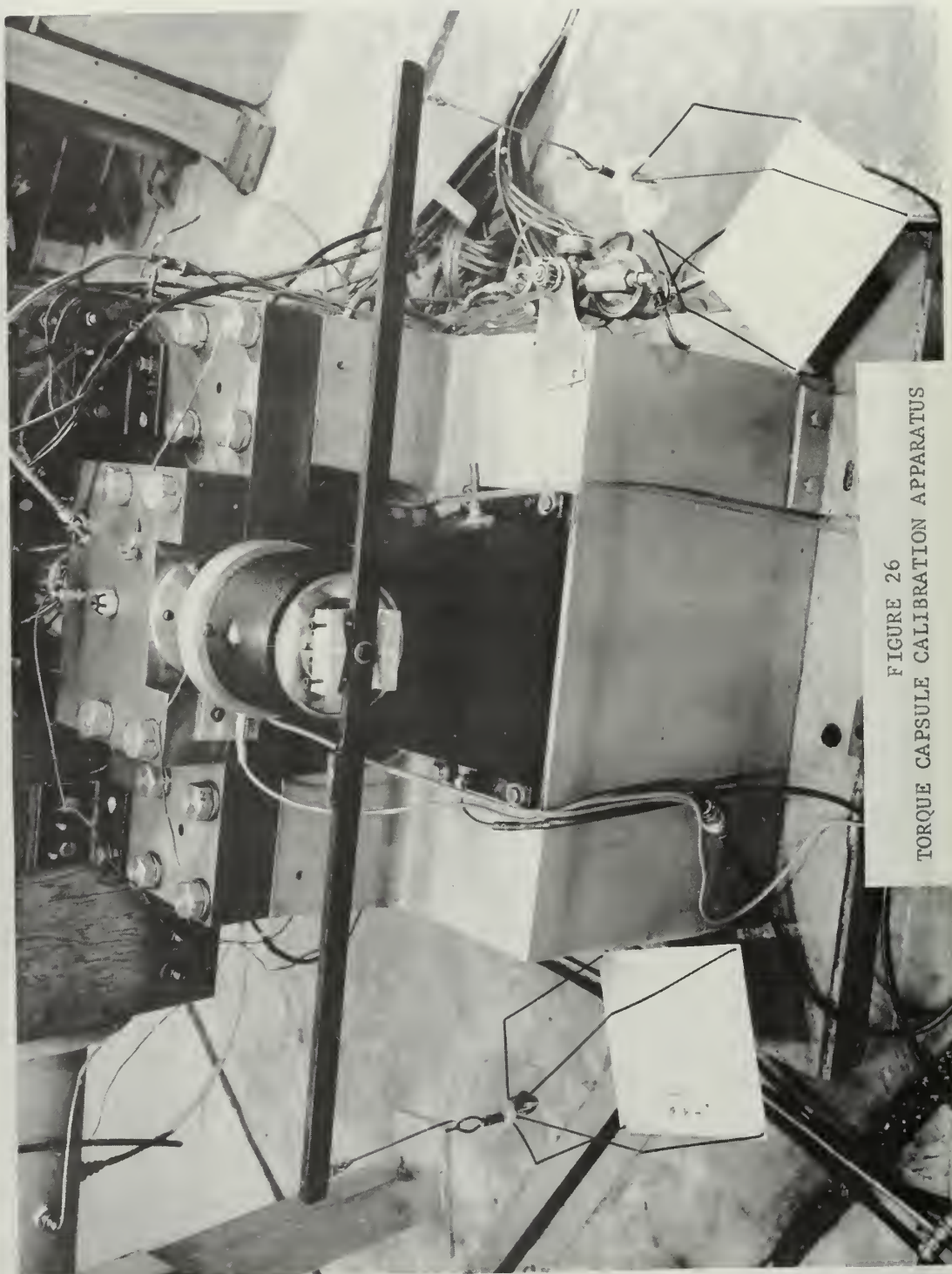


FIGURE 26
TORQUE CAPSULE CALIBRATION APPARATUS

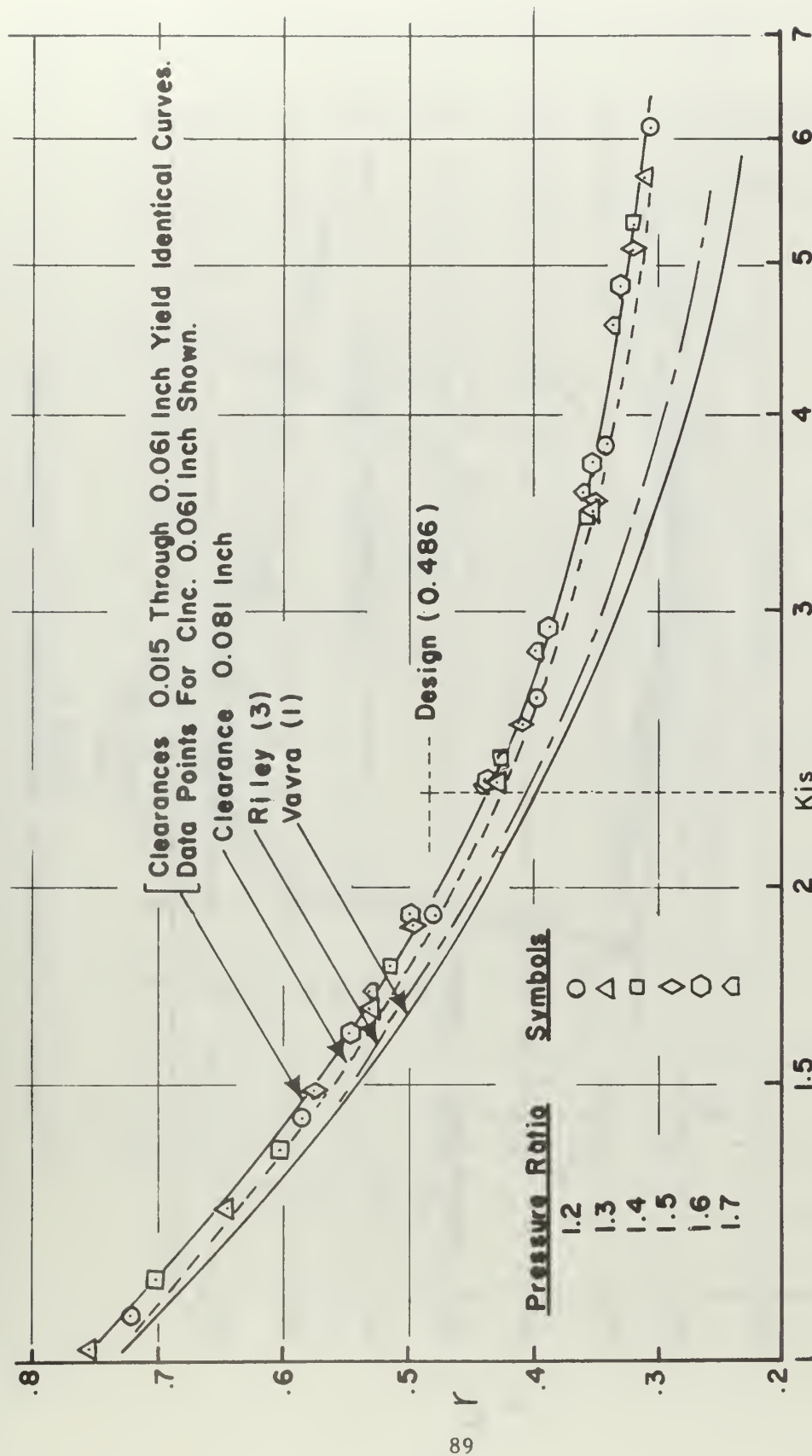


FIGURE 27
DEGREE OF REACTION VS. HEAD COEFFICIENT

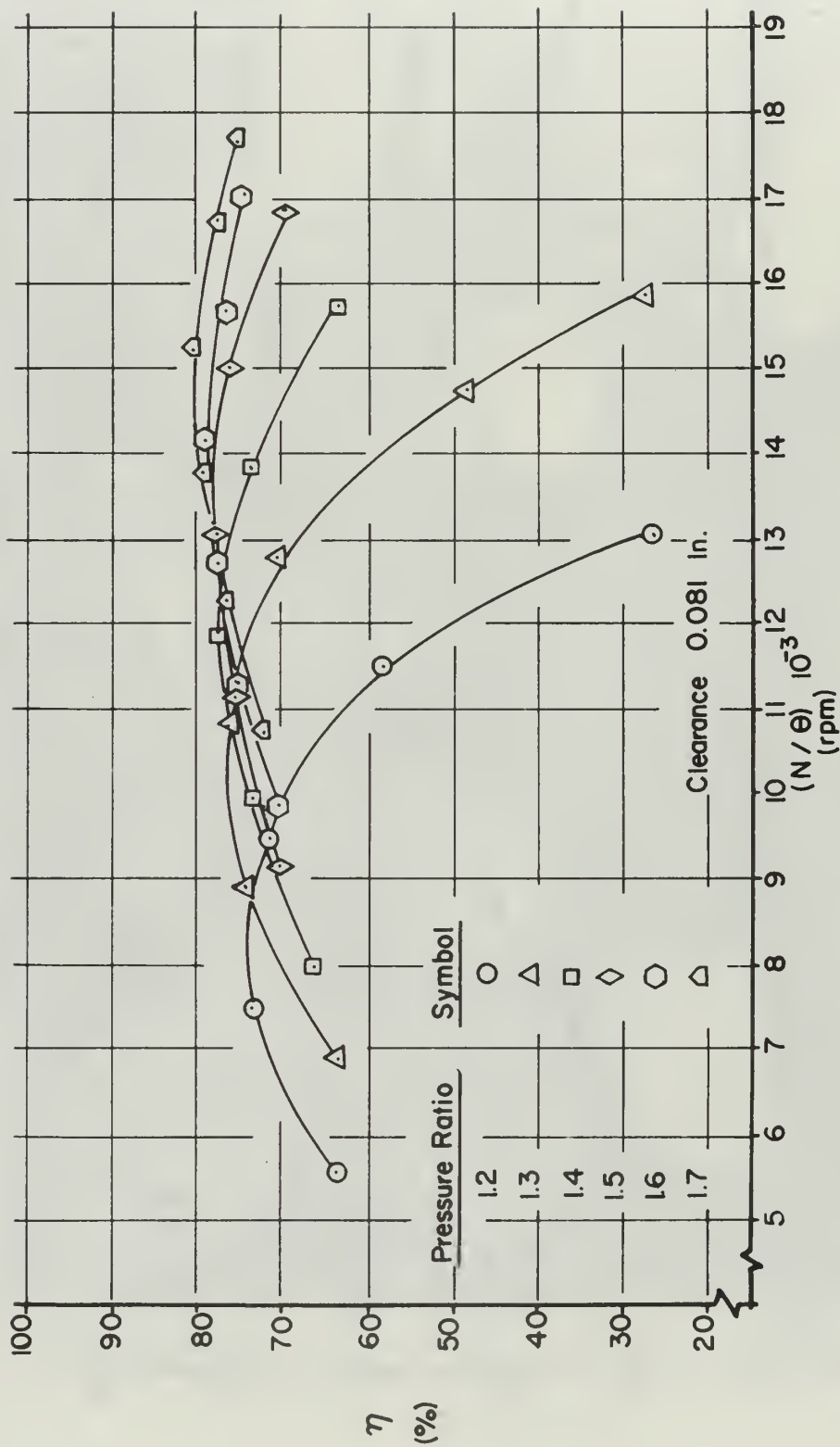


FIGURE 28
OVERALL EFFICIENCY (NO BEARING LOSSES) VS. REFERRED SPEED

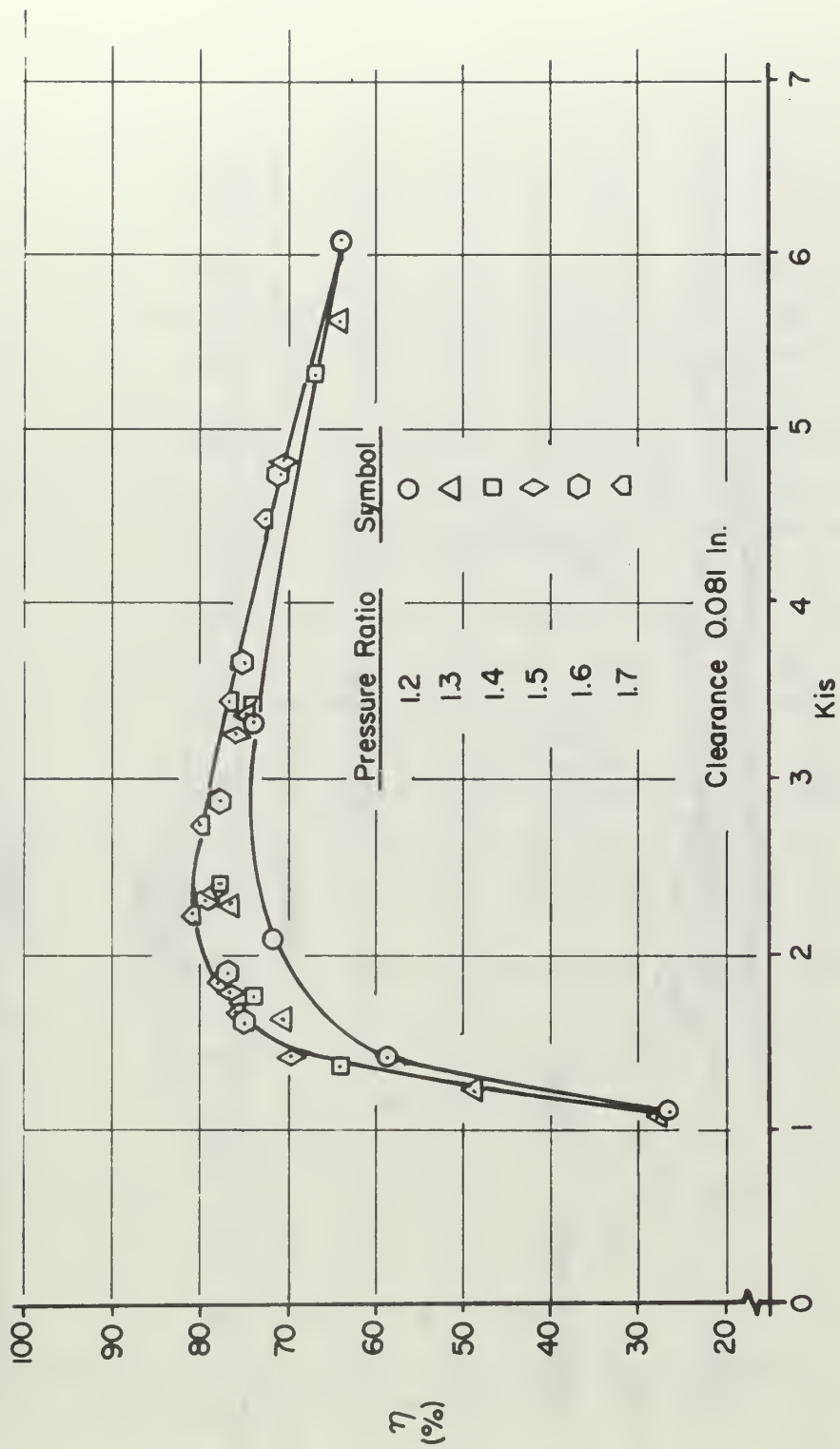


FIGURE 29
OVERALL EFFICIENCY (NO BEARING LOSSES) VS. HEAD COEFFICIENT

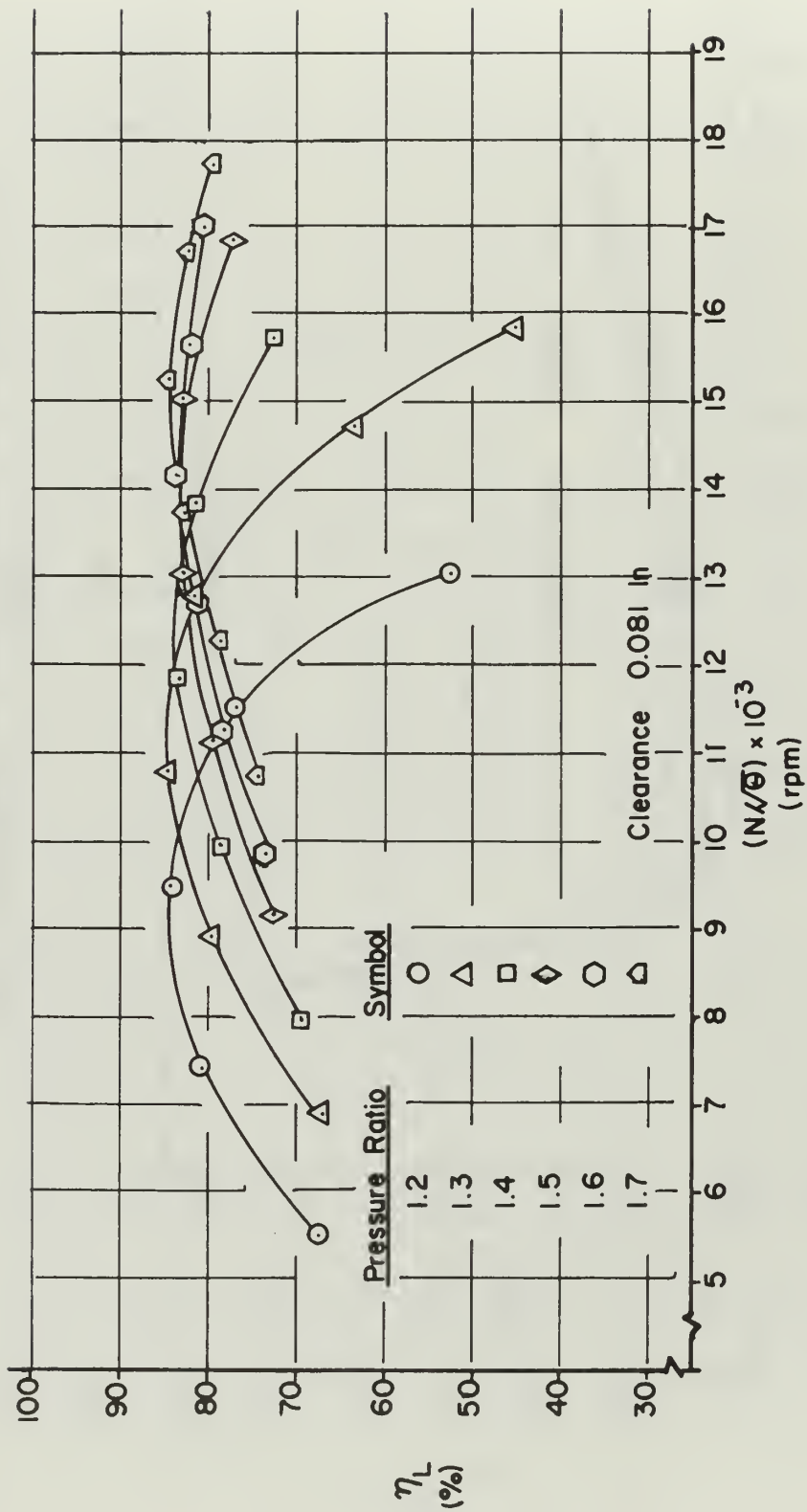


FIGURE 30
OVERALL EFFICIENCY (WITH BEARING LOSSES) VS. REFERRED SPEED

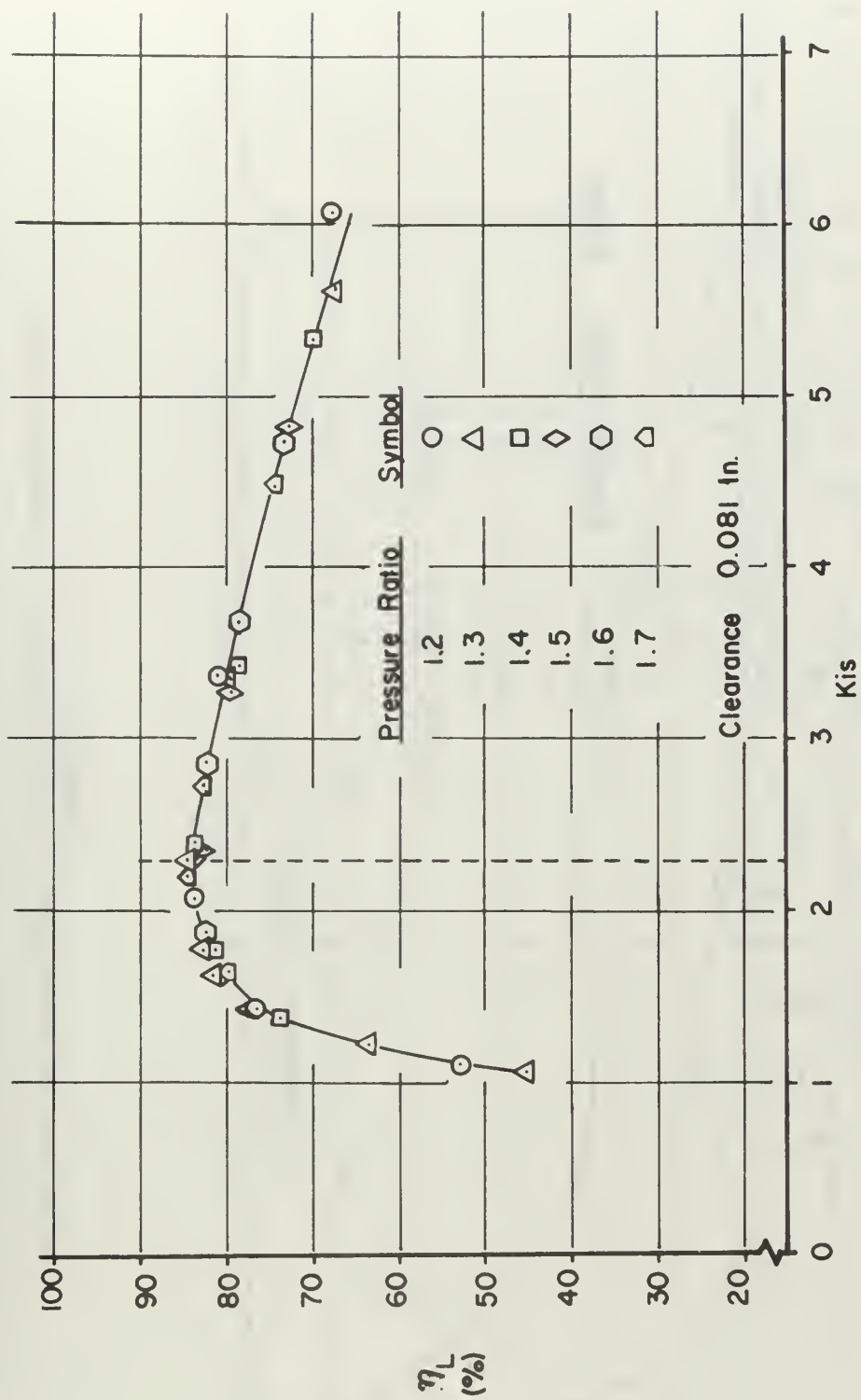


FIGURE 31
OVERALL EFFICIENCY (WITH BEARING LOSSES) VS. HEAD COEFFICIENT

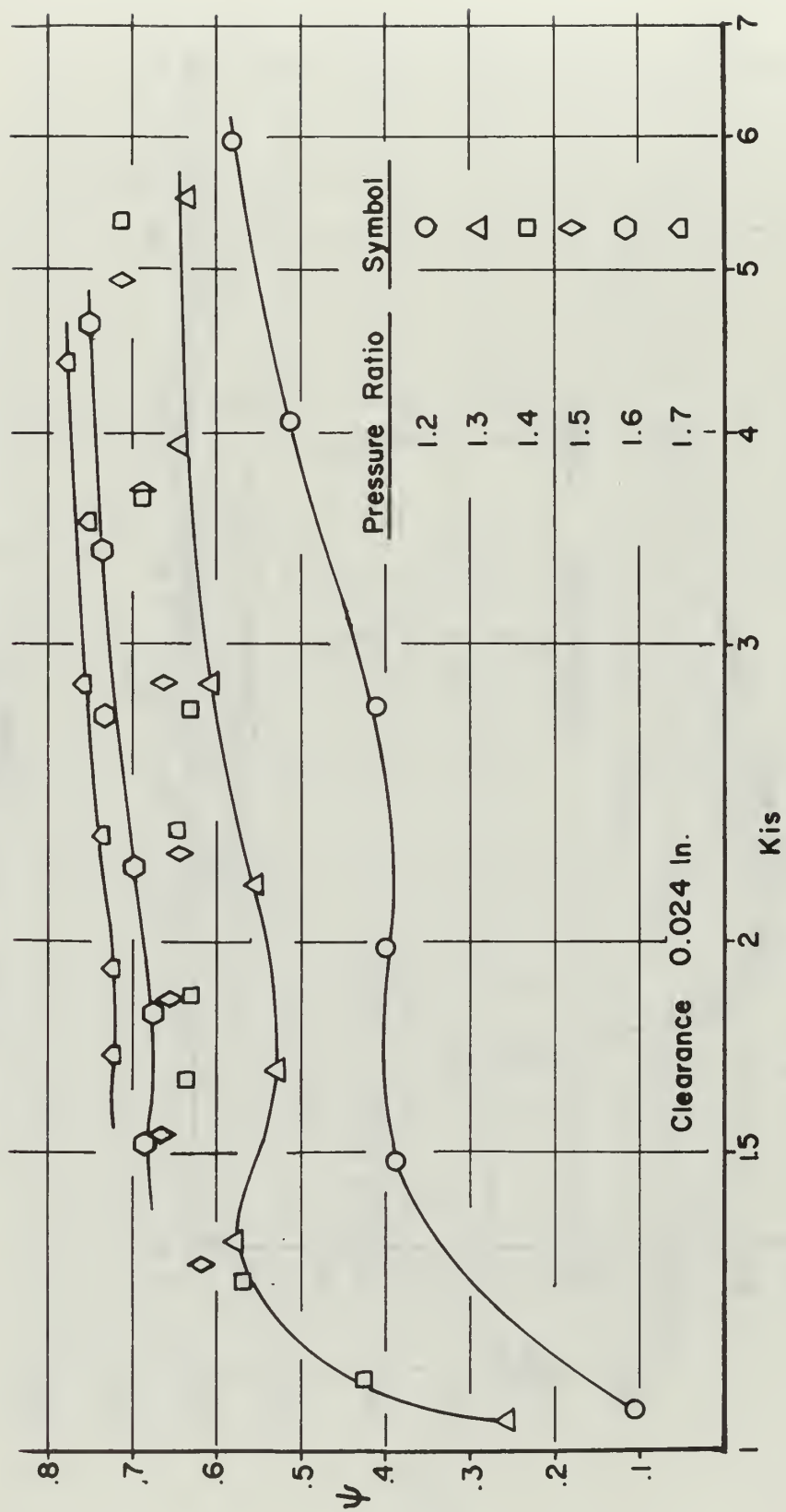


FIGURE 32
 ROTOR VELOCITY COEFFICIENT (NO BEARING LOSSES) VS. HEAD COEFFICIENT

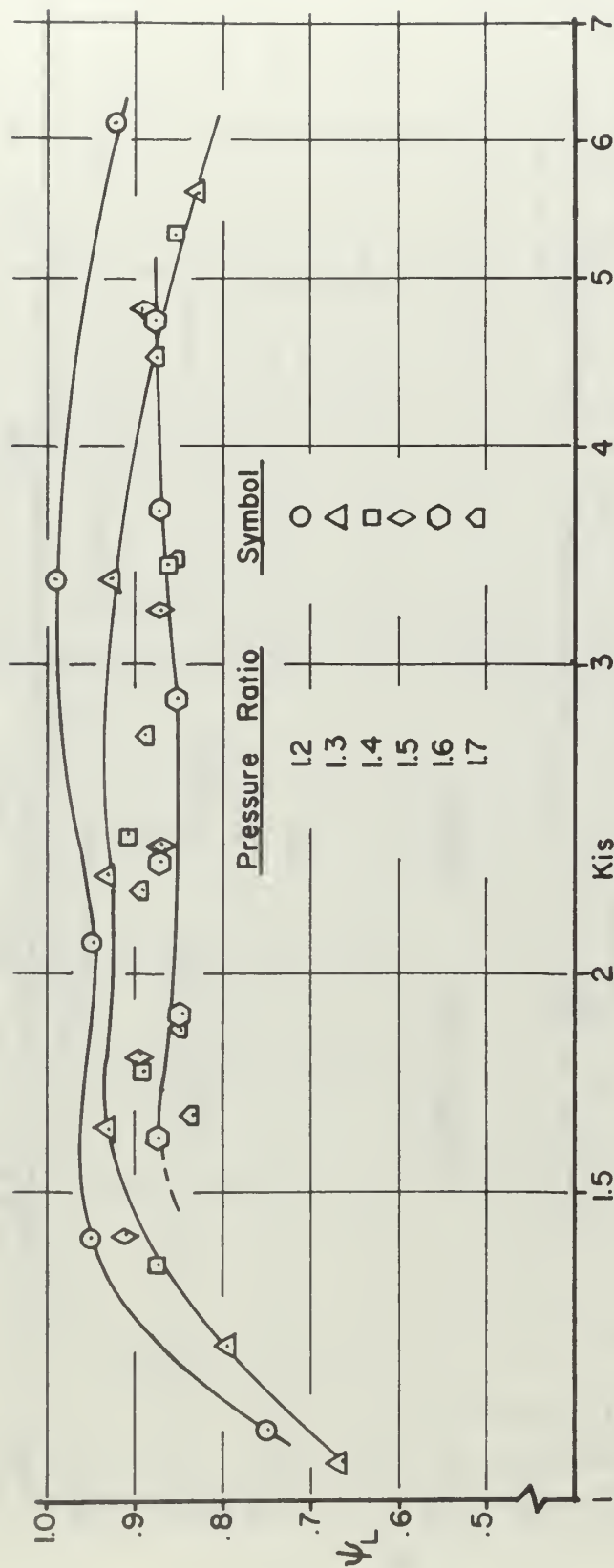


FIGURE 33
 ROTOR VELOCITY COEFFICIENT (WITH BEARING LOSSES) VS. HEAD COEFFICIENT
 CLEARANCE 0.081 IN.

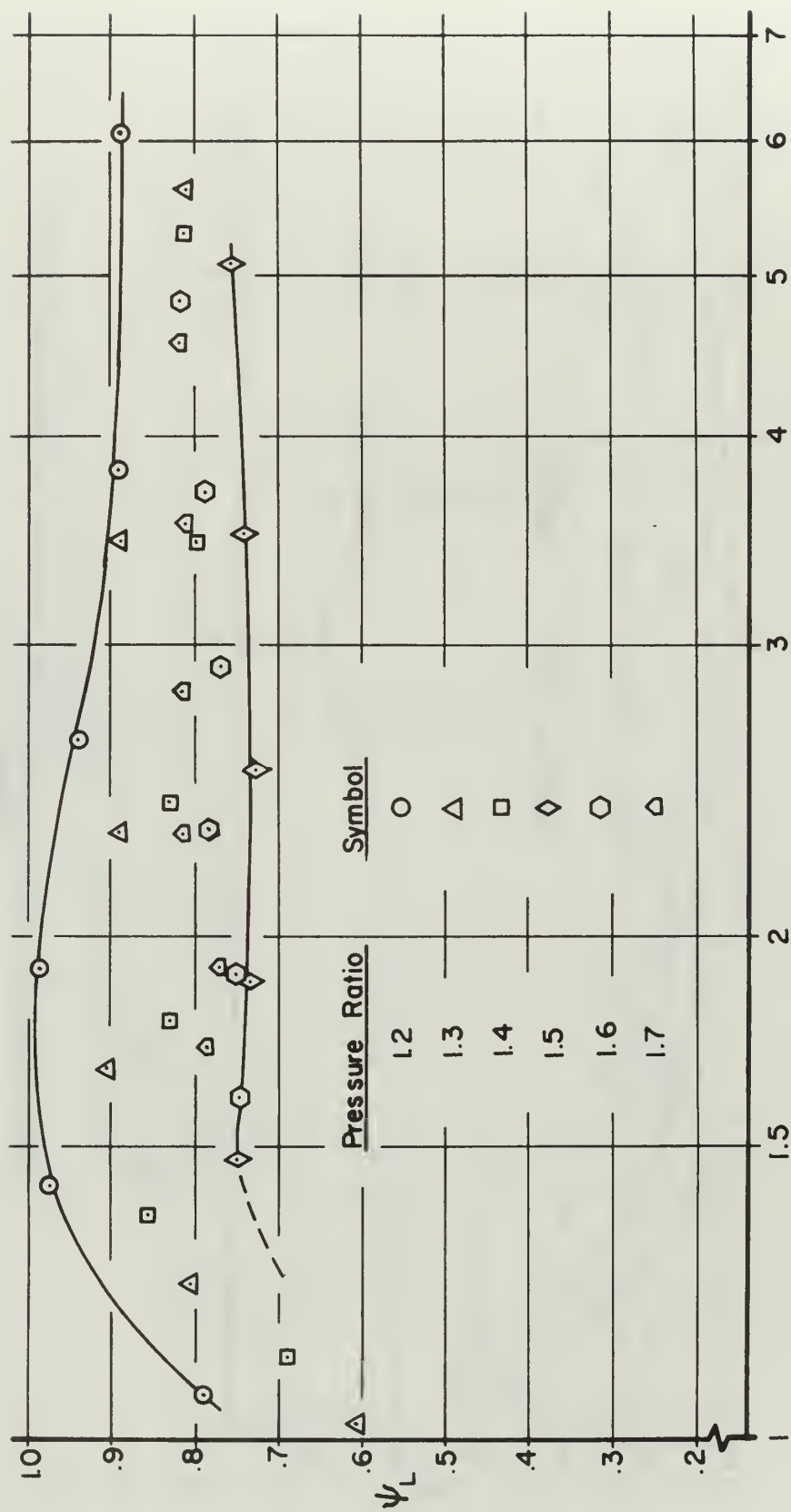


FIGURE 34
 ROTOR VELOCITY COEFFICIENT (WITH BEARING LOSSES) VS. HEAD COEFFICIENT
 CLEARANCE 0.061 IN.

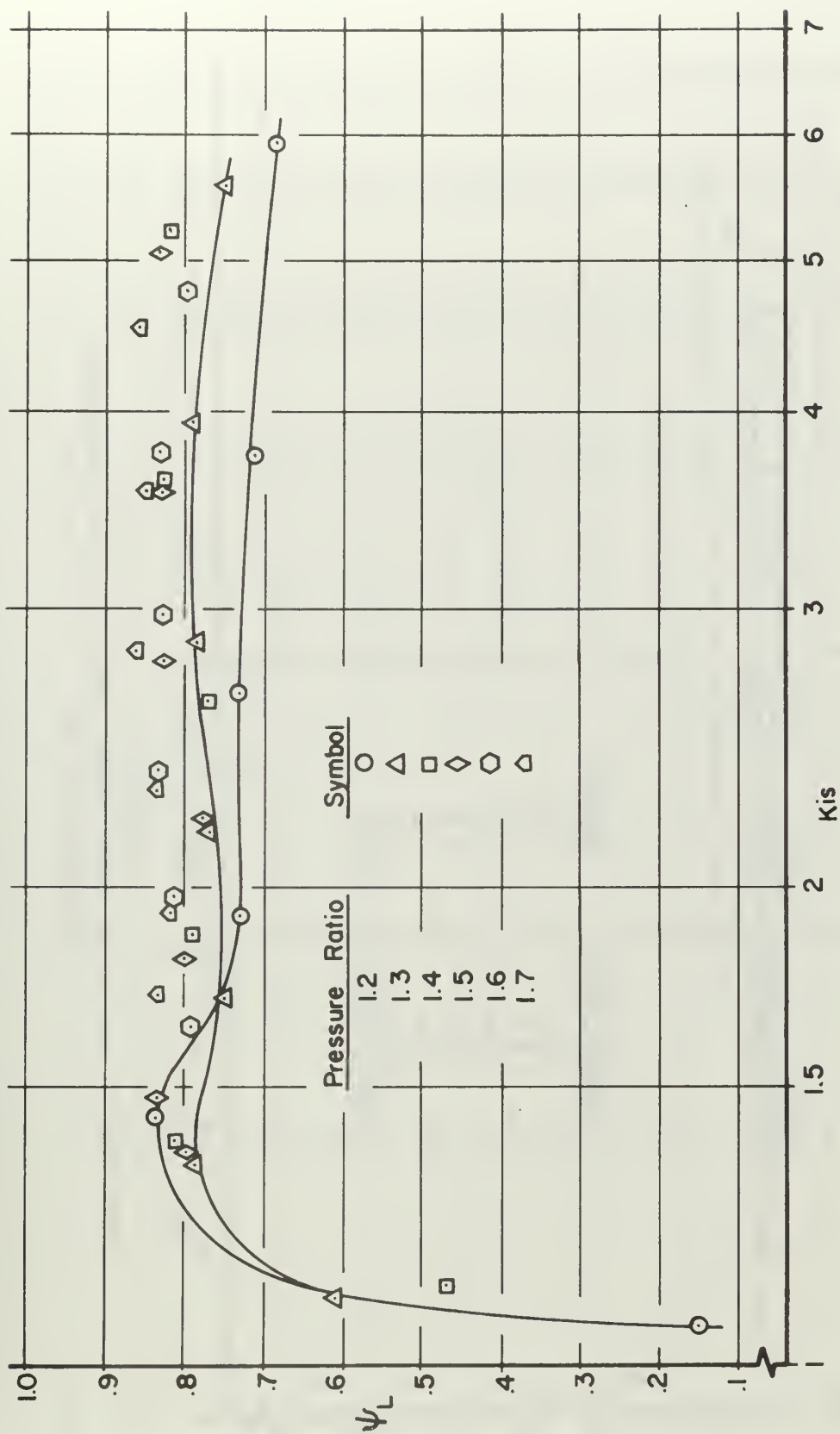


FIGURE 35
 ROTOR VELOCITY COEFFICIENT (WITH BEARING LOSSES) VS. HEAD COEFFICIENT
 CLEARANCE 0.041 IN.

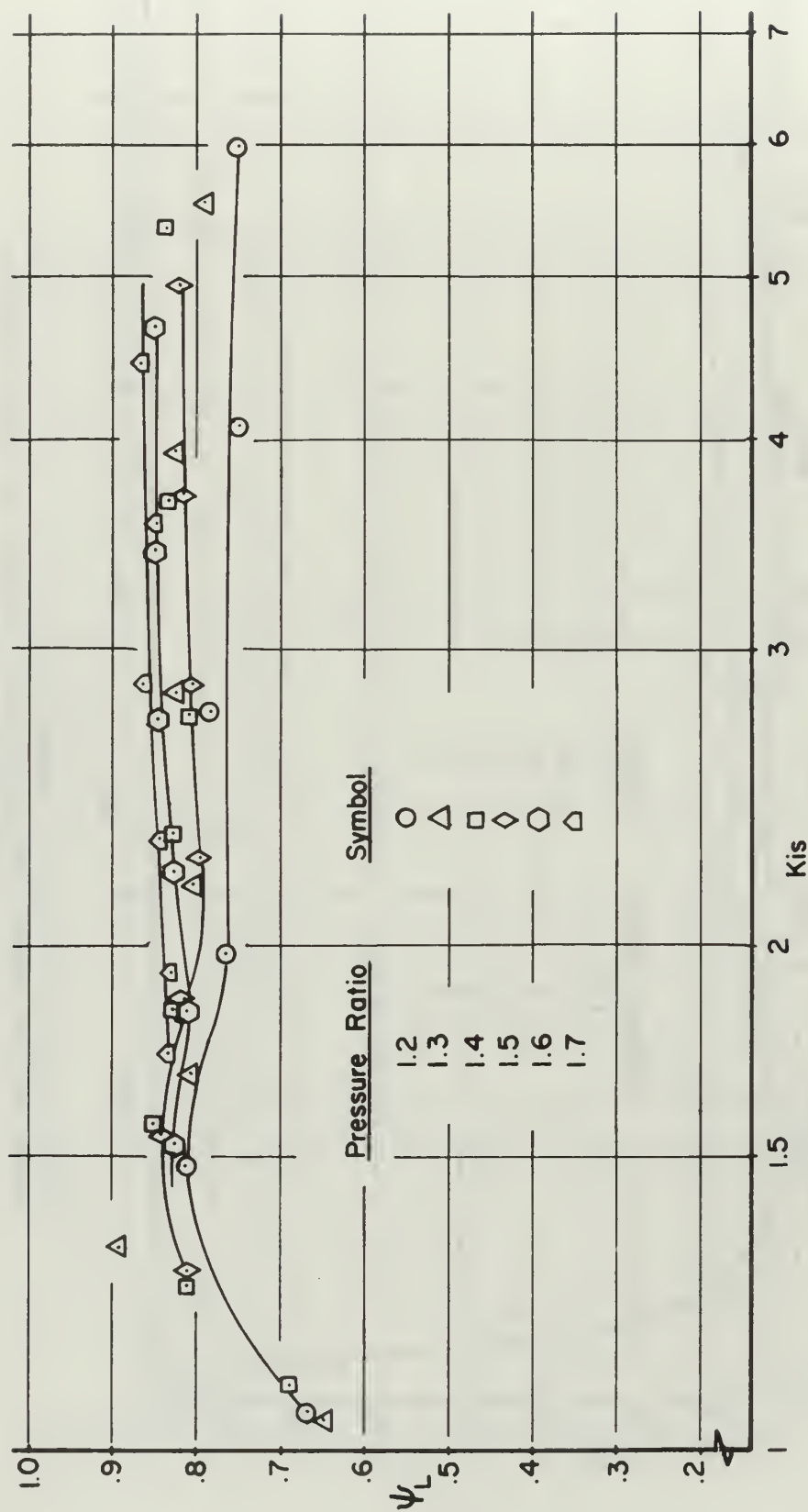


FIGURE 36
 ROTOR VELOCITY COEFFICIENT (WITH BEARING LOSSES) VS. HEAD COEFFICIENT
 CLEARANCE 0.024 IN.

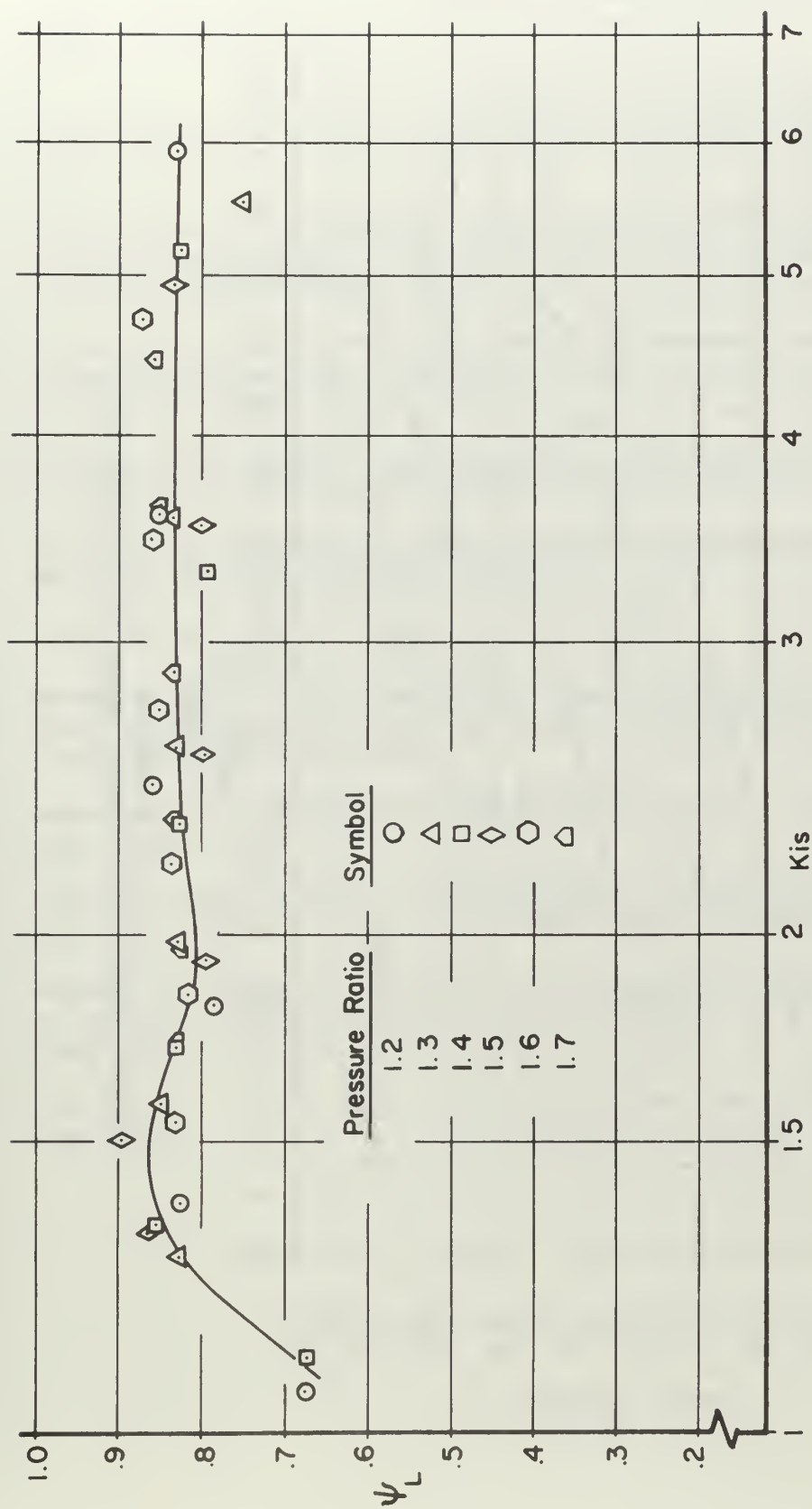


FIGURE 37
 ROTOR VELOCITY COEFFICIENT (WITH BEARING LOSSES) VS. HEAD COEFFICIENT
 CLEARANCE 0.015 IN.

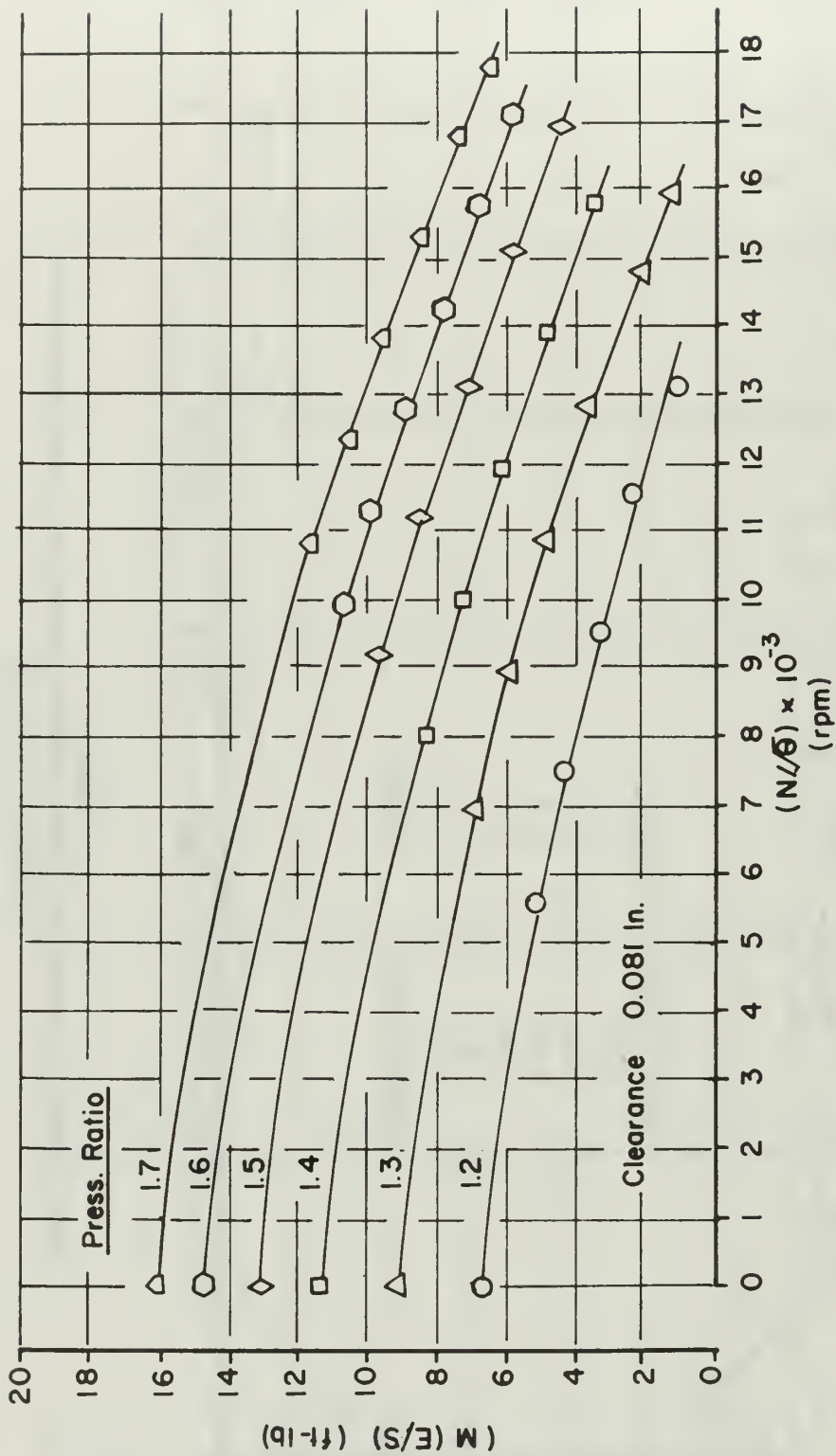


FIGURE 38
REFERRED MOMENT (WITH BEARING LOSSES) VS. REFERRED SPEED

REFERENCES

1. Vavra, M. H., Results of Turbine Air Testing Program, Phase II, Report AGLR-VA No. 29, for Aerojet General Corporation, January 1965.
2. Finn, W. A., "Performance Investigation of a Dual Discharge Radial Inflow Turbine." Master's thesis, Naval Postgraduate School, May 1966.
3. Riley, M. W., "The Effect of Axial Clearance on the Performance of a Dual Discharge Radial Turbine." Master's thesis, Naval Postgraduate School, December 1966.
4. Boshoven, R. L., "An Investigation of Compressible Flows with Large Whirl Components." Engineer's thesis, Naval Postgraduate School, June 1967.
5. Stearns, R. F., et al. Flow Measurement with Orifice Meters. New York: D. van Nostrand Company, 1951.
6. Vavra, M. H. Aero-Thermodynamics and Flow in Turbomachines. New York: John Wiley and Sons, 1960.
7. Vavra, M. H., Private communication, 1968.
8. Vavra, M. H., "Flow in Radial Turbines." Lecture notes for a short course on flow in turbines, von Karman Institute for Fluid Dynamics, March 1968.
9. Csanady, G. T. Theory of Turbomachines. New York: McGraw-Hill Book Company, 1964.
10. National Research Council. International Critical Tables, Vol. III. New York: McGraw-Hill Book Company, 1928.
11. Shenker, H. Reference Tables for Thermocouples. National Bureau of Standards, United States Department of Commerce, Circular 561. Washington: Government Printing Office, 1955.
12. Keenan, J. M. and J. Kaye. Gas Tables. New York: John Wiley and Sons, 1948.

APPENDIX A

PROGRAM SCROLL

Program SCROLL computes the losses in the scroll and guide vanes and the absolute rotor inlet flow angle from torque, mass flow rate, pressure, and temperature data obtained in the dummy rotor tests. The program is essentially that used by Riley (3) and by Boshoven (4), with several changes as specified below. It can process any number of runs, with a maximum of ten sets of data per run. A listing of program SCROLL is given in Table A1. The input and output values which constitute the results of the eight sets of dummy rotor test data obtained are presented in Tables A2 through A9.

A1 Main Program

The value of the specific gravity of mercury, G_{hg} , at room temperature t_{rm} , was determined from

$$G_{hg} = 13.63905 - (1.36303 \times 10^{-3}) t_{rm} \quad (A1)$$

for temperatures between 32°F and 113°F. The factor for converting inches Hg to lb/ft^2 is

$$C_{f1} = 70.438824 (G_{hg} / 13.54) \quad (A2)$$

The value of the specific gravity of water at room temperature is

$$G_{H_2O} = 0.9983763 + (1.060576 \times 10^{-4}) t_{rm} - (1.593186 \times 10^{-6}) t_{rm}^2 \quad (A3)$$

The specific gravity relations were obtained from the tabulated data of Reference 10.. These equations are slightly different from those used previously.

A2 Subroutine TEMP

The relations for the evaluation of the temperatures in this subroutine from the thermocouple readings in millivolts are different from those previously used because of the substitution of iron-constantan thermocouples for the chromel-alumel type. Thus, for iron-constantan thermocouples producing a millivolt output V , and using a cold junction reference temperature, t_{cj} , the temperature relations are

$$t = t_{cj} + 0.144 + 35.77 V - 0.4518 V^2 \quad (A4)$$

for $t \leq 100^\circ\text{F}$

$$t = t_{cj} + 1.252 + 34.86 V - 0.1855 V^2 \quad (A5)$$

for $100^\circ\text{F} < t \leq 200^\circ\text{F}$

Equations (A4) and (A5) were obtained from data tabulated in Reference 11.

A3 Subroutine FLOW

The evaluation of the flow rate using the measured data from the particular flow orifices employed in the radial turbine test setup was carried out in accordance with a method developed originally by Vavra (1), after the techniques given by Stearns, et al. (5). The values thus determined by Vavra applied to a sharp-edged orifice of 2.800 inches diameter. Before this series of tests was begun, the flow orifice diameter was measured and found to be 2.7965 inches. Additionally, the conversion factors and the value of the specific gravity of mercury used herein are slightly different than those previously used, the latter being 13.54 vice 13.59. The equations given below are thus those of Vavra (1), with these

modifications introduced. Computations were made for the vena contracta taps only, although flange tap data were available, because these data give a more accurate flow rate (1).

The relation for the flow rate is

$$\dot{W} = C \propto Y_1 F_r \sqrt{\frac{P_{1vc} \Delta h_{1vc}}{T_4}} \quad (A6)$$

where:

- C - factor dependent on orifice diameter, type of pressure taps, and dimensional units
- \propto - area multiplier to account for thermal expansion of orifice
- Y_1 - factor which accounts for compressibility effects
- F_r - Reynolds number correction factor
- P_{1vc} - absolute pressure at upstream tap
- Δh_{1vc} - pressure differential across orifice
- T_4 - temperature ahead of orifice

For vena contracta taps, $C = 0.9057$.

For a stainless steel orifice:

$$\propto = 1.0 + (1.85 \times 10^{-5}) (T_4 - 532.) \quad (A7)$$

$$Y_1 = 1.0 - 0.351 \frac{\Delta h_{1vc}}{P_{1vc}} \quad (A8)$$

Also,

$$F_r = 1.0 + \frac{0.001275}{X} \quad (A9)$$

where

$$X = 0.8131 \frac{\dot{W}}{Z} \quad (A10)$$

$$Z = 1.9 + (2.4 \times 10^{-3}) (T_4 - 559.69) \quad (A11)$$

where Equation (A11) is valid for air between 50°F and 300°F.

The resulting flow rate equation used herein is then given by

$$\dot{W} = 2.2854 \propto Y_1 F_r \sqrt{\frac{P_{1VC} \Delta h_{1VC}}{T_4}} \quad (A12)$$

where: \dot{W} is in lb_m/sec

P_{1VC} , Δh_{1VC} are in in. Hg.

T_4 is in °R

and where \propto , Y_1 and F_r are as given previously.

A4 Subroutine PRESS

It has been previously mentioned that a regulated reference pressure was used on the 96-inch water manometer board. This pressure must therefore be accounted for in computing p_1 , the absolute static pressure at the rotor inlet. This is done in the equation

$$p_1 = \frac{(P_{atm} + H_{refl})(G_{Hg}) + (H_L)(G_{H_2O})}{13.54} \quad (A13)$$

where the quantity $(P_{atm} + H_{refl})$ represents the total reference pressure applied to the manometer reservoir.

A5 Method of Assembly of Input Data

The items of input data necessary in performing computations with program SCROLL are given below in the order in which they must appear on the data cards. Specific formats for the numerical entries are given in the program listing.

| <u>Card No.</u> | <u>FORTRAN</u> | <u>Description</u> |
|-----------------|----------------|---|
| 1 | NRUNS | Number of runs (clearances) to be processed |
| 2 | NPTS | Number of points (pressure ratios) in run |
| 3 | DPVC | Measured pressure differential across flow orifice, from vena contracta taps (in. Hg) |

| <u>Card No.</u> | <u>FORTTRAN</u> | <u>Description</u> |
|-----------------|-----------------|--|
| | PUVC | Measured pressure upstream of flow measuring orifice, from vena contracta taps (in. Hg gage) |
| | P5P | Measured static pressure at turbine inlet (in. Hg gage) |
| | PATM | Barometric pressure (in. Hg) |
| | HREF1 | Measured reference pressure applied to H ₂ O manometer board (in. Hg gage) |
| | H1 | Average static pressure ahead of rotor (in. H ₂ O gage) |
| | SR | Torque scale reading (lb.) |
| | TRM | Control room temperature (°F) |
| | V4 | Thermocouple reading ahead of orifice (mv.) |
| | V5 | Thermocouple reading at turbine inlet (mv.) |
| 4 | TCJ | Cold junction temperature (°F) |
| | STARE | Torque scale tare (lb.) |
| | B1 | Perpendicular distance between shroud inner extremities (in.) |

Cards 3 and 4 comprise the input data for one test point and are repeated for a total of NPTS test points for each run. Each new run begins with card 2.

TABLE A1
LISTING OF PROGRAM SCROLL

```

C PROGRAM SCROLL
  DIMENSION CPVC(10),PUVC(10),P5P(10),PATM(10),HREF1(10),H1(10),
  1SR(10),TRM(10),V4(10),V5(10),WVCP(10),PRP(10),PHIP(10),ALPH(10),
  2VEL(10),TS(10),ACH(10),PS(10)
  COMMON GHG,GWR,CFI,TCJ,STARE,T4,T5,WVC,PR,PI,PHI,ALF1,PAT,V1,T1,
  *ACH1,B1
  READ(5,10) NRUNS
  DC 99 J=1,NRUNS
  READ(5,10) NPTS
  READ(5,11) (DFVC(K),PUVC(K),P5P(K),PATM(K),HREF1(K),H1(K),SR(K),
  *TRM(K),V4(K),V5(K),K=1,NPTS)
  READ(5,12) TCJ,STARE,B1
  CLNC=(R1-.894)/2.
  WRITE(6,20) CLNC
  *WRITE(6,20) (K,DPVC(K),PUVC(K),P5P(K),PATM(K),HREF1(K),H1(K),SR(K)
  * ,TRM(K),V4(K),V5(K),K=1,NPTS)
  DO 100 K=1,NPTS
    GWR=13.039C5-1.363C3OF-3*TRM(K)
    GHG=.0983763+1.060576E-4*TRM(K)-1.593186E-6*TRM(K)**2
    CFI=70.438824*GHG/13.54
    DPV=DPVC(K)
    PUV=PUVC(K)
    P5=P5P(K)
    PAT=PATM(K)
    HREF1=HREF1(K)
    PIP=H1(K)
    S=SR(K)
    V4T=V4(K)
    V5T=V5(K)
    CALL TEMP (V4T,V5T)
    CALL FLOW (DPV,PIV)
    CALL PRESS (P5,HREF1,PIF)
    CALL ALPSI (S)
    WVCP(K)=WVC
    PRP(K)=PR
    PHIP(K)=PHI
    ALPH(K)=ALF1
    VEL(K)=V1
    TS(K)=T1
    ACH(K)=ACH1
    PS(K)=PI
    CONTINUE
  100 WRITE(6,22) (K,PRP(K),WVCP(K),PHIP(K),ALPH(K),

```



```

1 VEL(K), TS(K), ACH(K), PS(K), K=1, NPTS)
99 CONTINUE
10 FORMAT(I4)
11 FORMAT(10F7.3)
12 FORMAT(3F7.3)
20 * FORMAT(1H1, 'PROGRAM SCROLL', T74, 'D.D. WILLIAMS', //, T21,
* 'SCROLL AND GUIDE VANE TESTS OF ICP RADIAL TURBINE', //, T17, 'TABLE
* ', T53, 'CLEARANCE = ', F5.3, 'IN.', //, T41, 'INPUT DATA', //, T5, 'PT
* ', DPVC PUVV P5P PATM HREF1 H1 SR TRM
* V4 V5, //)
21 FORMAT(16, 10F8.3)
22 * FORMAT(//, T40, 'OUTPUT DATA', //, T1C, 'PT PTO/PI WVC PHI
* ALPH(1) V1 MACH1 P1, //)
23 * FORMAT(5X, 16, 2F8.3, F8.4, 3F9.2, 2F9.3)
24 * FORMAT(//19X5HTCJ -F6.2, 9X7HSTARE -F5.2, 9X4HB1 -F6.3)
RETURN
END

```

C

```

SURROUTINE TEMP (V4, V5)
COMMON GHG, GWR, CF1, TCJ, STARE, T4, T5, WVC, PR, P1, PHI, ALP1, PAT, V1, T1,
* ACH1, B1
V=V4
J=1
100 T=TCJ+J.144+35.77-V-C.4518*V**2
101 IF(T-100.) 102, 101
102 T=TCJ+1.252+34.86*V-C.1855*V**2
103 T=T+459.69
104 IF(J-1) 103, 103, 104
J=2
T4=T
V=V5
GO TO 100
104 T5=T
RETURN
END

```

C

```

SUBROUTINE FLOW (DPVC,PUVC)
COMMON GHG,GWR,CFL,TCJ,STARF,T4,T5,WVC,PR,PI,PHI,ALPI,PAT,VJ,TI,
*ACH1,R1
DVC=DPVC*GHG/13.54
PVC=(PUVC+PAT)*GHG/13.54
A=1.+1.85E-5*(T4-532.)
Z=1.9+2.4E-3*(T4-560.)
Y=1.-.351*PVC/PVC
WVC=2.2854*A*Y*SQRT(PVC*DVC/T4)
X=WVC*.8131/Z
WVC=(1.+0.001275/X)*WVC
RETURN
END

```

C

```

SUBROUTINE PRESS(PSF,HOF1,H1)
COMMON GHG,GWP,CFL,TCJ,STARE,T4,T5,WVC,PR,PI,PHI,ALPI,PAT,V1,T1,
*ACH1,B1
A=T5-459.69
CP=.23943+3.4E-6*A+2.F-8*A**2
PI=((PAT+HOF1)*GHG+H1*GWP)/13.54
PS5=(PAT+PSF)*GHG/13.54
TT=T5
100 RHO=PS5*CFL/(TT*53.3448)
VO=WVC/(RHO*3.14159*6.25/144.)
TO=T5-(VO**2)/(2.*32.174*778.16*CP)
DTT=TT-TO
TT=TO
IF(ABS(DTT)-.01)101,101,100
101 PTO=PS5+RHO*(VO**2)/(2.*32.174*CFL)
PR=PTO/PI
RETURN
END

```

C

```

SUBROUTINE ALPSI (SR)
COMMON GHG,GWR,CFI,TCJ,STAPE,T4,T5,WVC,PR,PL,PHI,ALP1,PAT,VJ,T1,
*ACH1,B1
T=T5-459.6C
GAM=1.4018-2.E-5*T
EXP=(GAM-1.)/GAM
CP=.23943+3.4E-6*T+2.E-8*T**2
G=2.*32.174*778.16*CP
RM=(SR-STAPE)*12.0
VUI=RM*32.174/(WVC*4.75)
B=T5*(1.-1./PR**EXP)
A1=2.*3.14159*4.75*B1/144.
PHI=1.
100 V1=PHI*SQRT(G*B)
TI=T5-(V1**2)/G
RHO=P1*CF1/(T1*53.3448)
VM1=WVC/(A1*RHO)
V1A=SQRT(VM1**2+VUI**2)
IF(ABS(V1-V1A)-.5)102,102,101
101 PHI=PHI-.0001
GO TO 100
102 ALP1=57.29578*ATAN(VUI/VM1)
ACH1=V1/SQRT(32.174*GAM*53.3448*T1)
RETURN
END

```

SCROLL AND GUIDE VANE TESTS OF ICP RADIAL TURBINE

TABLE A2

CLEARANCE = 0.081 IN.

| INPUT DATA | | | | | | | | | | |
|-------------|--------|--------|--------|--------|-------|--------|--------|-------------|------------|-------|
| PT | CPVC | PVVC | P5P | PATM | HREF1 | H1 | SR | TRM | V4 | V5 |
| 1 | 1.134 | 2.640 | 1.520 | 30.040 | C.C | 2.089 | 1.820 | 83.000 | 1.597 | 1.495 |
| 2 | 2.259 | 5.350 | 3.160 | 30.040 | 0.0 | 4.306 | 3.800 | 83.600 | 1.625 | 1.540 |
| 3 | 3.399 | 8.310 | 4.990 | 30.040 | 0.0 | 6.799 | 6.010 | 84.000 | 1.643 | 1.560 |
| 4 | 4.410 | 11.000 | 6.700 | 30.040 | 0.0 | 9.103 | 8.040 | 84.500 | 1.660 | 1.582 |
| 5 | 5.443 | 14.000 | 8.640 | 30.040 | 0.0 | 11.781 | 10.330 | 85.000 | 1.655 | 1.590 |
| 6 | 6.619 | 18.600 | 12.080 | 30.030 | 0.0 | 15.045 | 13.060 | 85.000 | 1.660 | 1.600 |
| 7 | 7.768 | 21.290 | 13.550 | 30.030 | C.C | 18.561 | 15.940 | 85.200 | 1.665 | 1.605 |
| 8 | 9.278 | 26.410 | 17.210 | 30.030 | 0.0 | 24.234 | 19.850 | 85.600 | 1.675 | 1.615 |
| 9 | 10.795 | 31.850 | 21.110 | 30.030 | 0.0 | 30.913 | 24.000 | 86.000 | 1.680 | 1.630 |
| 10 | 11.582 | 37.830 | 23.250 | 30.030 | C.C | 34.725 | 26.300 | 86.000 | 1.685 | 1.635 |
| TCJ - 32.00 | | | | | | | | STARE - 0.0 | R1 - 1.056 | |

| OUTPUT DATA | | | | | |
|-------------|--------|-------|--------|---------|--------|
| PT | PTO/PI | WVC | PHI | ALPH(1) | VI |
| 1 | 1.047 | 0.590 | 0.8697 | 81.72 | 254.01 |
| 2 | 1.097 | 0.855 | 0.8825 | 81.77 | 365.49 |
| 3 | 1.152 | 1.081 | 0.8954 | 81.83 | 457.18 |
| 4 | 1.203 | 1.263 | 0.8989 | 81.77 | 523.08 |
| 5 | 1.260 | 1.445 | 0.9061 | 81.76 | 587.52 |
| 6 | 1.363 | 1.666 | 0.8636 | 81.49 | 644.58 |
| 7 | 1.400 | 1.843 | 0.9148 | 81.66 | 710.85 |
| 8 | 1.499 | 2.101 | 0.9154 | 81.54 | 776.70 |
| 9 | 1.600 | 2.364 | 0.9176 | 81.41 | 835.10 |
| 10 | 1.654 | 2.567 | 0.8981 | 80.87 | 843.95 |
| | | | | | PI |
| | | | | | 30.162 |
| | | | | | 30.324 |
| | | | | | 30.506 |
| | | | | | 30.674 |
| | | | | | 30.869 |
| | | | | | 31.099 |
| | | | | | 31.357 |
| | | | | | 31.773 |
| | | | | | 32.263 |
| | | | | | 32.543 |
| | | | | | MACH1 |
| | | | | | 0.223 |
| | | | | | 0.322 |
| | | | | | 0.405 |
| | | | | | 0.466 |
| | | | | | 0.526 |
| | | | | | 0.580 |
| | | | | | 0.645 |
| | | | | | 0.710 |
| | | | | | 0.769 |
| | | | | | 0.778 |
| | | | | | T1 |
| | | | | | 538.93 |
| | | | | | 534.73 |
| | | | | | 529.13 |
| | | | | | 524.51 |
| | | | | | 518.83 |
| | | | | | 513.32 |
| | | | | | 506.01 |
| | | | | | 498.20 |
| | | | | | 490.88 |
| | | | | | 489.82 |

PROGRAM SCROLL

D.D. WILLIAMS

SCROLL AND GUIDE VANE TESTS OF ICP RADIAL TURBINE

TABLE A3

CLEARANCE = 0.072 IN.

| INPUT DATA | | | | | | | | | |
|------------|--------|--------|--------|--------|-------|--------|--------|--------|-------|
| PT | DPVC | PUVC | P5P | PATM | HREF1 | H1 | SR | TRM | V5 |
| 1 | 1.147 | 2.690 | 1.550 | 29.880 | 0.0 | 2.308 | 1.860 | 79.100 | 1.675 |
| 2 | 2.278 | 5.460 | 3.210 | 29.880 | 0.0 | 4.708 | 3.880 | 80.000 | 1.702 |
| 3 | 2.234 | 7.960 | 4.750 | 29.880 | 0.0 | 6.958 | 5.750 | 80.200 | 1.710 |
| 4 | 2.232 | 10.660 | 6.460 | 29.880 | 0.0 | 9.406 | 7.750 | 81.300 | 1.755 |
| 5 | 3.392 | 13.960 | 8.180 | 29.880 | 0.0 | 12.517 | 10.300 | 82.200 | 1.785 |
| 6 | 6.653 | 17.750 | 11.180 | 29.880 | 0.0 | 16.517 | 13.160 | 83.000 | 1.800 |
| 7 | 7.832 | 21.560 | 13.780 | 29.880 | 0.0 | 20.593 | 16.100 | 84.000 | 1.820 |
| 8 | 9.392 | 26.950 | 17.560 | 29.880 | 0.0 | 26.829 | 20.330 | 84.700 | 1.830 |
| 9 | 10.837 | 32.200 | 21.330 | 29.880 | 0.0 | 33.722 | 24.210 | 85.000 | 1.835 |
| 10 | 11.796 | 35.780 | 24.020 | 29.880 | 0.0 | 38.925 | 26.990 | 85.500 | 1.840 |

TCJ - 32.00

STARE - 0.0

B1 - 1.038

OUTPUT DATA

| PT | PTO/PI | WVC | PHI | ALPH(1) | V1 | T1 | MACH1 | PI |
|----|--------|-------|--------|---------|--------|--------|-------|--------|
| 1 | 1.048 | 0.591 | 0.8789 | 81.66 | 259.13 | 541.12 | 0.227 | 30.031 |
| 2 | 1.098 | 0.856 | 0.8929 | 81.72 | 372.74 | 537.03 | 0.328 | 30.204 |
| 3 | 1.145 | 1.047 | 0.9038 | 81.76 | 451.70 | 532.47 | 0.399 | 30.369 |
| 4 | 1.195 | 1.228 | 0.9043 | 81.69 | 518.06 | 528.60 | 0.460 | 30.546 |
| 5 | 1.257 | 1.430 | 0.9134 | 81.68 | 592.06 | 523.01 | 0.528 | 30.784 |
| 6 | 1.331 | 1.645 | 0.9116 | 81.57 | 658.04 | 517.00 | 0.590 | 31.064 |
| 7 | 1.404 | 1.843 | 0.9174 | 81.53 | 718.94 | 510.61 | 0.649 | 31.361 |
| 8 | 1.504 | 2.111 | 0.9252 | 81.47 | 791.94 | 502.04 | 0.721 | 31.817 |
| 9 | 1.599 | 2.361 | 0.9225 | 81.30 | 843.57 | 495.25 | 0.773 | 32.323 |
| 10 | 1.664 | 2.528 | 0.9249 | 81.25 | 878.58 | 490.51 | 0.809 | 32.704 |

PROGRAM SCRCLL

D.O. WILLIAMS

SCRCLL AND GUIDE VANE TESTS OF ICP RADIAL TURBINE

TABLE A4

CLEARANCE = 0.061 IN.

| INPUT DATA | | | | | | | | | | |
|--|--------|--------|--------|--------|-------|--------|--------|--------|-------|-------|
| PT | DPVC | PVVC | P5P | PATM | HPEF1 | H1 | SR | TRM | V4 | V5 |
| 1 | 1.185 | 2.785 | 1.600 | 29.970 | 0.00 | 2.512 | 1.940 | 82.000 | 1.625 | 1.540 |
| 2 | 2.393 | 5.765 | 3.390 | 29.970 | 0.00 | 5.337 | 4.100 | 82.000 | 1.630 | 1.560 |
| 3 | 4.012 | 10.015 | 6.060 | 29.970 | 0.00 | 9.401 | 7.310 | 82.000 | 1.645 | 1.590 |
| 4 | 4.610 | 11.700 | 7.130 | 29.970 | 0.00 | 11.001 | 8.510 | 83.100 | 1.635 | 1.595 |
| 5 | 5.554 | 14.410 | 8.900 | 29.970 | 0.00 | 13.866 | 10.640 | 83.600 | 1.640 | 1.605 |
| 6 | 6.720 | 17.590 | 11.310 | 29.970 | 0.00 | 17.546 | 13.350 | 83.400 | 1.642 | 1.610 |
| 7 | 7.912 | 21.880 | 13.920 | 29.970 | 0.00 | 21.975 | 16.370 | 83.000 | 1.650 | 1.620 |
| 8 | 9.405 | 26.560 | 17.580 | 29.970 | 0.00 | 28.241 | 20.320 | 83.300 | 1.660 | 1.630 |
| 9 | 10.924 | 32.500 | 21.580 | 29.970 | 0.00 | 35.484 | 24.180 | 83.300 | 1.660 | 1.630 |
| 10 | 11.886 | 36.100 | 24.170 | 29.970 | 0.00 | 40.753 | 27.080 | 83.400 | 1.660 | 1.630 |
| TCJ - 32.00 STARE - 0.0 RI - 1.016 | | | | | | | | | | |

| OUTPUT DATA | | | | | | | | | | |
|-------------|--------|-------|--------|---------|--------|--------|-------|--------|--|--|
| PT | PTO/PI | WVC | PHI | ALPH(1) | V1 | T1 | MACH1 | PI | | |
| 1 | 1.049 | 0.603 | 0.8901 | 81.55 | 265.03 | 540.00 | 0.233 | 30.127 | | |
| 2 | 1.102 | 0.883 | 0.8991 | 81.56 | 381.76 | 534.39 | 0.337 | 30.335 | | |
| 3 | 1.181 | 1.193 | 0.9100 | 81.56 | 503.00 | 526.44 | 0.448 | 30.634 | | |
| 4 | 1.263 | 1.301 | 0.9060 | 81.49 | 539.19 | 523.64 | 0.480 | 30.748 | | |
| 5 | 1.331 | 1.466 | 0.9171 | 81.41 | 597.13 | 518.91 | 0.535 | 30.057 | | |
| 6 | 1.402 | 1.671 | 0.9247 | 81.38 | 650.80 | 511.01 | 0.594 | 31.228 | | |
| 7 | 1.499 | 1.871 | 0.9271 | 81.30 | 719.26 | 505.12 | 0.653 | 31.556 | | |
| 8 | 1.599 | 2.126 | 0.9155 | 81.02 | 832.78 | 491.20 | 0.719 | 32.017 | | |
| 9 | 1.660 | 2.366 | 0.9238 | 81.02 | 871.05 | 485.77 | 0.767 | 32.548 | | |
| 10 | | | | | | | 0.806 | 32.936 | | |

PRCGRAM SCROLL

SCROLL AND GUIDE VANE TESTS OF ICP RADIAL TURBINE

D.O. WILLIAMS

TABLE A5

CLEARANCE = 0.050 IN.

| INPUT DATA | | | | | | | | | | |
|------------------------------------|--------|--------|--------|---------|--------|--------|--------|--------|-------|-------|
| PT | DPVC | PLVC | P5P | PATM | HREF1 | H1 | SP | TRM | V4 | V5 |
| 1 | 1.158 | 2.720 | 1.560 | 29.920 | 0.0 | 2.547 | 1.880 | 78.000 | 1.493 | 1.435 |
| 2 | 2.305 | 5.480 | 3.190 | 29.920 | 0.0 | 5.204 | 3.900 | 79.000 | 1.530 | 1.490 |
| 3 | 3.285 | 8.110 | 4.840 | 29.920 | 0.0 | 7.926 | 5.860 | 79.200 | 1.540 | 1.515 |
| 4 | 4.423 | 11.280 | 6.860 | 29.920 | 0.0 | 10.989 | 8.200 | 79.200 | 1.500 | 1.485 |
| 5 | 5.333 | 13.820 | 8.540 | 29.920 | 0.0 | 13.858 | 10.040 | 79.600 | 1.530 | 1.510 |
| 6 | 6.676 | 17.800 | 11.170 | 29.920 | 0.0 | 18.247 | 13.180 | 80.000 | 1.540 | 1.520 |
| 7 | 7.788 | 21.460 | 13.610 | 29.920 | 0.0 | 22.750 | 16.020 | 80.000 | 1.550 | 1.530 |
| 8 | 9.262 | 26.400 | 17.110 | 29.920 | 0.0 | 29.118 | 19.740 | 80.200 | 1.560 | 1.545 |
| 9 | 10.712 | 31.350 | 20.690 | 29.920 | 0.0 | 35.069 | 23.520 | 80.600 | 1.575 | 1.558 |
| 10 | 11.753 | 35.500 | 23.700 | 29.920 | 0.0 | 42.194 | 26.780 | 80.600 | 1.595 | 1.575 |
| TCJ - 32.00 STARE - 0.0 RI - 0.994 | | | | | | | | | | |
| OUTPUT DATA | | | | | | | | | | |
| PT | PTO/PI | WVC | PHI | ALPH(1) | V1 | T1 | MACH1 | PI | | |
| 1 | 1.047 | 0.598 | 0.8857 | 81.29 | 259.21 | 536.64 | 0.228 | 30.091 | | |
| 2 | 1.096 | 0.866 | 0.9005 | 81.29 | 370.67 | 532.69 | 0.328 | 30.284 | | |
| 3 | 1.145 | 1.063 | 0.9111 | 81.41 | 453.76 | 527.85 | 0.403 | 30.484 | | |
| 4 | 1.204 | 1.275 | 0.9112 | 81.36 | 529.32 | 520.63 | 0.473 | 30.709 | | |
| 5 | 1.251 | 1.433 | 0.9049 | 81.20 | 576.79 | 517.12 | 0.517 | 30.919 | | |
| 6 | 1.325 | 1.662 | 0.9177 | 81.20 | 652.60 | 509.70 | 0.590 | 31.241 | | |
| 7 | 1.390 | 1.854 | 0.9271 | 81.14 | 711.14 | 503.40 | 0.647 | 31.572 | | |
| 8 | 1.481 | 2.106 | 0.9249 | 81.05 | 771.79 | 496.95 | 0.707 | 32.041 | | |
| 9 | 1.574 | 2.351 | 0.9226 | 80.88 | 823.91 | 489.95 | 0.759 | 32.477 | | |
| 10 | 1.641 | 2.539 | 0.9328 | 80.92 | 868.80 | 484.21 | 0.805 | 33.002 | | |

PROGRAM SCRCLL

SCRCLL AND GUIDE VANE TESTS OF ICP RADIAL TURBINE

D.D. WILLIAMS

TABLE A6

CLEARANCE = 0.041 IN.

| INPUT DATA | | | | | | | | | | | |
|-------------|--------|--------|--------|---------|--------|--------|--------|--------|-------|-------|--|
| PT | DPVC | PLVC | P5P | PATM | HREF1 | HI | SP | TRM | V4 | V5 | |
| 1 | 1.159 | 2.700 | 1.560 | 30.010 | 0.0 | 2.694 | 1.890 | 80.000 | 1.610 | 1.530 | |
| 2 | 2.348 | 5.610 | 3.310 | 30.010 | 0.0 | 5.815 | 3.310 | 80.200 | 1.620 | 1.560 | |
| 3 | 3.549 | 8.770 | 5.260 | 30.010 | 0.0 | 9.279 | 6.310 | 80.900 | 1.625 | 1.580 | |
| 4 | 4.422 | 11.170 | 6.800 | 30.010 | 0.0 | 11.986 | 8.120 | 80.000 | 1.635 | 1.595 | |
| 5 | 5.682 | 14.810 | 9.770 | 30.010 | 0.0 | 16.047 | 10.870 | 80.100 | 1.635 | 1.598 | |
| 6 | 6.823 | 18.700 | 11.390 | 30.010 | 0.0 | 22.428 | 13.870 | 80.000 | 1.645 | 1.605 | |
| 7 | 8.094 | 22.450 | 14.390 | 30.010 | 0.0 | 25.019 | 16.750 | 81.000 | 1.675 | 1.640 | |
| 8 | 9.715 | 27.990 | 18.280 | 30.010 | 0.0 | 33.769 | 21.020 | 81.900 | 1.675 | 1.660 | |
| 9 | 11.254 | 33.650 | 22.400 | 30.010 | 0.0 | 41.769 | 25.290 | 82.000 | 1.702 | 1.675 | |
| 10 | 12.258 | 37.450 | 25.200 | 30.010 | 0.0 | 47.581 | 28.050 | 82.000 | 1.720 | 1.690 | |
| ICJ - 32.00 | | | | | | | | | | | |
| STARE - 0.0 | | | | | | | | | | | |
| R1 - 0.976 | | | | | | | | | | | |
| OUTPUT DATA | | | | | | | | | | | |
| PT | PTO/PI | WVC | PHI | ALPH(1) | V1 | T1 | MACH1 | PI | | | |
| 1 | 1.047 | 0.596 | 0.890 | 81.14 | 259.91 | 539.83 | 0.228 | 30.186 | | | |
| 2 | 1.098 | 0.874 | 0.899 | 81.15 | 374.02 | 534.83 | 0.331 | 30.415 | | | |
| 3 | 1.155 | 1.110 | 0.909 | 81.17 | 458.02 | 528.99 | 0.415 | 30.668 | | | |
| 4 | 1.199 | 1.269 | 0.914 | 81.17 | 526.87 | 524.63 | 0.469 | 30.870 | | | |
| 5 | 1.265 | 1.489 | 0.918 | 81.12 | 600.87 | 517.78 | 0.539 | 31.169 | | | |
| 6 | 1.335 | 1.704 | 0.922 | 81.06 | 666.68 | 511.08 | 0.602 | 31.522 | | | |
| 7 | 1.405 | 1.900 | 0.928 | 81.04 | 725.68 | 505.44 | 0.653 | 31.855 | | | |
| 8 | 1.503 | 2.177 | 0.933 | 80.94 | 795.34 | 497.31 | 0.723 | 32.412 | | | |
| 9 | 1.601 | 2.445 | 0.934 | 80.82 | 852.15 | 490.03 | 0.785 | 33.055 | | | |
| 10 | 1.666 | 2.620 | 0.931 | 80.69 | 882.28 | 486.20 | 0.816 | 33.481 | | | |

SCROLL AND GUIDE VANE TESTS OF ICP RADIAL TURBINE

TABLE A7
CLEARANCE = 0.030 IN.

| INPUT DATA | | | | | | | | | |
|------------|-------|--------|--------|--------|-------|--------|--------|--------|-------|
| PT | DPVC | PLVC | P5P | PATM | HREF1 | H1 | SR | TRM | V5 |
| 1 | 0.840 | 2.000 | 1.150 | 30.000 | 0.0 | 2.096 | 1.360 | 75.200 | 1.390 |
| 2 | 0.352 | 5.670 | 3.350 | 30.000 | 0.0 | 6.133 | 4.000 | 76.000 | 1.420 |
| 3 | 0.228 | 7.900 | 4.750 | 30.000 | 0.0 | 8.606 | 5.670 | 76.300 | 1.435 |
| 4 | 0.555 | 10.900 | 6.620 | 30.000 | 0.0 | 12.080 | 7.900 | 78.000 | 1.440 |
| 5 | 0.538 | 14.450 | 8.920 | 30.000 | 0.0 | 16.384 | 10.630 | 78.400 | 1.485 |
| 6 | 0.202 | 18.950 | 11.980 | 30.000 | 0.0 | 22.088 | 13.940 | 78.800 | 1.505 |
| 7 | 0.802 | 22.830 | 14.600 | 30.000 | 0.0 | 27.082 | 16.940 | 78.800 | 1.520 |
| 8 | 0.295 | 28.550 | 18.650 | 30.000 | 0.0 | 35.422 | 21.450 | 79.000 | 1.555 |
| 9 | 0.406 | 34.000 | 22.550 | 30.000 | 0.0 | 45.122 | 25.657 | 79.300 | 1.570 |
| 10 | 0.473 | 37.600 | 25.400 | 30.000 | 0.0 | 50.191 | 28.350 | 79.800 | 1.595 |

TCJ - 32.00

STARE - 0.0

RI - 0.954

| OUTPUT DATA | | | | |
|-------------|--------|-------|--------|---------|
| PT | PTO/PI | WVC | PHI | ALPH(I) |
| 1 | 1.034 | 0.508 | 0.8848 | 80.97 |
| 2 | 1.099 | 0.881 | 0.8956 | 80.95 |
| 3 | 1.139 | 1.056 | 0.9063 | 80.96 |
| 4 | 1.193 | 1.255 | 0.9174 | 81.01 |
| 5 | 1.256 | 1.475 | 0.9254 | 80.96 |
| 6 | 1.339 | 1.728 | 0.9193 | 80.78 |
| 7 | 1.407 | 1.929 | 0.9280 | 80.73 |
| 8 | 1.504 | 2.216 | 0.9366 | 80.65 |
| 9 | 1.597 | 2.477 | 0.9432 | 80.65 |
| 10 | 1.663 | 2.654 | 0.9342 | 80.46 |

| T1 | MACH1 | P1 |
|--------|-------|--------|
| 536.79 | 0.195 | 30.147 |
| 529.72 | 0.332 | 30.442 |
| 525.59 | 0.394 | 30.623 |
| 519.67 | 0.464 | 30.873 |
| 514.43 | 0.532 | 31.189 |
| 507.69 | 0.602 | 31.603 |
| 501.38 | 0.659 | 31.975 |
| 493.05 | 0.733 | 32.589 |
| 485.97 | 0.790 | 33.302 |
| 482.96 | 0.818 | 33.673 |

PROGRAM SCROLL

D.D. WILLIAMS

SCROLL AND GUIDE VANE TESTS OF ICP RADIAL TURBINE

TABLE A8

CLEARANCE = 0.024 IN.

| INPUT DATA | | | | | | | | | | | |
|------------------------------------|--------|--------|--------|--------|-------|--------|--------|--------|-------|-------|--|
| PT | DPVC | PVVC | P5P | PATM | HREF1 | H1 | SR | TRM | V4 | V5 | |
| 1 | 1.237 | 2.920 | 1.700 | 29.960 | 0.0 | 3.193 | 2.020 | 72.900 | 1.520 | 1.435 | |
| 2 | 2.295 | 5.500 | 3.250 | 29.960 | 0.0 | 6.135 | 3.890 | 73.900 | 1.535 | 1.465 | |
| 3 | 3.391 | 8.340 | 5.000 | 29.960 | 0.0 | 9.529 | 5.990 | 74.500 | 1.540 | 1.495 | |
| 4 | 4.514 | 11.400 | 6.930 | 29.960 | 0.0 | 13.098 | 8.270 | 75.100 | 1.543 | 1.525 | |
| 5 | 5.747 | 14.930 | 9.230 | 29.960 | 0.0 | 17.457 | 10.960 | 75.800 | 1.560 | 1.523 | |
| 6 | 6.904 | 18.540 | 11.660 | 29.960 | 0.0 | 21.845 | 13.680 | 76.200 | 1.580 | 1.545 | |
| 7 | 8.201 | 22.750 | 14.570 | 29.970 | 0.0 | 27.859 | 17.000 | 77.000 | 1.590 | 1.555 | |
| 8 | 9.913 | 28.600 | 18.200 | 29.970 | 0.0 | 35.859 | 21.440 | 77.900 | 1.600 | 1.565 | |
| 9 | 11.395 | 34.050 | 22.700 | 29.970 | 0.0 | 44.934 | 25.670 | 78.800 | 1.610 | 1.580 | |
| 10 | 12.397 | 37.900 | 25.420 | 29.970 | 0.0 | 51.838 | 28.210 | 79.000 | 1.625 | 1.598 | |
| TCJ - 32.00 STARE - 0.0 R1 - 0.942 | | | | | | | | | | | |

| OUTPUT DATA | | | | | | |
|-------------|--------|-------|--------|---------|--------|--------|
| PT | PTO/PI | WVC | PHI | ALPH(1) | V1 | T1 |
| 1 | 1.050 | 0.619 | 0.8922 | 80.87 | 269.11 | 536.20 |
| 2 | 1.096 | 0.866 | 0.9036 | 80.87 | 370.45 | 531.84 |
| 3 | 1.146 | 1.083 | 0.9134 | 80.87 | 455.73 | 527.01 |
| 4 | 1.200 | 1.288 | 0.9181 | 80.83 | 529.07 | 521.34 |
| 5 | 1.263 | 1.502 | 0.9242 | 80.79 | 601.13 | 515.18 |
| 6 | 1.329 | 1.701 | 0.9260 | 80.74 | 662.65 | 509.46 |
| 7 | 1.405 | 1.923 | 0.9349 | 80.74 | 728.65 | 502.16 |
| 8 | 1.492 | 2.215 | 0.9469 | 80.60 | 797.81 | 493.72 |
| 9 | 1.600 | 2.474 | 0.9515 | 80.55 | 855.57 | 485.28 |
| 10 | 1.658 | 2.650 | 0.9533 | 80.33 | 877.98 | 483.67 |
| MACH1 PI | | | | | | |
| | | | | | | |
| | | | | | | |
| | | | | | | |
| | | | | | | |
| | | | | | | |
| | | | | | | |
| | | | | | | |
| | | | | | | |
| | | | | | | |

PROGRAM SCROLL
 SCROLL AND GUIDE VANE TESTS OF ICP RADIAL TURBINE
 D.D. WILLIAMS

TABLE A9
 CLEARANCE = 0.015 IN.

| INPUT DATA | | | | | | | | | |
|------------|--------|--------|--------|--------|-------|--------|--------|--------|-------|
| PT | DPVC | PUVC | PSP | FATM | HREF1 | H1 | SR | TRM | V5 |
| 1 | 1.309 | 3.070 | 1.780 | 30.120 | 0.0 | 3.548 | 2.120 | 75.000 | 1.545 |
| 2 | 2.428 | 5.820 | 3.430 | 30.120 | 0.0 | 6.792 | 4.120 | 76.000 | 1.562 |
| 3 | 3.503 | 8.590 | 5.130 | 30.120 | 0.0 | 10.197 | 6.170 | 76.900 | 1.580 |
| 4 | 4.611 | 11.960 | 7.090 | 30.120 | 0.0 | 13.879 | 8.440 | 77.200 | 1.590 |
| 5 | 5.776 | 14.900 | 9.250 | 30.120 | 0.0 | 18.168 | 10.970 | 78.100 | 1.605 |
| 6 | 7.046 | 18.050 | 11.910 | 30.060 | 0.0 | 23.169 | 13.980 | 79.000 | 1.620 |
| 7 | 8.328 | 23.050 | 14.840 | 30.060 | 0.0 | 28.109 | 17.240 | 79.200 | 1.615 |
| 8 | 9.992 | 28.890 | 18.810 | 30.060 | 0.0 | 38.719 | 21.790 | 80.100 | 1.570 |
| 9 | 11.853 | 35.650 | 23.810 | 30.060 | 0.0 | 50.909 | 26.050 | 80.100 | 1.570 |
| 10 | 12.683 | 38.820 | 26.150 | 30.060 | 0.0 | 56.909 | 29.050 | 80.600 | 1.580 |

TCJ - 32.00 STARE - 0.0 R1 - 0.924

| OUTPUT DATA | | | | | |
|-------------|--------|-------|--------|---------|--------|
| PT | PTO/P1 | WVC | PHI | ALPH(1) | V1 |
| 1 | 1.052 | 0.639 | 0.8542 | 80.60 | 273.91 |
| 2 | 1.099 | 0.894 | 0.9090 | 80.68 | 379.91 |
| 3 | 1.147 | 1.104 | 0.9177 | 80.67 | 460.69 |
| 4 | 1.202 | 1.305 | 0.9201 | 80.64 | 533.13 |
| 5 | 1.260 | 1.507 | 0.9262 | 80.61 | 600.20 |
| 6 | 1.332 | 1.724 | 0.9305 | 80.58 | 668.98 |
| 7 | 1.404 | 1.943 | 0.9397 | 80.56 | 732.03 |
| 8 | 1.503 | 2.230 | 0.9447 | 80.49 | 802.56 |
| 9 | 1.612 | 2.553 | 0.9462 | 80.36 | 865.81 |
| 10 | 1.660 | 2.698 | 0.9440 | 80.26 | 888.48 |

| T1 | MACH1 | P1 |
|--------|-------|--------|
| 536.85 | 0.241 | 30.374 |
| 531.94 | 0.336 | 30.610 |
| 527.15 | 0.409 | 30.858 |
| 522.01 | 0.476 | 31.128 |
| 516.20 | 0.539 | 31.441 |
| 508.98 | 0.604 | 31.747 |
| 493.09 | 0.666 | 32.160 |
| 484.07 | 0.737 | 32.843 |
| 481.50 | 0.802 | 33.771 |
| | 0.826 | 34.225 |

APPENDIX B

PROGRAM RADIAL

Program RADIAL computes the referred flow rate, head coefficient, degree of reaction, relative and absolute rotor inlet flow angles, velocity and loss coefficients for the scroll and guide vanes, referred moment, absolute discharge flow angle, velocity and loss coefficients for the rotor, and efficiencies from the torque, speed, mass flow rate, and the pressure and temperature data obtained during the active rotor tests. The calculation technique generally follows that given in the theory of Section 4.3. It can process any number of clearances (sets) and any number of pressure ratios (runs) per clearance with a maximum of ten different speed settings (points) per run. A listing of program RADIAL is given in Table B1.

In program RADIAL, use was made of temporary memory disc storage of the input data in order to avoid the awkward procedure of subscripting the input variables. This procedure permits the processing and printing of the input data on a point-by-point basis and the presentation of the results in a compact, tabular form. Appropriate comments appear in the main program at the points where this procedure was used. The additional control cards required to implement this technique and to obtain necessary additional memory core storage space are shown in Table B2. As the table indicates, these cards are inserted just ahead of the data cards in the assembled deck.

The torque calibration data used for all runs are given in Table B3. The input and output values resulting from the five sets of test data are presented in Tables B4 through B13.

B1 Subroutines TEMP and FLOW

These subroutines perform the same functions as in program SCROLL, namely those of obtaining temperatures from the thermocouple readings and calculating mass flow rate, respectively. Subroutine TEMP has been expanded to include calculation of the temperatures of the bearing lubricating oil at the inlet and at the discharge of each bearing. However for reasons discussed in Section 4, these values were not used in this experiment.

B2 Subroutine PRESS

Subroutine PRESS establishes the total-to-static pressure ratios across the scroll and guide vanes (P_{to}/p_1) and across the turbine (P_{to}/p_2) and the ratio p_1/p_2 . An iteration process is necessary in order to determine an average value of the total pressure at the turbine inlet, P_{to} . Three relations are used to accomplish this, these being the gas law,

$$\rho_o = C_{f1} \frac{P_o}{R_g T_o} \quad (B1)$$

the continuity equation,

$$\dot{V}_o = \frac{\dot{W}}{\rho_o A_5} \quad (B2)$$

and the energy equation,

$$T_o = T_{to} - \frac{V_o^2}{2gJc_p} \quad (B3)$$

where A_5 is the area of the five-inch inlet pipe and C_p is the specific heat of air at the temperature T_{to} . Using T_{to} as a first approximation of ρ_o , an initial value of V_o is found, and from this, by Equation (B3), a new value of T_o . The iteration continues until a difference of 0.01

degrees or less exists between any two successive values of T_0 . Since velocities are low, the total pressure P_{t0} is then obtained from

$$P_{t0} = P_0 + \frac{\rho_0 V_0^2}{2 g C_{f1}} \quad (B4)$$

B3 Subroutine EDC

This subroutine computes the mean values of γ and C_p based on the arithmetic mean of total turbine inlet and static isentropic discharge temperatures. From Reference 3, the variations of γ and C_p with temperature are

$$\gamma = 1.4018 - (2 \times 10^{-5}) t \quad (B5)$$

$$C_p = 0.23943 + (3.4 \times 10^{-6}) t + (2 \times 10^{-8}) t^2 \quad (B6)$$

These relations were originally obtained from data tabulated in Reference 12 and are valid from approximately 40°F to 170°F.

The values of γ_{avg} and $C_{p(avg)}$ correspond to the average temperature through the turbine based on an isentropic expansion. This average temperature, t , is given by

$$t = (T_{t0} - 459.69) - \frac{\Delta T_{is}}{2} \quad (B7)$$

where

$$\Delta T_{is} = T_{t0} \left[1 - (P_2 / P_{t0})^{\frac{\gamma-1}{\gamma}} \right] \quad (B8)$$

Using an iteration process, the first approximation of ΔT_{is} is based on a value of γ corresponding to T_{t0} . The value of t resulting from Equation (B6) is compared with the previous value of t in each iteration until the difference between any two successive values of t is less than

1.0°. Using the final value of t , values of γ_{avg} , $C_{P(avg)}$, and ΔT_{is} are computed from Equations (B5), (B6), and (B8), respectively. The reference parameter Θ , given by

$$\Theta = (\gamma_{avg}/1.4) (T_5/518.7) \quad (B9)$$

is also computed in this subroutine.

The subscript indicating the average values of γ and C_p will be dropped in subsequent discussions. The average values of these quantities are assumed in the remainder of the program unless otherwise stated.

B4 Subroutines TORQ and DYNA

These subroutines compute the net torque produced by the turbine by evaluating the bearing friction moment and the torque measured by the dynamometer.

In subroutine TORQ, the bearing friction moment is evaluated from turbine rpm by Equations (27), (28), and (29). The net moment is calculated by Equation (30), where the dynamometer torque output is found in subroutine DYNA, called from subroutine TORQ.

Subroutine DYNA determines the torque from the dynamometer calibration data obtained for each run. These data are tabulated in Table B3 for all runs.

The values of the torque calibration data constitute a one-dimensional array with five elements, representing the torque scale reading for loads of zero to 400 inch-pounds, respectively, taken at 100 inch-pound intervals. Thus, TCD(1) represents the torque scale readout value for the no load condition. Using a DO loop with index I , the torque indicator reading for the test point being processed, TQ , is compared with the values of TCD(I) to determine the interval (I , $I+1$) within which TQ lies. Since

the calibration curve data are very nearly linear, the torque is computed assuming a straight line approximation between TCD(I) and TCD(I-1), by the equation

$$T = 100(I-1) + 100 \left[\frac{TQ - TCD(I)}{TCD(I+1) - TCD(I)} \right] \quad (B10)$$

This procedure was adapted from that used by Riley (3).

B5 Subroutine TURB

The turbine performance parameters described in Section 4 are calculated by subroutine TURB in a manner which follows the theory previously given. No iterations are involved, and the equations used are self-explanatory. Therefore, the steps will not be discussed here. The velocity coefficient, ϕ , and the absolute rotor inlet flow angle, α_1 , are provided from subroutine PHIAL, for which TURB is the calling subroutine.

B6 Subroutine PHIAL

This subroutine calculates the values of ϕ , α_1 , V_1 , and ζ_N , from the results of program SCROLL. The values of γ and C_p used are based on the total inlet temperature, rather than the average temperature as computed in subroutine EDC, because the values of ϕ and α_1 obtained in program SCROLL were computed in this manner.

The values of ϕ and α_1 are obtained from Equations (13) and (14), for which the entering arguments are CLNC, the axial clearance, and ACH1, or M_1 , the Mach number at the rotor inlet. Since V_1 and T_1 are not known at this point in the computations, they must be obtained by iteration. An initial value of V_1 is obtained from Equation (4) by assuming $\phi = 1.0$, and initial values of T_1 and M_1 are obtained from Equations (35) and (36), respectively. Using this value of M_1 , called ACHIA, and CLNC, a value of

ϕ , called PHIA, is obtained from Equation (13). The assumed value of ϕ is reduced in increments of 0.001 until succeeding values of ϕ and ϕ_A differ by no more than 0.001. Thus, values of V_1 , M_1 , and ϕ are established, and α_1 is then computed from Equation (14). The loss coefficient for the scroll and guide vanes, ζ_N , is then obtained from Equation (12).

B7 Subroutine REFER

This subroutine computes the referred speed, referred flow rate, and referred moment in accordance with Equations (60), (61), and (62), respectively.

B8 Method of Assembly of Input Data

In order to facilitate future use of program RADIAL, the order of assembly of the input data cards is given. The actual formats for the numerical entries may be obtained directly from the program listing. All items of data are given in the order in which they must appear on the data cards. For convenience, the symbols are redefined.

| <u>Card No.</u> | <u>FORTTRAN</u> | <u>Description</u> |
|-----------------|-----------------|--|
| 1 | NSETS | Number of sets of data (clearances to be processed) |
| 2 | CLNC | Clearance for set |
| 3 | NRUNS | Number of runs (pressure ratios) in data set |
| 4 | TCD | Torque calibration data for run (5 values). |
| 5 | NPTS | Number of data points (speeds) in run |
| 6 | RPM | Measured turbine speed (rpm) |
| | TQ | Torque indicator reading (counts) |
| | PUVC | Measured pressure upstream of flow measuring orifice, from vena contracta taps (in. Hg gage) |

| <u>Card No.</u> | <u>FORTTRAN</u> | <u>Description</u> |
|-----------------|-----------------|--|
| | P5P | Measured static pressure at turbine inlet (in. Hg gage) |
| | H1 | Average static pressure ahead of rotor (in H ₂ O gage) |
| | DPVC | Measured pressure differential across flow orifice, from vena contracta taps (in. Hg) |
| | PATM | Barometric pressure (in. Hg) |
| | HREF1 | Measured reference pressure applied to water manometer board (in. Hg gage) |
| | V4 | Thermocouple reading ahead of orifice (mv.) |
| | V5 | Thermocouple reading at turbine inlet (mv.) |
| 7 | V20 | Thermocouple reading at lube oil inlet (mv.) |
| | V21 | Thermocouple reading at lube oil discharge from right bearing (mv.) |
| | V22 | Thermocouple reading at lub oil discharge from left bearing (mv.) |
| | TRM | Control room temperature (°F) |
| | TCJ | Cold junction temperature (°F) |

Cards 6 and 7 comprise the input data for one test point and are repeated for a total of NPTS test points for each run. Each new run begins with card 4, and each new set begins with card 2.

TABLE B1

www

```

C WRITE INPLT DATA.
  WRITE(6,7) J,K,RPM(K),TQ(K),PUVC(K),P5P(K),H1(K),DPVC(K),PATM(K),
  *HREF1(K),V4(K),V5(K),V20(K),V21(K),V22(K),TRM(K),TCJ(K)
  7 FORMAT(2X,2I3,1X,F7.0,2X,F6.0,3F8.2,F9.3,2F8.2,5F8.3,2F7.1)
  IF(K.EQ.NPTS) GC TO R
    GC TC 12
  R WRITE(6,1C3)
  1C3 FORMAT(/)
  13 CONTINUE
C WRITE DATA FOR CNE RUN CN TEMPORARY DATA SET.
  WRITE(8)(RPM(I),TC(I),PUVC(I),P5P(I),H1(I),DPVC(I),PATM(I),HREF1(I)
  *,V4(I),V5(I),V20(I),V21(I),V22(I),TRM(I),TCJ(I),I=1,NPTS)
  12 CONTINUE
C WRITE HEADING FOR PRINTOUT OF RESULTS.
  WRITE(6,2C0)
  2C0 FORMAT(1F1,///,T44,'PERFORMANCE EVALUATION OF ICP RADIAL TURRINE',
  *///)
  WRITE(6,2C1) CLNC
  2C1 FORMAT(T22,'TABLE',T61,'OUTPUT DATA',T91,'CLEARANCE = ',F5.3,1X,
  *,IN,///)
  WRITE(6,2C2)
  2C2 FORMAT(T25,'REDUCED TC STANDARD AIR IN ACCORDANCE WITH NASA METHOD
  *,',T25,'TCTAL INLET PRESS. = 14.7 PSIA, TCTAL INLET TEMPERATURE',
  *,',T35,'= 518.7 DEG.R., GAMMA = 1.4, CP = 0.24 BTU/LBM-DEG.F.,//)
  WRITE(6,2C3)
  2C3 FORMAT(/,T76,'NO BEARING LCASSES',T106,'MAXIMUM BEARING LOSSES',/,
  *T69,/,T10,'PRESS REF. REF. HEAD DEG ANGLE ANGLE VEL LOS
  *S',/,T2,'RUN/PT REF ANGLE ANGLE VEL LOSS EFF
  *IC-',/,T2,'RATIO SPEED FLOW COEFF REACT ALPHA1 BETAL CO
  *EFF CCEFF WCM ALF20 CCEFF IENCY DEG GV ROTOR',/)
  *EFF IENCY',/,T17,'RPM FT.LR DEG
  *LB CEG RCTOR',/)
  WRITE(6,2C4)
  2C4 FORMAT(T2,/,
  *-----,
  *REWIND 8
C PROCESS DATA POINTS.
DO 21 J=1,NRUNS
C READ TOPQUE CALIBRATION DATA FROM TEMPORARY DATA SET.
  READ(8)(TCD(I),I=1,5)
  READ(8) NPTS
C READ DATA FOR CNE RUN FROM TEMPORARY DATA SET.
  READ(8)(PPM(I),TQ(I),FUVVC(I),P5P(I),H1(I),DPVC(I),PATM(I),HREF1(I)

```



```

* V4(I), V5(I), V20(I), V21(I), V22(I), TRM(I), TCJ(I), I=1, NPTS)
WRITE(6,205)
205 FORMAT(/)
DO 22 K=1, NPTS
  GHG=13.63905-1.363030E-3*TRM(K)
  GWR=.9983763+1.060576E-4*TRM(K)-1.593186E-6*TRM(K)**2
  CF1=70.428824*GHG/13.54
  CALL TEMP (V4(K), V5(K), V20(K), V21(K), V22(K), TCJ(K))
  CALL FLCW (GHG, DPVC(K), PUVC(K), PATM(K))
  CALL PRESS (PATM(K), HREF1(K), GHG, GWR, H1(K), P5P(K), CF1)
  CALL EDC (THETA)
  CALL TCRC (RPM(K), TCD, TQ(K))
  CALL TURB (RPM(K), CLNC)
  CALL REFER (RPM(K), THETA, GHG)
C WRITE OUTPUT DATA.
  WRITE(6,9) J,K, PR2, RPWR, WVCR, HEAD, DR, ALPH1, RETAI, PHI, ZETAN, TR, ALF2
  * PSI, ZETR, ETA, TNETR, ALF2L, PSIL, ZETRL, ETAL
  9 FORMAT(2I3, F8.3, F7.0, F7.3, 2F6.3, F6.2, F7.2, 2F6.3,
  * F6.2, F8.2, F7.2, 2F6.3, F6.2)
  22 CONTINUE
  21 CONTINUE
  11 RETURN
END

```

```

C SUBROUTINE TEMP (V4, V5, V20, V21, V22, TCJ)
C CALCULATES TEMPERATURES FROM THERMOCOUPLE READINGS.
C THERMOCOUPLE EQUATIONS VALID FOR IRON-CONSTANTAN ONLY.
COMMON T4, T5, T20, T21, T22, WVC, P1, PTO, PR1, PR2, PSR, DTIS,
  * XP, TNETR, ROISP, TETA, ETAL, ACH1, PHI, V1, ALPH1, ZETAN, BETAI, PSI, PSIL,
  * ZETR, ZETRL, TR, TNETR, ALF2, ALF2L, RPWR, WVCR, BFM, HEAD, DR
DO 122 J=1,5
  GO TO (110,111,112,113,114), J
110 V=V4
111 GC TO 123
112 V=V5
113 GC TO 123
114 V=V20

```

```

113 GC TC 123
114 V=V21 GC TC 123
115 V=V22
116 T=TCJ+C.144+35.77*V-0.4518*V**2
117 IF(T.LE.100.) GO TO 115
118 T=TCJ+1.252+34.86*V-0.1855*V**2
119 IF(J.GT.2) GC TC 116
120 T=T+455.69
121 GO TO (117,118,119,120,121),J
122 T4=T GC TC 122
123 T5=T GC TC 122
124 T20=T GC TC 122
125 T21=T GC TC 122
126 T22=T GC TC 122
127 CONTINUE
128 RETURN
129 END

```

```

C CAL SUBROUTINE FLOW (GHG,DPVC,PVVC,PATM)
CALCULATES FLOW RATE FROM ORIFICE MEASUREMENTS.
COMMON T4,T5,T20,T21,T22,WVC,P1,PTO,PR1,PR2,PSR,DTIS,DHIS,CP,GAM,E
*XP,TNET,RCSP,T,FETA,ETAL,ACH1,PHI,V1,ALPH1,ZETAN,RETAL,PSI,PSIL,
*ZETR,ZETPL,TR,TNETR,ALF2,ALF2L,RPMR,WVCR,BFM,HEAD,DR
DVC=DPVC*GHG/13.54
PVC=(PLVVC+PATM)*GHG/13.54
A=1.+1.85E-5*(T4-532.)
Z=1.9+2.4E-3*(T4-560.)
Y=1.-.351*DVC/PVC
WVC=.2+.2854*A*Y*SQRT(PVC*DVC/T4)
X=WVC*.8131/Z
WVC=(1.+0.001275/X)*WVC
RETURN
END

```

```

C  SUBROUTINE PRESS (PATM,HREF1,GHG,GWR,H1,P5P,CF1)
CALCULATES INLET TOTAL PRESSURE AND PRESSURE RATIOS WITHIN TURBINE.
COMMON T4,T5,T20,T21,T22,WVC,P1,PTO,PR1,PR2,PSR,DTIS,DHIS,CP,GAM,E
*XP,TNET,ROSP,T,ETA,ETAL,ACH1,PHI,V1,ALPH1,ZETAN,BETAL,PSI,PSIL,
*ZETR,ZETRL,TR,TNETR,ALF2,ALF2L,RPMR,WVCR,BFM,HEAD,DR
A=T5-459.69
CP5=.23943+3.4E-6*A+2.E-8*A**2
P1=((PATM+HREF1)*GHG+(H1*GWR))/13.54
PS5=(PATM+P5F)*GHG/13.54
TT=T5
100 RHO=PS5*CF1/(TT*53.3448)
VO=WVC/(RHO*3.14159*6.25/144.)
TO=T5-(VC**2)/(2.*32.174*778.16*CP5)
DTT=TT-TC
TT=TO
IF(ABS(CIT)-.01) 101,101,100
101 PTO=PS5*RHC*(VO**2)/(2.*32.174*CF1)
PR1=PTC/P1
PR2=PTC/(PATM*GHG/13.54)
PSR=P1/(PATM*GHG/13.54)
RETURN
END

```

```

C  SUBROUTINE ECC (THETA)
CALCULATES AVERAGE TEMP. FOR DETERMINATION OF CP,GAMMA, AND SQ. ROOT
OF TEMP. RATIO (THETA), AND ISENTROPIC ENTHALPY DROP (DHIS).
COMMON T4,T5,T20,T21,T22,WVC,P1,PTO,PR1,PR2,PSR,DTIS,DHIS,CP,GAM,E
*XP,TNET,ROSP,T,ETA,ETAL,ACH1,PHI,V1,ALPH1,ZETAN,BETAL,PSI,ZETAR,AL
*F20,RPMR,WVCR,TNETR,BFM,HEAD,DR
A=T5-459.69

```

```

105 GA=1.4C1E-2.E-5*A
   EX=(GA-1.)/GA
   DT=T5*(1.-1./PR2**EX)
   AA=T5-459.69-DT/2.
   AAA=ABS(AA-A)
   IF(AAA-1.) 1C7,107,1C6
106 A=AA
   GC TG 1C5
1C7 GAM=GA
   EXP=EX
   DTIS=CT
   CP=.23942+3.4E-6*AA+2.E-8*AA**2
   DHIS=CP*DTIS
   IF(GAM*T5) 2C50,2C51,2C51
2C50 WRITE(6,2052) K,GAM,T5
2052 FORMAT(//,6X,I4,2F8.3)
2051 CONTINUE
   THETA=(GAM/1.4)*(T5/518.7)
   RETURN
   END

```

```

C  SUBROUTINE TCRG (RPM,ICD,TQ)
CALCULATES NET TORQUE (MEASURED PLUS THAT DUE TO BEARING FRICTION).
DIMENSION TCD(5)
COMMON T4,T5,T2C,T21,T22,WVC,P1,PTO,PR1,PR2,PSR,DTIS,DHIS,CP,GAM,E
*XP,TNET,ROSP,T,ETA,ETAL,ACH1,PHI,V1,ALPH1,ZETAN,BETA1,PSI,PSIL,
*ZETR,ZETRL,TR,TNETR,ALF2,ALF2L,RPMR,WVCR,BFM,HEAD,DR
ROSP=3.14159*RPM/30.
C  CCMPUTE BEARING FRICTION MCMNT FROM COAST-DOWN DATA OF VAVRA, FOR
   MAXIMUM LCSS CONDITION.
   IF(RPM.LE.10500.) GO TO 99
   HPF=-.6+((.17143)*(RPM/1000.)-(4.898E-3)*(RPM/1000.-10.5)**2
   GC TO 1CC
99 HPF=-.6+((.17143)*(RPM/1000.)
100 BFM=(HPF*550.)/RCSP
   CALL CYNA (TC,TCD,T)
   TNET=T+BFM
   RETURN

```


END

```

C SUBROUTINE DYNA (TQ,TCD,T)
C CALCULATES DYNAMOMETER TORQUE FROM TORQUE READOUT AND TORQUE CAPSULE
C CALIBRATION DATA.
C DIMENSION TCD(5)
DO 100 I=1,5
IF (TCD(I)-TQ) 100,100,101
100 CONTINUE
AI=100.*(I-1)
T=AI+100.*((TQ-TCD(I))/(TCD(I+1)-TCD(I)))
T=T/12.
RETURN
END

```

```

C SUBROUTINE TURB (RPM,CLNC)
C CALCULATES HEAD COEFFICIENT, LOSS COEFFICIENTS, EFFICIENCIES, AND FLOW
C ANGLES.
COMMON T4,T5,T2C,T21,T22,WVC,P1,PTO,PR1,PR2,PSR,DTIS,DHIS,CP,GAM,E
*XP,TNET,ROSP,T,ETA,ETAL,ACH1,PHI,V1,ALPH1,ZETAN,BETA1,PSI,PSIL,
*ZETR,ZETRL,TR,TNETR,ALF2,ALF2L,RPMR,WVCR,8FM,HEAD,DR
DTW=(TNET*ROSP)/(CP*WVC*778.16)
ETAL=CTH/DTIS
DTWNL=(T*RCSF)/(CP*WVC*778.16)
ETA=DTWNL/DTIS
CC=SQRT(2.*32.174*778.16*CP*DTIS)
D1=9.40
U1=3.14159*RFM*D1/720.
CC=CC/U1
HEAD=CC**2
DR=1.-(T5/DTIS)*(1.-(1./PR1)**EXP)

```

```

C THE LETTER U AT END OF VARIABLE NAME INDICATES DIVISION BY U1.

CALL PHIAL (CLAC)
V1U=V1/U1
X=ALPH1/57.29578
V1U=V1U*SIN(X)
W1U=V1U-1.
VM1U=V1U*CCS(X)
C W1U12=(W1/U1)**2
W1U12=VM1U**2+W1U**2
Y=W1U/V1U
BET=ATAN(Y)
BETA1=BET*57.29578
R1=4.7
R20=2.54
VU2U=(R1/R20)*((V1U-(ETA/2.)*HEAD)
VU2UL=(R1/R20)*((V1U-(ETAL/2.)*HEAD)
C BET20 = -69.85 DEGREES.
BET20=(-69.85)/57.29578
W20U=(VU2U-R20/R1)/SIN(BET20)
W20UL=(VU2UL-R20/R1)/SIN(BET20)
C W20TU=W20CTH/U1
W20TU=SQRT(DR*HEAD+(VM1U**2)+((R20/R1)**2)-1.)
PSI=W20U/W20TU
PSIL=W20UL/W20TU
ZETRL=1.-PSI**2
ZETRL=1.-PSIL**2
VM2U=W20U*CCS(BET20)
VM2UL=W20UL*CCS(BET20)
ALF2=57.29578*ATAN(VU2U/VM2U)
ALF2L=57.29578*ATAN(VU2UL/VM2UL)
ETA=100.*ETA
ETAL=100.*ETAL
RETURN
END

```

```

C SUBROUTINE PHIAL (CLNC)
C CALCULATES VALUES OF PHI, ALPHA, V1, ZETAN, FROM RESULTS OF PROGRAM
  SCRCLL.
  COMMON T4,T5,T20,T21,T22,WVC,P1,PTO,PR1,PR2,PSR,DTIS,CHIS,CP,GAM,E
  *XP,TNET,ROSP,T,ETA,ETAL,ACH1,PHI,V1,ALPH1,ZETAN,BETAI,PSI,PSIL,
  *ZETR,ZETRL,TR,TNETR,ALF2,ALF2L,RPMR,WVCR,BFM,HEAD,DR
  A=T5-.459.69
  GAMMA=1.4018-2.E-5*A
  EXP=(GAMMA-1.)/GAMMA
  CP5=.23943+3.4E-6*A+2.E-8*A**2
  G=2.*32.174*778.16*CP5
  B=T5*(1.-1./PR1**EXP)
  PHI=1.
  100 V1=PHI*.SQRT(G*B)
      T1=T5-(V1**2)/G
      ACH1A=V1/SQRT(32.174*GAMMA*53.3448*T1)
      PHIA=((.92473)*(1.01433-1.24601*CLNC+24.06839*CLNC**2-180.36258*CLN
      *C**3)*(0.53149+.18292*ACH1A-.09202*ACH1A**2)
      IF(ABS(PHI-PHIA)-.0001) 102,102,101
  101 PHI=PHI-.0001
      GO TO 100
  102 ACH1=ACH1A
      PHI=PHIA
      ALPH1=(81.762)*((.98267+.26958*CLNC-.65080*CLNC**2)*(.99624+.02223*
      *ACH1-.02940*ACH1**2)
      ZETAN=1.-PHI**2
      RETURN
      END

```

```

C SUBROUTINE REFER (RPM,THETA,GHG)
C COMPUTES SPEED, NET MOMENT, FLOW RATE, REDUCED TO STANDARD AIR IN
  ACCORDANCE WITH NASA METHOD.
  COMMON T4,T5,T20,T21,T22,WVC,P1,PTO,PR1,PR2,PSR,DTIS,CHIS,CP,GAM,E
  *XP,TNET,ROSP,T,ETA,ETAL,ACH1,PHI,V1,ALPH1,ZETAN,BETAI,PSI,PSIL,
  *ZETR,ZETRL,TR,TNETR,ALF2,ALF2L,RPMR,WVCR,BFM,HEAD,DR
  *REFERRED SPEED, T(THETA)
  RPMR=RPM/SQRT(T(THETA))
  DEL=(PTC*(GHG/13.54))/29.92
  X=(GAM+1.)/(2.*(GAM-1.))

```

```

C   EPS=(.81C/GAM)*((GAM+1.)/2.)**X
C   REFERRED FLCW RATE.
C   WVCR=WVC*(SQRT(THETA))*EPS/DEL
C   REFERRED MCMENT.
    TR=T*EPS/DEL
    TNETR=TNET*EPS/DEL
    RETURN
  END

```



```

      END
/*
//GØ.FT06F001    DD SYSOUT=A,SPACE=(CYL,(15,1))
//GØ.FT08F001    DD UNIT=SYSDA,SPACE=(TRK,(2,1)),
//               DCB=(RECFM=V,LRECL=500,BLKSIZE=504)
//GØ.SYSIN DD*

```

| | | | | |
|---|---|----|--------|----|
| 1 | 7 | 16 | COLUMN | 72 |
|---|---|----|--------|----|

TABLE B2
ADDITIONAL CONTROL CARDS REQUIRED FOR PROGRAM RADIAL

TABLE B3
TORQUE CALIBRATION DATA

| SET | CLEARANCE (IN) | RUNS | APPLIED TORQUE (IN-LB) | | | | |
|-----|-------------------|-----------------|------------------------|------|------|------|-------|
| | | | 0 | 100 | 200 | 300 | 400 |
| 1 | 0.081 | 1-4 | 5. | 261. | 518. | 768. | 1013. |
| | | 5-6, NOSPD 1 | 2. | 255. | 510. | 762. | 1009. |
| 2 | 0.061 | 1-3 | 0. | 255. | 511. | 760. | 1007. |
| | | 4-6, NOSPD 2 | 3. | 259. | 514. | 762. | 1007. |
| 3 | 0.041 | 1-3 | 0. | 257. | 511. | 760. | 1007. |
| | | 4-6, NOSPD 3 | 0. | 257. | 510. | 759. | 1004. |
| 4 | 0.024 | 1-3 | 0. | 256. | 510. | 760. | 1006. |
| | | 4-6, NOSPD 4 | 1. | 259. | 513. | 762. | 1007. |
| 5 | 0.015 | 1-4 | 0. | 255. | 511. | 760. | 1008. |
| | | 5-6, NOSPD 5 | -2. | 255. | 510. | 759. | 1004. |

PERFORMANCE EVALUATION OF ICP RADIAL TURPINE

TABLE B4 INPUT DATA CLEARANCE = 0.081 IN

| RUN/PT | RPM | TORQUE COUNTS | PVVC IN.HG | P5P IN.HG | H1 IN.H2O | DPVC IN.HG | PATM IN.HG | HREF1 IN.HG | V4 MM | V5 MM | V21 MM | V22 MM | TRM DEG F | TCJ DEG F |
|--------|--------|------------------|---------------|--------------|--------------|---------------|---------------|----------------|----------|----------|-----------|-----------|--------------|--------------|
| 1 | 5650. | 185. | 9.06 | 5.85 | 23.25 | 3.246 | 30.07 | 0.0 | 1.340 | 1.245 | 0.0 | 0.0 | 77.8 | 32.3 |
| 1 | 7620. | 149. | 8.76 | 5.90 | 27.05 | 2.801 | 30.07 | 0.0 | 1.365 | 1.280 | 0.0 | 0.0 | 78.8 | 32.3 |
| 1 | 9670. | 107. | 8.27 | 5.50 | 35.51 | 1.883 | 30.07 | 0.0 | 1.380 | 1.305 | 0.0 | 0.0 | 79.2 | 32.3 |
| 1 | 11720. | 65. | 7.77 | 5.91 | 45.76 | 1.883 | 30.07 | 0.0 | 1.380 | 1.305 | 0.0 | 0.0 | 80.5 | 32.3 |
| 1 | 13330. | 25. | 7.30 | 5.56 | 55.79 | 1.366 | 30.07 | 0.0 | 1.380 | 1.320 | 0.0 | 0.0 | 81.5 | 32.3 |
| 2 | 7040. | 272. | 13.36 | 8.82 | 34.78 | 4.517 | 30.07 | 0.0 | 1.380 | 1.325 | 0.0 | 0.0 | 85.7 | 32.3 |
| 2 | 9090. | 228. | 12.97 | 9.83 | 40.31 | 4.208 | 30.07 | 0.0 | 1.390 | 1.335 | 0.0 | 0.0 | 85.7 | 32.3 |
| 2 | 11030. | 181. | 12.50 | 9.85 | 49.78 | 3.689 | 30.07 | 0.0 | 1.385 | 1.340 | 0.0 | 0.0 | 85.5 | 32.3 |
| 2 | 13050. | 131. | 11.98 | 8.50 | 62.08 | 3.113 | 30.07 | 0.0 | 1.390 | 1.340 | 0.0 | 0.0 | 85.5 | 32.3 |
| 2 | 15050. | 170. | 11.21 | 8.87 | 75.39 | 2.388 | 30.07 | 0.0 | 1.405 | 1.360 | 0.0 | 0.0 | 86.2 | 32.3 |
| 2 | 16220. | 35. | 10.81 | 8.91 | 85.26 | 1.932 | 30.07 | 0.0 | 1.405 | 1.360 | 0.0 | 0.0 | 86.2 | 32.3 |
| 3 | 8140. | 356. | 17.52 | 11.76 | 4.84 | 5.806 | 30.06 | 3.02 | 1.375 | 1.330 | 0.0 | 0.0 | 87.0 | 32.3 |
| 3 | 10140. | 307. | 16.10 | 11.75 | 10.35 | 5.391 | 30.06 | 3.02 | 1.375 | 1.335 | 0.0 | 0.0 | 87.4 | 32.3 |
| 3 | 12120. | 251. | 16.60 | 11.78 | 21.33 | 4.834 | 30.06 | 3.02 | 1.380 | 1.335 | 0.0 | 0.0 | 87.5 | 32.3 |
| 3 | 14120. | 192. | 16.00 | 11.80 | 29.33 | 4.219 | 30.06 | 5.05 | 1.390 | 1.335 | 0.0 | 0.0 | 87.7 | 32.3 |
| 3 | 16040. | 135. | 15.35 | 11.81 | 23.27 | 3.560 | 30.06 | 5.05 | 1.400 | 1.335 | 0.0 | 0.0 | 87.7 | 32.3 |
| 4 | 9320. | 438. | 21.62 | 14.67 | 11.33 | 6.981 | 30.06 | 3.40 | 1.310 | 1.255 | 0.0 | 0.0 | 84.1 | 32.3 |
| 4 | 11330. | 380. | 21.20 | 14.71 | 18.93 | 6.518 | 30.06 | 3.40 | 1.315 | 1.265 | 0.0 | 0.0 | 85.0 | 32.3 |
| 4 | 13310. | 320. | 20.64 | 14.74 | 8.02 | 5.964 | 30.06 | 5.10 | 1.325 | 1.265 | 0.0 | 0.0 | 85.0 | 32.3 |
| 4 | 15300. | 255. | 20.01 | 14.78 | 24.05 | 5.346 | 30.06 | 5.10 | 1.340 | 1.285 | 0.0 | 0.0 | 85.5 | 32.3 |
| 4 | 17200. | 194. | 19.43 | 14.81 | 39.14 | 4.575 | 30.06 | 5.10 | 1.340 | 1.290 | 0.0 | 0.0 | 85.5 | 32.3 |
| 5 | 10130. | 509. | 25.65 | 17.60 | 14.16 | 8.081 | 30.07 | 4.02 | 1.665 | 1.470 | 0.0 | 0.0 | 84.7 | 32.3 |
| 5 | 11480. | 467. | 25.37 | 17.60 | 19.03 | 7.782 | 30.07 | 4.02 | 1.585 | 1.390 | 0.0 | 0.0 | 85.3 | 32.3 |
| 5 | 12980. | 417. | 25.04 | 17.65 | 12.66 | 7.381 | 30.07 | 5.20 | 1.575 | 1.375 | 0.0 | 0.0 | 86.0 | 32.3 |
| 5 | 14450. | 369. | 24.61 | 17.66 | 8.02 | 6.919 | 30.07 | 6.42 | 1.565 | 1.365 | 0.0 | 0.0 | 86.4 | 32.3 |
| 5 | 16000. | 313. | 24.04 | 17.70 | 8.21 | 6.424 | 30.07 | 7.70 | 1.560 | 1.360 | 0.0 | 0.0 | 86.4 | 32.3 |
| 5 | 17350. | 275. | 23.76 | 17.83 | 17.66 | 6.079 | 30.07 | 7.70 | 1.560 | 1.360 | 0.0 | 0.0 | 86.6 | 32.3 |
| 6 | 10960. | 590. | 30.00 | 20.55 | 7.53 | 9.120 | 30.07 | 5.40 | 1.525 | 1.300 | 0.0 | 0.0 | 87.0 | 32.3 |
| 6 | 12500. | 535. | 29.34 | 20.57 | 14.58 | 8.766 | 30.07 | 5.38 | 1.525 | 1.295 | 0.0 | 0.0 | 87.0 | 32.3 |
| 6 | 14020. | 482. | 28.91 | 20.58 | 11.75 | 8.329 | 30.07 | 6.37 | 1.540 | 1.310 | 0.0 | 0.0 | 87.0 | 32.3 |
| 6 | 15550. | 428. | 28.40 | 20.61 | 12.32 | 7.853 | 30.07 | 7.31 | 1.560 | 1.310 | 0.0 | 0.0 | 87.1 | 32.3 |
| 6 | 17030. | 369. | 28.93 | 20.69 | 16.48 | 7.331 | 30.07 | 8.12 | 1.560 | 1.310 | 0.0 | 0.0 | 87.1 | 32.3 |
| 6 | 18070. | 326. | 28.53 | 20.66 | 12.88 | 6.923 | 30.07 | 9.11 | 1.560 | 1.320 | 0.0 | 0.0 | 87.3 | 32.3 |

PERFORMANCE EVALUATION OF ICP RADIAL TURBINE

TABLE B5

OUTPUT DATA

CLEARANCE = 0.001 IN.

REDUCED TO STANDARD AIR IN ACCORDANCE WITH NASA METHOD.
 TOTAL INLET PRESS. = 14.7 PSIA, TOTAL INLET TEMPERATURE
 = 518.7 DEG.R., GAMMA = 1.4, CP = 0.24 RTU/LBM-DEG.F.

| RUN/PT | PRESS RATIO | REF. SPEED RPM | REF. FLOW LB/SEC | NO BEARING LOSSES | | | | | MAXIMUM BEARING LOSSES | | | | |
|--------|----------------|----------------------|------------------------|---------------------|----------------------|--------------|------------------------|-----------------|------------------------|----------------------|--------------|------------------------|-----------------|
| | | | | REF MOM FT.LB | ANGLE ALF2 DEG | VEL COEFF | LOSS COEFF ROTNR | EFFIC- TENCY | REF MOM FT.LB | ANGLE ALF2 DEG | VEL COEFF | LOSS COEFF ROTNR | EFFIC- TENCY |
| 1 | 1 | 200 | 5559. | 4.87 | -32.22 | 0.751 | 0.437 | 63.43 | 5.15 | -44.35 | 0.82 | 0.153 | 67.33 |
| 1 | 1 | 201 | 7489. | 3.97 | -32.48 | 0.775 | 0.512 | 73.24 | 4.30 | -18.17 | 0.89 | 0.111 | 63.80 |
| 1 | 1 | 200 | 9497. | 1.64 | 79.65 | 0.473 | 0.776 | 58.73 | 2.16 | 53.59 | 0.951 | 0.166 | 69.10 |
| 1 | 1 | 200 | 11509. | 0.57 | 87.80 | 0.157 | 0.975 | 26.73 | 1.10 | 73.12 | 0.740 | 0.140 | 65.10 |
| 2 | 1 | 301 | 6908. | 6.49 | -12.73 | 0.675 | 0.544 | 63.93 | 6.84 | -32.40 | 0.829 | 0.115 | 47.35 |
| 2 | 1 | 300 | 8917. | 5.57 | -27.42 | 0.720 | 0.482 | 74.32 | 5.09 | -11.91 | 0.920 | 0.128 | 47.95 |
| 2 | 1 | 301 | 10818. | 4.70 | 56.66 | 0.682 | 0.537 | 76.21 | 4.40 | 20.35 | 0.935 | 0.123 | 44.44 |
| 2 | 1 | 301 | 12800. | 3.16 | 70.27 | 0.635 | 0.597 | 48.58 | 3.65 | 45.01 | 0.798 | 0.131 | 42.44 |
| 2 | 1 | 299 | 14752. | 1.64 | 81.46 | 0.443 | 0.804 | 27.31 | 2.20 | 68.08 | 0.708 | 0.162 | 42.45 |
| 2 | 1 | 299 | 15899. | 0.77 | 86.29 | 0.256 | 0.934 | 27.31 | 1.17 | 76.79 | 0.665 | 0.159 | 42.45 |
| 3 | 1 | 401 | 7986. | 8.02 | -17.20 | 0.723 | 0.478 | 66.47 | 8.39 | -34.33 | 0.855 | 0.169 | 42.40 |
| 3 | 1 | 400 | 9950. | 6.87 | -34.22 | 0.689 | 0.525 | 73.76 | 7.29 | 0.35 | 0.859 | 0.178 | 28.28 |
| 3 | 1 | 399 | 11889. | 5.71 | 53.97 | 0.704 | 0.503 | 77.46 | 6.16 | 24.35 | 0.922 | 0.181 | 27.62 |
| 3 | 1 | 399 | 13857. | 3.03 | 65.97 | 0.668 | 0.608 | 63.80 | 3.55 | 60.75 | 0.875 | 0.173 | 27.62 |
| 4 | 1 | 499 | 9165. | 9.31 | -17.78 | 0.773 | 0.402 | 70.11 | 9.68 | -32.59 | 0.891 | 0.204 | 27.82 |
| 4 | 1 | 500 | 11140. | 8.02 | -28.75 | 0.732 | 0.465 | 75.03 | 8.45 | 31.82 | 0.875 | 0.204 | 27.82 |
| 4 | 1 | 500 | 13082. | 6.69 | 54.20 | 0.705 | 0.503 | 76.58 | 7.12 | 36.80 | 0.866 | 0.200 | 27.95 |
| 4 | 1 | 500 | 15032. | 4.00 | 62.92 | 0.713 | 0.492 | 69.76 | 4.53 | 59.12 | 0.800 | 0.174 | 27.12 |
| 5 | 1 | 598 | 9894. | 10.37 | -18.03 | 0.776 | 0.398 | 70.60 | 10.74 | -31.31 | 0.879 | 0.227 | 27.10 |
| 5 | 1 | 598 | 12411. | 9.51 | 36.80 | 0.758 | 0.425 | 75.03 | 9.00 | 31.35 | 0.875 | 0.235 | 27.37 |
| 5 | 1 | 598 | 14167. | 8.44 | 36.80 | 0.730 | 0.467 | 77.06 | 8.89 | 42.91 | 0.868 | 0.247 | 27.37 |
| 5 | 1 | 599 | 15679. | 7.49 | 48.50 | 0.706 | 0.501 | 76.97 | 7.74 | 45.73 | 0.846 | 0.284 | 27.42 |
| 5 | 1 | 603 | 17015. | 5.53 | 66.68 | 0.726 | 0.473 | 74.95 | 5.90 | 55.30 | 0.877 | 0.230 | 27.42 |
| 6 | 1 | 698 | 10762. | 11.27 | -15.61 | 0.782 | 0.388 | 72.05 | 11.63 | -28.25 | 0.875 | 0.234 | 27.35 |
| 6 | 1 | 698 | 12276. | 10.18 | 32.88 | 0.751 | 0.436 | 76.06 | 10.56 | 12.08 | 0.882 | 0.270 | 27.88 |
| 6 | 1 | 698 | 13769. | 9.24 | 32.88 | 0.772 | 0.394 | 79.58 | 9.43 | 26.28 | 0.894 | 0.262 | 27.57 |
| 6 | 1 | 700 | 16717. | 8.19 | 45.64 | 0.729 | 0.448 | 75.12 | 8.59 | 46.79 | 0.887 | 0.260 | 27.10 |
| 6 | 1 | 698 | 17732. | 6.21 | 59.02 | 0.714 | 0.490 | 75.12 | 6.59 | 55.30 | 0.837 | 0.290 | 27.10 |

PERFORMANCE EVALUATION OF ICP RADIAL TURPINE

TABLE B6

INPUT DATA

CLEARANCE = 0.061 IN.

| RUN/PT | RPM | TORQUE COUNTS | P5P IN. HG | H1 IN. H2O | DPVC IN. HG | PATM IN. HG | HREF1 IN. HG | V4 MV | V5 MV | V20 MV | V21 MV | V22 MV | TRM DEG. F | TCJ DEG. F |
|--------|--------|------------------|---------------|---------------|----------------|----------------|-----------------|----------|----------|-----------|-----------|-----------|---------------|---------------|
| 1 | 5710. | 179. | 5.84 | 9.88 | 3.241 | 30.03 | 1.01 | 1.780 | 1.665 | 1.180 | 1.260 | 1.345 | 80.5 | 32.0 |
| 1 | 7200. | 151. | 5.84 | 12.64 | 2.986 | 30.03 | 1.00 | 1.805 | 1.695 | 1.170 | 1.280 | 1.340 | 81.0 | 32.0 |
| 1 | 8570. | 125. | 5.86 | 12.09 | 2.680 | 30.03 | 1.37 | 1.800 | 1.685 | 1.165 | 1.325 | 1.380 | 82.5 | 32.0 |
| 1 | 10000. | 97. | 5.90 | 8.92 | 2.320 | 30.03 | 2.75 | 1.800 | 1.685 | 1.185 | 1.375 | 1.450 | 83.5 | 32.0 |
| 1 | 11810. | 63. | 5.91 | 9.12 | 1.866 | 30.03 | 2.75 | 1.795 | 1.675 | 1.185 | 1.445 | 1.680 | 84.0 | 32.0 |
| 1 | 13660. | 17. | 5.95 | 10.10 | 1.254 | 30.03 | 3.53 | 1.805 | 1.675 | 1.205 | 1.505 | 1.915 | 84.0 | 32.0 |
| 2 | 7080. | 266. | 8.78 | 16.65 | 4.573 | 30.03 | 1.35 | 1.845 | 1.750 | 1.195 | 1.265 | 1.345 | 84.0 | 32.0 |
| 2 | 9050. | 223. | 8.80 | 13.68 | 4.176 | 30.03 | 2.69 | 1.855 | 1.760 | 1.230 | 1.395 | 1.400 | 84.5 | 32.0 |
| 2 | 10600. | 177. | 8.81 | 12.79 | 3.729 | 30.03 | 3.59 | 1.855 | 1.775 | 1.230 | 1.505 | 1.595 | 84.5 | 32.0 |
| 2 | 13050. | 128. | 8.84 | 13.00 | 3.125 | 30.03 | 3.59 | 1.865 | 1.785 | 1.230 | 1.505 | 1.895 | 84.5 | 32.0 |
| 2 | 15100. | 170. | 8.85 | 9.11 | 2.453 | 30.03 | 4.93 | 1.865 | 1.780 | 1.230 | 1.605 | 2.040 | 85.0 | 32.0 |
| 2 | 16740. | 18. | 8.91 | 12.80 | 1.706 | 30.03 | 5.70 | 1.855 | 1.770 | 1.290 | 1.690 | 2.095 | 85.0 | 32.0 |
| 3 | 8270. | 348. | 11.72 | 8.85 | 5.825 | 30.03 | 2.80 | 1.870 | 1.795 | 1.295 | 1.320 | 1.425 | 85.0 | 32.0 |
| 3 | 10330. | 299. | 11.73 | 18.12 | 5.399 | 30.03 | 3.30 | 1.835 | 1.775 | 1.275 | 1.315 | 1.445 | 85.0 | 32.0 |
| 3 | 12320. | 243. | 11.73 | 19.19 | 4.873 | 30.03 | 3.31 | 1.830 | 1.755 | 1.255 | 1.365 | 1.775 | 85.0 | 32.0 |
| 3 | 14320. | 187. | 11.79 | 9.265 | 4.261 | 30.03 | 5.10 | 1.820 | 1.750 | 1.295 | 1.495 | 1.925 | 84.5 | 32.0 |
| 3 | 16260. | 131. | 11.83 | 8.35 | 3.578 | 30.03 | 6.25 | 1.810 | 1.740 | 1.295 | 1.605 | 1.980 | 84.0 | 32.0 |
| 3 | 17940. | 165. | 11.88 | 12.41 | 2.744 | 30.03 | 7.24 | 1.805 | 1.725 | 1.305 | 1.705 | 2.190 | 84.0 | 32.0 |
| 4 | 9150. | 425. | 14.66 | 11.57 | 6.945 | 30.14 | 3.42 | 1.674 | 1.615 | 1.130 | 1.172 | 1.283 | 68.2 | 32.0 |
| 4 | 10400. | 374. | 14.69 | 18.05 | 6.554 | 30.14 | 3.42 | 1.715 | 1.662 | 1.163 | 1.273 | 1.506 | 69.8 | 32.0 |
| 4 | 12800. | 317. | 14.70 | 4.15 | 6.034 | 30.14 | 5.30 | 1.731 | 1.684 | 1.166 | 1.385 | 1.935 | 69.8 | 32.0 |
| 4 | 15060. | 247. | 14.72 | 11.61 | 5.455 | 30.14 | 6.01 | 1.750 | 1.703 | 1.255 | 1.588 | 2.029 | 70.1 | 32.0 |
| 4 | 17040. | 186. | 14.76 | 12.92 | 4.679 | 30.14 | 7.15 | 1.762 | 1.709 | 1.316 | 1.857 | 2.204 | 71.0 | 32.0 |
| 5 | 10100. | 512. | 17.61 | 12.54 | 8.042 | 30.14 | 4.29 | 1.774 | 1.729 | 1.318 | 1.304 | 1.512 | 71.0 | 32.0 |
| 5 | 11800. | 467. | 17.61 | 17.78 | 7.337 | 30.14 | 4.21 | 1.782 | 1.739 | 1.302 | 1.277 | 1.792 | 72.0 | 32.0 |
| 5 | 13000. | 418. | 17.64 | 11.10 | 7.337 | 30.14 | 5.40 | 1.786 | 1.745 | 1.304 | 1.345 | 1.987 | 72.0 | 32.0 |
| 5 | 14540. | 370. | 17.65 | 6.30 | 6.813 | 30.14 | 6.60 | 1.774 | 1.745 | 1.326 | 1.594 | 2.020 | 72.0 | 32.0 |
| 5 | 16070. | 312. | 17.69 | 7.67 | 6.332 | 30.14 | 7.65 | 1.765 | 1.737 | 1.345 | 1.685 | 2.143 | 73.0 | 32.0 |
| 5 | 17500. | 262. | 17.70 | 6.04 | 5.811 | 30.14 | 8.67 | 1.772 | 1.736 | 1.385 | 1.685 | 2.204 | 73.0 | 32.0 |
| 6 | 11000. | 589. | 20.52 | 10.47 | 9.063 | 30.10 | 5.32 | 1.828 | 1.779 | 1.275 | 1.159 | 1.472 | 76.0 | 32.0 |
| 6 | 12480. | 549. | 20.55 | 11.27 | 8.733 | 30.10 | 5.72 | 1.831 | 1.753 | 1.297 | 1.276 | 1.722 | 78.0 | 32.0 |
| 6 | 13990. | 489. | 20.59 | 14.79 | 8.341 | 30.10 | 6.24 | 1.831 | 1.738 | 1.350 | 1.391 | 1.883 | 78.0 | 32.0 |
| 6 | 15460. | 437. | 20.62 | 8.78 | 7.844 | 30.10 | 7.60 | 1.810 | 1.722 | 1.361 | 1.529 | 1.981 | 78.0 | 32.0 |
| 6 | 16970. | 371. | 20.63 | 5.83 | 7.218 | 30.10 | 8.99 | 1.801 | 1.722 | 1.376 | 1.699 | 2.058 | 78.0 | 32.0 |
| 6 | 17950. | 337. | 20.66 | 15.42 | 6.933 | 30.10 | 9.00 | 1.784 | 1.718 | 1.376 | 1.707 | 2.140 | 78.0 | 32.0 |

PERFORMANCE EVALUATION OF ICP RADIAL TURBINE

TABLE B7

OUTPUT DATA

CLEARANCE = 0.061 IN.

REDUCED TO STANDARD AIR IN ACCORDANCE WITH NASA METHOD.
TOTAL INLET PRESS. = 14.7 PSIA; TOTAL INLET TEMPERATURE
= 518.7 DEG.R.; GAMMA = 1.4; CP = 0.24 BTU/LBM-DEG.F.

| RUN/PT | PRESS RATIO | REF. SPEED RPM | REF. FLOW LBS/SEC | HEAD COEFF | DEG REACT | ANGLE ALPH1 DEG | ANGLE BETAI DEG | VEL COEFF GV | LOSS COEFF GV | NO BEARING LOSSES | | | | | MAXIMUM BEARING LOSSES | | | | |
|--------|----------------|----------------------|-------------------------|---------------|--------------|-----------------------|-----------------------|--------------------|---------------------|---------------------|-----------------------|--------------|---------------|-----------------|------------------------|-----------------------|--------------|---------------|-----------------|
| | | | | | | | | | | REF MOM FT.LB | ANGLE ALF20 DEG | VEL COEFF | LOSS ROTOR | EFFIC- IENCY | REF MOM FT.LB | ANGLE ALF20 DEG | VEL COEFF | LOSS ROTOR | EFFIC- IENCY |
| 1 | 1.200 | 5544. | 0.911 | 6.108 | 0.303 | 81.53 | 71.93 | 0.802 | 0.187 | 4.87 | -27.34 | 0.716 | 0.499 | 63.25 | 5.14 | -43.27 | 0.885 | 0.215 | 67.12 |
| 1 | 1.199 | 6984. | 0.874 | 3.841 | 0.337 | 81.53 | 63.34 | 0.971 | 0.189 | 4.12 | 51.14 | 0.638 | 0.593 | 70.33 | 4.51 | -18.65 | 0.843 | 0.209 | 67.92 |
| 1 | 1.199 | 8413. | 0.827 | 2.649 | 0.353 | 81.53 | 37.25 | 0.899 | 0.192 | 3.41 | 58.21 | 0.617 | 0.620 | 74.15 | 3.83 | 7.62 | 0.843 | 0.179 | 76.86 |
| 1 | 1.200 | 9997. | 0.769 | 1.921 | 0.478 | 81.52 | -40.46 | 0.896 | 0.205 | 2.65 | 68.51 | 0.519 | 0.730 | 72.03 | 3.14 | 25.64 | 0.978 | 0.163 | 76.68 |
| 1 | 1.200 | 11463. | 0.694 | 1.429 | 0.586 | 81.51 | -72.52 | 0.892 | 0.207 | 1.73 | 77.27 | 0.462 | 0.730 | 61.42 | 2.26 | 46.93 | 0.978 | 0.163 | 76.68 |
| 1 | 1.200 | 13259. | 0.563 | 1.070 | 0.724 | 81.48 | -82.27 | 0.885 | 0.217 | 0.49 | 87.15 | 0.192 | 0.963 | 24.42 | 1.03 | 70.57 | 0.730 | 0.377 | 61.58 |
| 2 | 1.200 | 6856. | 1.044 | 5.687 | 0.306 | 81.51 | 71.28 | 0.910 | 0.173 | 6.50 | -11.79 | 0.658 | 0.567 | 64.00 | 6.85 | -34.25 | 0.810 | 0.244 | 67.44 |
| 2 | 1.300 | 8761. | 0.997 | 3.483 | 0.350 | 81.52 | 61.15 | 0.905 | 0.175 | 5.60 | 29.28 | 0.685 | 0.531 | 73.77 | 6.02 | -11.15 | 0.890 | 0.208 | 70.25 |
| 2 | 1.299 | 10702. | 0.941 | 2.331 | 0.427 | 81.53 | 12.84 | 0.905 | 0.180 | 4.25 | 59.93 | 0.643 | 0.586 | 75.99 | 4.92 | 24.22 | 0.893 | 0.182 | 84.05 |
| 2 | 1.299 | 12623. | 0.859 | 1.676 | 0.529 | 81.53 | -60.49 | 0.901 | 0.188 | 3.21 | 69.43 | 0.616 | 0.621 | 71.33 | 3.72 | 44.77 | 0.904 | 0.154 | 85.80 |
| 2 | 1.299 | 14608. | 0.760 | 1.249 | 0.646 | 81.52 | -77.96 | 0.895 | 0.199 | 1.78 | 80.44 | 0.462 | 0.786 | 51.33 | 2.28 | 46.12 | 0.804 | 0.154 | 85.80 |
| 2 | 1.299 | 16200. | 0.633 | 1.017 | 0.756 | 81.50 | -83.36 | 0.889 | 0.211 | 0.48 | 87.17 | 0.195 | 0.962 | 19.25 | 0.98 | 77.89 | 0.605 | 0.334 | 67.15 |
| 3 | 1.400 | 7997. | 1.139 | 5.306 | 0.313 | 81.47 | 70.40 | 0.915 | 0.163 | 8.00 | -11.60 | 0.681 | 0.537 | 66.30 | 8.37 | -31.47 | 0.912 | 0.341 | 69.37 |
| 3 | 1.399 | 9898. | 1.096 | 3.458 | 0.352 | 81.49 | 60.09 | 0.913 | 0.166 | 5.83 | 39.56 | 0.634 | 0.598 | 72.92 | 7.25 | -5.35 | 0.799 | 0.362 | 70.46 |
| 3 | 1.399 | 11831. | 1.040 | 2.418 | 0.424 | 81.50 | 21.69 | 0.913 | 0.171 | 5.67 | 56.61 | 0.645 | 0.585 | 76.37 | 6.43 | 28.93 | 0.833 | 0.306 | 81.64 |
| 3 | 1.399 | 13769. | 0.970 | 1.788 | 0.512 | 81.52 | -52.32 | 0.907 | 0.185 | 4.37 | 67.42 | 0.623 | 0.611 | 73.21 | 4.83 | 28.08 | 0.859 | 0.262 | 84.74 |
| 3 | 1.400 | 15749. | 0.887 | 1.368 | 0.601 | 81.53 | -73.90 | 0.893 | 0.196 | 3.06 | 74.07 | 0.618 | 0.618 | 64.28 | 3.53 | 40.30 | 0.859 | 0.262 | 84.74 |
| 3 | 1.400 | 17385. | 0.774 | 1.123 | 0.704 | 81.52 | -81.14 | 0.896 | 0.216 | 1.53 | 82.04 | 0.424 | 0.820 | 40.58 | 1.99 | 73.24 | 0.693 | 0.520 | 69.74 |
| 4 | 1.498 | 8897. | 1.201 | 5.100 | 0.316 | 81.43 | 69.85 | 0.919 | 0.156 | 9.05 | -0.07 | 0.646 | 0.593 | 66.56 | 9.42 | -22.26 | 0.759 | 0.423 | 69.27 |
| 4 | 1.498 | 10719. | 1.165 | 3.515 | 0.349 | 81.47 | 61.01 | 0.918 | 0.158 | 7.92 | 42.05 | 0.674 | 0.575 | 72.47 | 8.32 | -16.20 | 0.777 | 0.423 | 70.25 |
| 4 | 1.498 | 12594. | 1.117 | 2.544 | 0.408 | 81.47 | 33.55 | 0.915 | 0.162 | 6.65 | 62.85 | 0.674 | 0.575 | 74.66 | 7.08 | 16.96 | 0.777 | 0.423 | 70.25 |
| 4 | 1.497 | 14603. | 0.980 | 1.891 | 0.456 | 81.52 | -41.89 | 0.912 | 0.169 | 5.26 | 69.70 | 0.571 | 0.677 | 65.98 | 5.69 | 56.09 | 0.749 | 0.423 | 70.25 |
| 4 | 1.497 | 16520. | 0.880 | 1.478 | 0.456 | 81.52 | -49.87 | 0.908 | 0.176 | 3.94 | 74.55 | 0.568 | 0.677 | 65.98 | 4.37 | 64.43 | 0.749 | 0.423 | 70.25 |
| 5 | 1.597 | 9785. | 1.255 | 4.844 | 0.326 | 81.39 | 68.90 | 0.931 | 0.151 | 10.31 | -12.56 | 0.715 | 0.489 | 69.42 | 10.67 | -27.92 | 0.815 | 0.337 | 70.88 |
| 5 | 1.597 | 11138. | 1.226 | 3.736 | 0.349 | 81.40 | 62.91 | 0.921 | 0.152 | 9.37 | 21.43 | 0.677 | 0.489 | 73.37 | 9.77 | -2.91 | 0.815 | 0.337 | 70.88 |
| 5 | 1.597 | 12590. | 1.196 | 2.926 | 0.385 | 81.45 | 50.01 | 0.919 | 0.154 | 8.35 | 46.57 | 0.677 | 0.489 | 75.91 | 8.75 | 24.36 | 0.769 | 0.408 | 70.54 |
| 5 | 1.597 | 14080. | 1.158 | 2.338 | 0.433 | 81.45 | 15.69 | 0.915 | 0.158 | 7.35 | 65.43 | 0.652 | 0.575 | 77.45 | 7.75 | 39.29 | 0.769 | 0.408 | 70.54 |
| 5 | 1.597 | 15566. | 1.108 | 1.914 | 0.458 | 81.45 | -40.47 | 0.915 | 0.163 | 6.14 | 65.43 | 0.652 | 0.575 | 77.45 | 6.54 | 52.64 | 0.741 | 0.441 | 70.54 |
| 5 | 1.597 | 16951. | 1.061 | 1.613 | 0.548 | 81.49 | -63.39 | 0.912 | 0.168 | 5.09 | 71.12 | 0.598 | 0.642 | 70.39 | 5.50 | 61.47 | 0.741 | 0.452 | 70.54 |
| 6 | 1.697 | 10641. | 1.295 | 4.585 | 0.331 | 81.34 | 67.85 | 0.924 | 0.147 | 11.20 | -10.79 | 0.727 | 0.471 | 71.31 | 11.56 | -25.20 | 0.818 | 0.332 | 72.29 |
| 6 | 1.697 | 12074. | 1.269 | 3.562 | 0.355 | 81.36 | 51.25 | 0.923 | 0.148 | 10.26 | 18.08 | 0.712 | 0.471 | 75.31 | 10.64 | -22.79 | 0.818 | 0.332 | 72.29 |
| 6 | 1.698 | 13544. | 1.200 | 2.833 | 0.394 | 81.38 | 39.04 | 0.922 | 0.151 | 9.27 | 38.04 | 0.705 | 0.501 | 78.31 | 9.63 | 17.98 | 0.818 | 0.332 | 72.29 |
| 6 | 1.698 | 14974. | 1.154 | 2.321 | 0.439 | 81.41 | 13.46 | 0.920 | 0.154 | 8.25 | 64.85 | 0.657 | 0.568 | 79.38 | 8.63 | 39.12 | 0.818 | 0.332 | 72.29 |
| 6 | 1.697 | 16445. | 1.125 | 1.921 | 0.456 | 81.45 | -38.62 | 0.916 | 0.158 | 6.95 | 64.85 | 0.657 | 0.568 | 79.38 | 7.33 | 49.95 | 0.771 | 0.340 | 70.58 |
| 6 | 1.698 | 17396. | 1.085 | 1.717 | 0.530 | 81.46 | -56.71 | 0.916 | 0.161 | 6.28 | 64.84 | 0.646 | 0.557 | 74.45 | 6.66 | 54.50 | 0.771 | 0.340 | 70.58 |

PERFORMANCE EVALUATION OF ICP RADIAL TURBINE

TABLE B8

CLEARANCE = 0.041 IN.

INPUT DATA

| RUN/PT | RPM | TORQUE COUNTS | P5P IN.HG | H1 IN.H2O | OPVC IN.HG | PATM IN.HG | HREF1 IN.HG | V4 MV | V5 MV | V20 MV | V21 MV | V22 MV | TRM DEG.F | ICJ DEG.F |
|--------|-----|------------------|--------------|--------------|---------------|---------------|----------------|----------|----------|-----------|-----------|-----------|--------------|--------------|
| 1 | 1 | 171. | 9.94 | 5.18 | 3.259 | 30.10 | 1.33 | 1.727 | 1.668 | 1.194 | 1.269 | 1.433 | 75.0 | 32. |
| 1 | 2 | 144. | 8.82 | 11.19 | 2.997 | 30.10 | 1.35 | 1.748 | 1.694 | 1.213 | 1.330 | 1.454 | 74.4 | 32. |
| 1 | 3 | 120. | 8.57 | 12.67 | 2.732 | 30.10 | 1.35 | 1.822 | 1.761 | 1.238 | 1.330 | 1.483 | 74.8 | 32. |
| 1 | 4 | 90. | 8.26 | 14.63 | 2.362 | 30.10 | 1.66 | 1.845 | 1.780 | 1.265 | 1.459 | 1.599 | 76.0 | 32. |
| 1 | 5 | 63. | 7.83 | 17.01 | 1.954 | 30.10 | 2.49 | 1.869 | 1.747 | 1.285 | 1.500 | 1.796 | 76.8 | 32. |
| 1 | 6 | 12. | 7.19 | 11.79 | 1.250 | 30.10 | 2.51 | 1.885 | 1.801 | 1.298 | 1.589 | 2.002 | 77.0 | 32. |
| 2 | 1 | 261. | 13.34 | 15.59 | 4.600 | 30.10 | 1.43 | 1.927 | 1.859 | 1.319 | 1.369 | 1.469 | 79.0 | 32. |
| 2 | 2 | 231. | 13.10 | 19.14 | 4.337 | 30.10 | 1.43 | 1.926 | 1.859 | 1.319 | 1.404 | 1.500 | 79.6 | 32. |
| 2 | 3 | 198. | 12.76 | 16.78 | 4.020 | 30.10 | 1.75 | 1.929 | 1.881 | 1.337 | 1.455 | 1.601 | 81.0 | 32. |
| 2 | 4 | 163. | 12.42 | 9.35 | 3.636 | 30.10 | 3.11 | 1.935 | 1.883 | 1.356 | 1.525 | 1.834 | 81.7 | 32. |
| 2 | 5 | 127. | 12.02 | 3.37 | 3.220 | 30.10 | 4.21 | 1.937 | 1.883 | 1.376 | 1.604 | 1.950 | 82.6 | 32. |
| 2 | 6 | 88. | 11.53 | 14.26 | 2.714 | 30.10 | 4.24 | 1.923 | 1.879 | 1.380 | 1.667 | 2.120 | 83.6 | 32. |
| 2 | 7 | 40. | 10.94 | 11.24 | 2.071 | 30.10 | 5.36 | 1.906 | 1.859 | 1.381 | 1.736 | 2.236 | 83.5 | 32. |
| 3 | 1 | 350. | 17.54 | 11.69 | 5.835 | 30.10 | 2.60 | 1.895 | 1.855 | 1.355 | 1.380 | 1.495 | 83.4 | 32. |
| 3 | 2 | 311. | 17.23 | 11.99 | 5.501 | 30.10 | 2.61 | 1.886 | 1.846 | 1.339 | 1.381 | 1.495 | 83.4 | 32. |
| 3 | 3 | 261. | 16.82 | 16.12 | 5.090 | 30.10 | 2.61 | 1.899 | 1.846 | 1.339 | 1.421 | 1.543 | 83.4 | 32. |
| 3 | 4 | 197. | 15.16 | 10.52 | 4.694 | 30.10 | 4.89 | 1.915 | 1.872 | 1.350 | 1.544 | 1.736 | 83.5 | 32. |
| 3 | 5 | 137. | 15.47 | 11.01 | 3.694 | 30.10 | 5.96 | 1.925 | 1.876 | 1.371 | 1.690 | 1.970 | 83.5 | 32. |
| 3 | 6 | 68. | 14.65 | 6.19 | 2.821 | 30.10 | 5.99 | 1.927 | 1.877 | 1.385 | 1.804 | 2.229 | 83.5 | 32. |
| 4 | 1 | 433. | 21.63 | 12.80 | 7.005 | 30.02 | 3.41 | 1.827 | 1.757 | 1.258 | 1.301 | 1.428 | 74.6 | 32. |
| 4 | 2 | 386. | 21.29 | 13.34 | 6.627 | 30.02 | 3.80 | 1.834 | 1.772 | 1.275 | 1.356 | 1.562 | 74.6 | 32. |
| 4 | 3 | 344. | 21.00 | 15.55 | 6.237 | 30.02 | 4.27 | 1.857 | 1.795 | 1.275 | 1.447 | 1.870 | 75.0 | 32. |
| 4 | 4 | 292. | 20.50 | 11.96 | 5.780 | 30.02 | 5.32 | 1.861 | 1.799 | 1.356 | 1.541 | 2.013 | 75.0 | 32. |
| 4 | 5 | 243. | 19.99 | 11.90 | 5.252 | 30.02 | 5.32 | 1.866 | 1.815 | 1.411 | 1.753 | 2.048 | 75.0 | 32. |
| 4 | 6 | 197. | 19.43 | 13.21 | 4.712 | 30.02 | 7.09 | 1.875 | 1.826 | 1.429 | 1.823 | 2.220 | 75.0 | 32. |
| 4 | 7 | 169. | 19.19 | 18.63 | 4.393 | 30.02 | 7.09 | 1.879 | 1.844 | 1.429 | 1.823 | 2.220 | 75.0 | 32. |
| 5 | 1 | 510. | 25.67 | 7.49 | 8.079 | 30.02 | 4.70 | 2.003 | 1.929 | 1.370 | 1.334 | 1.508 | 75.0 | 32. |
| 5 | 2 | 475. | 25.42 | 11.97 | 7.793 | 30.02 | 4.70 | 2.012 | 1.936 | 1.373 | 1.355 | 1.624 | 75.0 | 32. |
| 5 | 3 | 430. | 25.04 | 18.33 | 7.434 | 30.02 | 5.00 | 2.015 | 1.936 | 1.373 | 1.355 | 1.624 | 75.0 | 32. |
| 5 | 4 | 380. | 24.61 | 13.56 | 6.984 | 30.02 | 5.00 | 2.019 | 1.936 | 1.412 | 1.542 | 1.834 | 75.0 | 32. |
| 5 | 5 | 328. | 24.13 | 9.49 | 6.485 | 30.02 | 7.29 | 2.023 | 1.946 | 1.436 | 1.542 | 2.054 | 75.0 | 32. |
| 5 | 6 | 272. | 23.62 | 15.26 | 5.917 | 30.02 | 7.29 | 2.023 | 1.946 | 1.471 | 1.782 | 2.182 | 75.0 | 32. |
| 6 | 1 | 595. | 29.70 | 8.14 | 9.097 | 30.02 | 5.50 | 2.037 | 1.920 | 1.421 | 1.322 | 1.617 | 75.0 | 32. |
| 6 | 2 | 548. | 29.34 | 12.55 | 8.755 | 30.02 | 5.56 | 2.030 | 1.920 | 1.416 | 1.358 | 1.744 | 75.0 | 32. |
| 6 | 3 | 498. | 28.98 | 19.60 | 8.383 | 30.02 | 6.56 | 2.026 | 1.919 | 1.417 | 1.462 | 1.869 | 75.0 | 32. |
| 6 | 4 | 439. | 28.50 | 10.46 | 7.911 | 30.02 | 7.80 | 2.029 | 1.919 | 1.447 | 1.554 | 2.044 | 75.0 | 32. |
| 6 | 5 | 381. | 27.94 | 7.38 | 7.358 | 30.02 | 8.56 | 2.024 | 1.913 | 1.449 | 1.748 | 2.202 | 75.0 | 32. |
| 6 | 6 | 340. | 27.50 | 8.94 | 6.897 | 30.02 | 9.56 | 2.022 | 1.913 | 1.449 | 1.748 | 2.202 | 75.0 | 32. |

PERFORMANCE EVALUATION OF ICP RADIAL TURBINE

TABLE B9

OUTPUT DATA

CLEARANCE = 0.041 IN.

REDUCED TO STANDARD AIR IN ACCORDANCE WITH NASA METHOD.
 TOTAL INLET PRESS. = 14.7 PSIA, TOTAL INLET TEMPERATURE
 = 518.7 DEG. R., GAMMA = 1.4, CP = 0.24 BTU/LBM-DEG. F.

| RUN/PT | PRESS RATIO | REF. SPEED RPM | REF. FLOW LB/SEC | HEAD COEFF | DEG REACT | ANGLE ALPHA DEG | ANGLE BETA DEG | VEL COEFF GV | LOSS COEFF GV | NO BEARING LOSSES | | | | | MAXIMUM BEARING LOSSES | | | | |
|--------|----------------|----------------------|------------------------|---------------|--------------|-----------------------|----------------------|--------------------|---------------------|---------------------|-----------------------|--------------|------------------------|----------------|------------------------|-----------------------|--------------|------------------------|----------------|
| | | | | | | | | | | REF MOM FT.LB | ANGLE ALF20 DEG | VEL COEFF | LOSS COEFF ROTNR | EFFIC- ENCY | REF MOM FT.LB | ANGLE ALF20 DEG | VEL COEFF | LOSS COEFF ROTNR | EFFIC- ENCY |
| 1 | 1.198 | 5602. | 0.925 | 5.935 | 0.301 | 81.19 | 71.08 | 0.906 | 0.179 | 4.57 | 24.82 | 0.508 | 0.742 | 59.53 | 4.87 | -19.07 | 0.691 | 0.537 | 63.26 |
| 1 | 1.198 | 7043. | 0.876 | 3.765 | 0.341 | 81.20 | 61.87 | 0.905 | 0.181 | 3.94 | 62.57 | 0.459 | 0.790 | 66.18 | 4.22 | 15.66 | 0.710 | 0.496 | 72.85 |
| 1 | 1.199 | 8393. | 0.835 | 2.681 | 0.356 | 81.19 | -36.82 | 0.903 | 0.185 | 3.18 | 74.37 | 0.418 | 0.825 | 68.45 | 3.86 | 41.06 | 0.730 | 0.464 | 77.97 |
| 1 | 1.199 | 9849. | 0.776 | 1.927 | 0.474 | 81.18 | -70.88 | 0.896 | 0.197 | 2.37 | 81.27 | 0.378 | 0.891 | 64.52 | 2.86 | 58.76 | 0.730 | 0.464 | 77.97 |
| 1 | 1.199 | 11420. | 0.704 | 1.438 | 0.577 | 81.18 | -77.35 | 0.896 | 0.197 | 1.63 | 82.15 | 0.378 | 0.857 | 56.38 | 2.15 | 60.63 | 0.730 | 0.464 | 77.97 |
| 1 | 1.199 | 13304. | 0.563 | 1.059 | 0.579 | 81.18 | -77.35 | 0.896 | 0.197 | 0.24 | -84.64 | 2.023 | 0.891 | 12.38 | 0.70 | 89.43 | 0.154 | 0.076 | 29.68 |
| 2 | 1.295 | 6910. | 1.045 | 5.582 | 0.306 | 81.18 | 70.45 | 0.914 | 0.167 | 5.36 | 6.45 | 0.590 | 0.652 | 63.17 | 6.71 | -25.29 | 0.743 | 0.478 | 66.62 |
| 2 | 1.299 | 8252. | 1.015 | 3.921 | 0.336 | 81.18 | 63.63 | 0.913 | 0.170 | 5.73 | 37.45 | 0.597 | 0.689 | 68.20 | 6.35 | -4.57 | 0.788 | 0.387 | 74.87 |
| 2 | 1.299 | 9654. | 0.977 | 2.860 | 0.383 | 81.19 | 46.56 | 0.911 | 0.174 | 4.90 | 60.67 | 0.558 | 0.744 | 71.81 | 5.95 | 25.95 | 0.783 | 0.415 | 77.32 |
| 2 | 1.302 | 11200. | 0.926 | 1.717 | 0.441 | 81.19 | -33.67 | 0.906 | 0.179 | 4.01 | 72.33 | 0.506 | 0.782 | 66.60 | 3.44 | 49.14 | 0.751 | 0.437 | 77.24 |
| 2 | 1.302 | 12507. | 0.871 | 1.341 | 0.518 | 81.19 | -55.80 | 0.901 | 0.188 | 3.11 | 77.25 | 0.467 | 0.788 | 56.60 | 3.51 | 59.77 | 0.745 | 0.384 | 69.87 |
| 2 | 1.299 | 14101. | 0.800 | 1.106 | 0.610 | 81.18 | -74.33 | 0.896 | 0.197 | 2.14 | 80.03 | 0.461 | 0.944 | 31.10 | 2.64 | 65.70 | 0.745 | 0.384 | 69.87 |
| 2 | 1.299 | 15539. | 0.697 | 1.106 | 0.706 | 81.18 | -81.02 | 0.896 | 0.197 | 0.93 | 86.28 | 0.237 | 0.944 | 31.10 | 1.43 | 76.94 | 0.611 | 0.327 | 47.87 |
| 3 | 1.399 | 8050. | 1.140 | 5.227 | 0.314 | 81.14 | 69.57 | 0.919 | 0.156 | 8.03 | -11.87 | 0.687 | 0.527 | 67.05 | 8.40 | -31.56 | 0.819 | 0.320 | 70.16 |
| 3 | 1.399 | 9664. | 1.105 | 3.634 | 0.348 | 81.15 | 61.19 | 0.918 | 0.162 | 7.51 | -28.22 | 0.664 | 0.555 | 73.31 | 7.51 | -5.27 | 0.768 | 0.347 | 77.62 |
| 3 | 1.399 | 11339. | 1.062 | 2.674 | 0.406 | 81.17 | 36.75 | 0.916 | 0.169 | 5.91 | 59.22 | 0.588 | 0.655 | 74.58 | 6.39 | 32.76 | 0.790 | 0.347 | 80.41 |
| 3 | 1.399 | 13448. | 0.987 | 1.897 | 0.501 | 81.19 | -43.72 | 0.917 | 0.177 | 4.53 | 68.55 | 0.576 | 0.655 | 72.00 | 4.90 | 42.59 | 0.812 | 0.347 | 80.41 |
| 3 | 1.399 | 15548. | 0.901 | 1.327 | 0.566 | 81.19 | -75.36 | 0.909 | 0.175 | 3.12 | -89.32 | 0.112 | 0.987 | 39.62 | 1.98 | 86.60 | 0.469 | 0.327 | 51.61 |
| 4 | 1.499 | 8955. | 1.208 | 5.084 | 0.321 | 81.10 | 68.96 | 0.923 | 0.148 | 9.36 | -16.16 | 0.716 | 0.487 | 68.49 | 9.74 | -31.83 | 0.829 | 0.313 | 71.42 |
| 4 | 1.499 | 10624. | 1.175 | 3.589 | 0.356 | 81.13 | 60.30 | 0.922 | 0.150 | 8.32 | -22.96 | 0.690 | 0.524 | 74.52 | 8.73 | -4.91 | 0.823 | 0.320 | 78.17 |
| 4 | 1.499 | 12352. | 1.140 | 2.713 | 0.399 | 81.15 | 43.30 | 0.920 | 0.153 | 7.81 | 43.40 | 0.618 | 0.539 | 77.36 | 7.81 | 16.34 | 0.824 | 0.320 | 81.46 |
| 4 | 1.500 | 14997. | 1.094 | 2.045 | 0.474 | 81.17 | -49.31 | 0.915 | 0.162 | 6.23 | 61.80 | 0.635 | 0.597 | 74.59 | 6.67 | 50.57 | 0.835 | 0.320 | 81.46 |
| 4 | 1.500 | 17520. | 0.985 | 1.365 | 0.513 | 81.18 | -78.89 | 0.912 | 0.168 | 4.23 | 74.57 | 0.608 | 0.570 | 64.71 | 4.64 | 64.65 | 0.835 | 0.320 | 81.46 |
| 5 | 1.600 | 9851. | 1.258 | 4.752 | 0.328 | 81.05 | 68.03 | 0.926 | 0.143 | 10.30 | -8.95 | 0.697 | 0.515 | 69.47 | 10.57 | -25.64 | 0.797 | 0.366 | 71.96 |
| 5 | 1.600 | 11072. | 1.234 | 3.293 | 0.378 | 81.06 | 62.29 | 0.925 | 0.146 | 9.04 | -10.04 | 0.703 | 0.506 | 77.78 | 9.04 | -12.76 | 0.825 | 0.366 | 77.52 |
| 5 | 1.600 | 13494. | 1.166 | 2.373 | 0.430 | 81.11 | 51.73 | 0.922 | 0.154 | 7.67 | 36.50 | 0.678 | 0.540 | 79.39 | 7.67 | 29.61 | 0.835 | 0.366 | 81.46 |
| 5 | 1.600 | 15356. | 1.122 | 1.972 | 0.486 | 81.13 | -30.74 | 0.920 | 0.159 | 6.52 | 49.50 | 0.653 | 0.540 | 77.41 | 6.52 | 55.62 | 0.811 | 0.371 | 82.68 |
| 5 | 1.600 | 16818. | 1.071 | 1.643 | 0.543 | 81.16 | -60.48 | 0.917 | 0.159 | 5.42 | 67.02 | 0.653 | 0.573 | 73.41 | 5.83 | 43.83 | 0.793 | 0.371 | 82.68 |
| 6 | 1.699 | 10711. | 1.296 | 4.534 | 0.332 | 81.00 | 66.99 | 0.928 | 0.139 | 11.40 | -16.81 | 0.765 | 0.415 | 72.50 | 11.76 | -29.20 | 0.855 | 0.269 | 74.80 |
| 6 | 1.699 | 13069. | 1.242 | 3.271 | 0.359 | 81.02 | 60.54 | 0.926 | 0.143 | 10.46 | -28.91 | 0.744 | 0.446 | 78.01 | 10.46 | -8.46 | 0.860 | 0.269 | 80.24 |
| 6 | 1.699 | 14993. | 1.205 | 2.315 | 0.439 | 81.08 | 47.00 | 0.924 | 0.146 | 8.97 | 28.09 | 0.724 | 0.475 | 80.28 | 8.97 | 29.87 | 0.834 | 0.304 | 83.27 |
| 6 | 1.699 | 16369. | 1.160 | 1.941 | 0.493 | 81.11 | -34.24 | 0.922 | 0.154 | 7.63 | 56.60 | 0.706 | 0.501 | 78.17 | 7.63 | 48.03 | 0.819 | 0.304 | 83.27 |
| 6 | 1.698 | 17437. | 1.122 | 1.711 | 0.534 | 81.13 | -56.17 | 0.920 | 0.154 | 6.44 | 60.00 | 0.719 | 0.493 | 77.07 | 6.44 | 48.03 | 0.835 | 0.304 | 83.27 |

PERFORMANCE EVALUATION OF ICP RADIAL TURBINE

TABLE B10

INPUT DATA
CLEARANCE = 0.024 IN.

| RUN/PT | RPM | TORQUE COUNTS | P5P IN.HG | H1 IN.H2O | DPVC IN.HG | PATM IN.HG | HREF1 IN.HG | V4 MV | V5 MV | V20 MV | V21 MV | V22 MV | TRM DEG.F | TCJ DEG.F |
|--------|--------|------------------|--------------|--------------|---------------|---------------|----------------|----------|----------|-----------|-----------|-----------|--------------|--------------|
| 1 | 5770. | 175. | 9.10 | 23.48 | 3.306 | 30.11 | 0.0 | 1.809 | 1.739 | 1.234 | 1.287 | 1.462 | 80.9 | 32.0 |
| 1 | 7010. | 152. | 8.90 | 25.71 | 3.071 | 30.11 | 0.0 | 1.837 | 1.766 | 1.249 | 1.332 | 1.496 | 81.0 | 32.0 |
| 1 | 8510. | 126. | 8.66 | 25.34 | 2.797 | 30.11 | 0.0 | 1.838 | 1.768 | 1.262 | 1.393 | 1.492 | 81.0 | 32.0 |
| 1 | 10040. | 94. | 8.24 | 37.44 | 2.413 | 30.11 | 0.0 | 1.824 | 1.754 | 1.301 | 1.443 | 1.593 | 81.0 | 32.0 |
| 1 | 11600. | 65. | 5.88 | 45.66 | 2.008 | 30.11 | 0.0 | 1.836 | 1.763 | 1.310 | 1.510 | 1.783 | 81.0 | 32.0 |
| 1 | 13730. | 14. | 5.93 | 59.93 | 1.239 | 30.11 | 0.0 | 1.812 | 1.739 | 1.310 | 1.571 | 1.980 | 80. | 32.0 |
| 2 | 7170. | 265. | 13.38 | 35.06 | 4.641 | 30.11 | 0.0 | 1.862 | 1.796 | 1.300 | 1.345 | 1.419 | 79.9 | 32.0 |
| 2 | 8500. | 236. | 13.12 | 38.55 | 4.377 | 30.11 | 0.0 | 1.869 | 1.801 | 1.304 | 1.379 | 1.442 | 80.0 | 32.0 |
| 2 | 10000. | 202. | 12.15 | 44.76 | 4.056 | 30.11 | 0.0 | 1.876 | 1.796 | 1.309 | 1.408 | 1.527 | 80.0 | 32.0 |
| 2 | 11450. | 166. | 12.45 | 52.56 | 3.691 | 30.11 | 0.0 | 1.876 | 1.806 | 1.339 | 1.482 | 1.772 | 80.0 | 32.0 |
| 2 | 13000. | 128. | 12.01 | 62.11 | 3.238 | 30.11 | 0.0 | 1.889 | 1.821 | 1.377 | 1.574 | 1.971 | 80.0 | 32.0 |
| 2 | 14630. | 94. | 11.54 | 72.67 | 2.726 | 30.11 | 0.0 | 1.908 | 1.833 | 1.399 | 1.650 | 2.066 | 80.0 | 32.0 |
| 2 | 16520. | 28. | 10.67 | 89.40 | 1.805 | 30.11 | 0.0 | 1.937 | 1.848 | 1.411 | 1.764 | 2.160 | 80. | 32.0 |
| 3 | 8370. | 353. | 17.59 | 46.95 | 5.899 | 30.11 | 0.0 | 1.970 | 1.888 | 1.399 | 1.426 | 1.515 | 80.5 | 32.0 |
| 3 | 9950. | 314. | 17.67 | 52.75 | 5.483 | 30.11 | 0.0 | 1.986 | 1.909 | 1.388 | 1.431 | 1.515 | 80.5 | 32.0 |
| 3 | 11520. | 272. | 17.28 | 14.42 | 5.155 | 30.11 | 0.0 | 1.996 | 1.934 | 1.405 | 1.452 | 1.554 | 80.5 | 32.0 |
| 3 | 12510. | 244. | 17.05 | 21.20 | 4.887 | 30.11 | 0.0 | 2.001 | 1.946 | 1.415 | 1.500 | 1.584 | 80.5 | 32.0 |
| 3 | 13990. | 202. | 16.50 | 32.20 | 4.438 | 30.11 | 0.0 | 2.013 | 1.956 | 1.440 | 1.595 | 1.944 | 80.5 | 32.0 |
| 3 | 15340. | 160. | 16.02 | 42.55 | 3.929 | 30.11 | 0.0 | 2.008 | 1.960 | 1.455 | 1.680 | 2.065 | 80.5 | 32.0 |
| 3 | 17030. | 110. | 15.84 | 19.71 | 3.297 | 30.11 | 0.0 | 2.012 | 1.959 | 1.475 | 1.794 | 2.233 | 79.9 | 32.0 |
| 3 | 18250. | 162. | 14.68 | 33.07 | 2.649 | 30.11 | 0.0 | 2.015 | 1.952 | 1.488 | 1.884 | 2.306 | 79.8 | 32.0 |
| 4 | 9310. | 437. | 21.82 | 13.06 | 7.047 | 30.10 | 3.40 | 1.745 | 1.651 | 1.191 | 1.262 | 1.366 | 80.7 | 32.0 |
| 4 | 10810. | 398. | 21.42 | 11.38 | 6.763 | 30.10 | 3.89 | 1.872 | 1.777 | 1.252 | 1.346 | 1.534 | 80.5 | 32.0 |
| 4 | 12310. | 354. | 21.12 | 16.86 | 6.393 | 30.10 | 4.84 | 1.903 | 1.812 | 1.286 | 1.394 | 1.788 | 79.9 | 32.0 |
| 4 | 13840. | 307. | 20.60 | 11.65 | 5.941 | 30.10 | 5.28 | 1.936 | 1.851 | 1.354 | 1.459 | 1.981 | 80.0 | 32.0 |
| 4 | 15310. | 258. | 20.30 | 19.59 | 5.431 | 30.10 | 6.30 | 1.957 | 1.865 | 1.637 | 1.387 | 2.218 | 80.0 | 32.0 |
| 4 | 16800. | 212. | 19.62 | 11.59 | 4.875 | 30.10 | 7.03 | 1.959 | 1.874 | 1.427 | 1.752 | 2.297 | 79.9 | 32.0 |
| 4 | 18380. | 155. | 19.02 | 10.43 | 4.202 | 30.10 | 8.21 | 1.963 | 1.874 | 1.446 | 1.857 | 2.366 | 79.9 | 32.0 |
| 5 | 10350. | 525. | 25.80 | 8.70 | 8.170 | 30.10 | 4.60 | 1.982 | 1.887 | 1.386 | 1.367 | 1.528 | 79.1 | 32.0 |
| 5 | 12070. | 470. | 25.48 | 7.82 | 7.777 | 30.10 | 5.16 | 1.977 | 1.886 | 1.397 | 1.392 | 1.600 | 79.0 | 32.0 |
| 5 | 13500. | 424. | 25.10 | 9.65 | 7.393 | 30.10 | 5.80 | 1.975 | 1.880 | 1.420 | 1.487 | 1.886 | 79.0 | 32.0 |
| 5 | 15030. | 368. | 24.60 | 6.71 | 6.892 | 30.10 | 6.95 | 1.971 | 1.889 | 1.450 | 1.590 | 1.981 | 79.0 | 32.0 |
| 5 | 16510. | 314. | 24.10 | 6.58 | 6.327 | 30.10 | 7.92 | 1.970 | 1.891 | 1.477 | 1.699 | 2.152 | 78.1 | 32.0 |
| 5 | 18090. | 260. | 23.51 | 7.56 | 5.716 | 30.10 | 8.89 | 1.970 | 1.899 | 1.477 | 1.818 | 2.240 | 78.1 | 32.0 |
| 6 | 12200. | 605. | 29.80 | 10.44 | 9.214 | 30.04 | 5.30 | 1.968 | 1.902 | 1.437 | 1.370 | 1.655 | 76.0 | 32.0 |
| 6 | 14000. | 559. | 29.50 | 19.76 | 8.884 | 30.04 | 5.80 | 1.971 | 1.902 | 1.426 | 1.396 | 1.707 | 76.3 | 32.0 |
| 6 | 15550. | 509. | 29.10 | 19.16 | 8.490 | 30.04 | 6.42 | 1.966 | 1.896 | 1.435 | 1.456 | 1.819 | 76.3 | 32.0 |
| 6 | 17000. | 448. | 28.61 | 12.20 | 7.971 | 30.04 | 7.89 | 1.970 | 1.890 | 1.446 | 1.557 | 2.053 | 77.0 | 32.0 |
| 6 | 18030. | 389. | 28.02 | 16.59 | 7.391 | 30.04 | 8.89 | 1.970 | 1.887 | 1.471 | 1.739 | 2.149 | 77.1 | 32.0 |
| 6 | 18030. | 349. | 27.62 | 10.80 | 6.986 | 30.04 | 9.40 | 1.960 | 1.883 | 1.471 | 1.739 | 2.149 | 77.1 | 32.0 |

PERFORMANCE EVALUATION OF ICP RADIAL TURBINE

TABLE B11

OUTPUT DATA

CLEARANCE = 0.024 IN.

REDUCED TO STANDARD AIR IN ACCORDANCE WITH NASA METHOD:
 TOTAL INLET PRESS. = 14.7 PSIA, TOTAL INLET TEMPERATURE
 = 518.7 DEG.R., $G_{A,STD} = 1.4$, $C_p = 0.24$ BTU/LBM-DEG.F.

| RUN/PT | PRESS RATIO | REF. SPEED RPM | REF. FLOW LB/SEC | HEAD COEFF | DEG REACT | ANGLE ALPHA DEG | ANGLE BETA DEG | VEL COEFF GV | LOSS COEFF GV | NO BEARING LOSSES | | | | MAXIMUM BEARING LOSSES | | | | | |
|--------|----------------|----------------------|------------------------|---------------|--------------|-----------------------|----------------------|--------------------|---------------------|---------------------|-----------------------|--------------|---------------|------------------------|---------------------|-----------------------|--------------|---------------|-----------------|
| | | | | | | | | | | REF MOM FT.LB | ANGLE ALF20 DEG | VEL COEFF | LOSS ROTOR | EFFIC- IENCY | REF MOM FT.LB | ANGLE ALF20 DEG | VEL COEFF | LOSS ROTOR | EFFIC- IENCY |
| 1 | 1 | 199 | 0.920 | 5.997 | 0.302 | 80.88 | 70.62 | 0.910 | 0.171 | 4.71 | 2.27 | 0.578 | 0.665 | 61.15 | 5.00 | -30.67 | 0.750 | 0.437 | 64.97 |
| 1 | 1 | 200 | 0.886 | 4.075 | 0.329 | 80.88 | 63.81 | 0.910 | 0.173 | 4.08 | 51.91 | 0.510 | 0.740 | 66.73 | 4.46 | 0.08 | 0.749 | 0.439 | 72.85 |
| 1 | 1 | 199 | 0.845 | 2.760 | 0.476 | 80.87 | 48.91 | 0.904 | 0.182 | 3.38 | 78.50 | 0.398 | 0.834 | 70.39 | 3.82 | 52.88 | 0.784 | 0.416 | 78.56 |
| 1 | 1 | 199 | 0.784 | 1.982 | 0.577 | 80.86 | -31.69 | 0.900 | 0.189 | 2.50 | 81.36 | 0.382 | 0.854 | 66.42 | 2.99 | 51.59 | 0.763 | 0.417 | 78.56 |
| 1 | 1 | 199 | 0.560 | 1.058 | 0.749 | 80.82 | -82.38 | 0.891 | 0.205 | 1.72 | 82.51 | 0.102 | 0.854 | 57.60 | 0.87 | 74.67 | 0.671 | 0.550 | 44.17 |
| 2 | 2 | 6933 | 1.051 | 5.540 | 0.307 | 80.86 | 69.78 | 0.918 | 0.157 | 6.51 | -5.21 | 0.636 | 0.595 | 64.60 | 6.86 | -30.98 | 0.789 | 0.378 | 68.18 |
| 2 | 2 | 6933 | 1.020 | 3.949 | 0.336 | 80.86 | 63.17 | 0.917 | 0.162 | 5.88 | 26.62 | 0.640 | 0.591 | 71.17 | 5.28 | -12.98 | 0.823 | 0.316 | 76.18 |
| 2 | 2 | 6933 | 0.980 | 2.853 | 0.388 | 80.87 | 45.31 | 0.913 | 0.167 | 5.02 | 25.62 | 0.602 | 0.693 | 74.37 | 5.47 | 16.25 | 0.823 | 0.316 | 76.18 |
| 2 | 2 | 6933 | 0.934 | 2.176 | 0.453 | 80.88 | -67.19 | 0.909 | 0.173 | 4.17 | 69.67 | 0.555 | 0.719 | 68.18 | 4.50 | 40.03 | 0.808 | 0.347 | 81.86 |
| 2 | 2 | 6933 | 0.874 | 1.686 | 0.533 | 80.88 | -57.81 | 0.909 | 0.181 | 3.17 | 75.90 | 0.530 | 0.666 | 61.30 | 3.66 | 53.20 | 0.897 | 0.347 | 76.61 |
| 2 | 2 | 6933 | 0.800 | 1.335 | 0.617 | 80.88 | -74.11 | 0.909 | 0.181 | 2.31 | 75.90 | 0.530 | 0.666 | 61.30 | 2.81 | 56.20 | 0.897 | 0.347 | 76.61 |
| 2 | 2 | 6933 | 0.650 | 1.047 | 0.750 | 80.85 | -82.41 | 0.897 | 0.195 | 0.65 | 82.83 | 0.259 | 0.933 | 24.13 | 1.11 | 75.53 | 0.645 | 0.585 | 42.61 |
| 3 | 3 | 8071 | 1.148 | 5.192 | 0.314 | 80.82 | 68.90 | 0.923 | 0.147 | 8.14 | -15.30 | 0.707 | 0.501 | 67.95 | 8.51 | -33.33 | 0.838 | 0.298 | 71.68 |
| 3 | 3 | 8071 | 1.107 | 3.749 | 0.352 | 80.85 | 62.86 | 0.922 | 0.150 | 7.21 | 20.95 | 0.682 | 0.535 | 73.83 | 7.62 | -13.70 | 0.837 | 0.299 | 76.50 |
| 3 | 3 | 8071 | 1.073 | 2.682 | 0.392 | 80.86 | 42.09 | 0.921 | 0.153 | 6.21 | 20.95 | 0.628 | 0.506 | 79.03 | 6.13 | 30.46 | 0.829 | 0.312 | 81.28 |
| 3 | 3 | 8071 | 1.045 | 2.036 | 0.436 | 80.87 | 13.91 | 0.916 | 0.161 | 5.65 | 51.20 | 0.626 | 0.609 | 74.86 | 5.40 | 30.46 | 0.829 | 0.312 | 81.28 |
| 3 | 3 | 8071 | 0.993 | 1.868 | 0.458 | 80.88 | -41.50 | 0.913 | 0.167 | 4.69 | 65.90 | 0.631 | 0.677 | 69.86 | 4.15 | 54.63 | 0.852 | 0.313 | 82.78 |
| 3 | 3 | 8071 | 0.933 | 1.517 | 0.567 | 80.88 | -66.63 | 0.908 | 0.175 | 3.62 | 76.38 | 0.568 | 0.677 | 57.34 | 2.98 | 54.63 | 0.852 | 0.313 | 82.78 |
| 3 | 3 | 8071 | 0.853 | 1.260 | 0.648 | 80.87 | -76.63 | 0.908 | 0.184 | 2.52 | 81.76 | 0.427 | 0.918 | 38.11 | 1.86 | 72.77 | 0.690 | 0.523 | 67.56 |
| 3 | 3 | 8071 | 0.761 | 1.100 | 0.726 | 80.87 | -81.22 | 0.903 | 0.184 | 1.40 | 81.76 | 0.427 | 0.918 | 38.11 | 1.86 | 72.77 | 0.690 | 0.523 | 67.56 |
| 4 | 4 | 9042 | 1.211 | 4.954 | 0.321 | 80.78 | 68.12 | 0.927 | 0.140 | 9.37 | -12.73 | 0.707 | 0.500 | 69.19 | 9.74 | -29.70 | 0.820 | 0.327 | 71.95 |
| 4 | 4 | 9042 | 1.184 | 3.704 | 0.347 | 80.79 | 61.37 | 0.926 | 0.145 | 8.50 | 20.44 | 0.687 | 0.528 | 74.26 | 8.91 | -14.30 | 0.818 | 0.332 | 77.80 |
| 4 | 4 | 9042 | 1.151 | 2.854 | 0.390 | 80.83 | 46.46 | 0.925 | 0.149 | 7.53 | 20.44 | 0.663 | 0.560 | 77.51 | 8.07 | 18.30 | 0.818 | 0.332 | 81.28 |
| 4 | 4 | 9042 | 1.109 | 2.263 | 0.445 | 80.85 | 27.31 | 0.923 | 0.154 | 6.54 | 44.69 | 0.646 | 0.569 | 76.22 | 7.09 | 30.46 | 0.818 | 0.332 | 81.28 |
| 4 | 4 | 9042 | 1.058 | 1.853 | 0.503 | 80.86 | -42.75 | 0.920 | 0.159 | 5.51 | 61.47 | 0.656 | 0.569 | 72.25 | 6.07 | 46.27 | 0.818 | 0.332 | 81.28 |
| 4 | 4 | 9042 | 1.000 | 1.541 | 0.560 | 80.86 | -64.75 | 0.917 | 0.166 | 4.42 | 68.54 | 0.665 | 0.558 | 61.83 | 5.04 | 55.27 | 0.818 | 0.332 | 81.28 |
| 4 | 4 | 9042 | 0.927 | 1.287 | 0.631 | 80.88 | -75.26 | 0.913 | 0.166 | 3.27 | 74.54 | 0.619 | 0.616 | 51.83 | 3.69 | 64.74 | 0.818 | 0.332 | 81.28 |
| 5 | 5 | 9975 | 1.263 | 4.671 | 0.327 | 80.73 | 67.07 | 0.930 | 0.135 | 10.53 | -15.90 | 0.749 | 0.439 | 71.66 | 10.90 | -29.88 | 0.850 | 0.285 | 74.18 |
| 5 | 5 | 9975 | 1.200 | 3.474 | 0.355 | 80.75 | 60.66 | 0.928 | 0.140 | 9.47 | 18.27 | 0.730 | 0.467 | 76.97 | 9.86 | -12.93 | 0.845 | 0.285 | 77.80 |
| 5 | 5 | 9975 | 1.151 | 2.746 | 0.400 | 80.77 | 42.42 | 0.925 | 0.144 | 8.51 | 18.27 | 0.723 | 0.477 | 79.38 | 8.92 | 13.29 | 0.845 | 0.285 | 81.28 |
| 5 | 5 | 9975 | 1.107 | 2.155 | 0.454 | 80.80 | 27.31 | 0.923 | 0.148 | 7.53 | 44.69 | 0.646 | 0.516 | 77.08 | 8.07 | 30.46 | 0.845 | 0.285 | 81.28 |
| 5 | 5 | 9975 | 1.051 | 1.835 | 0.508 | 80.83 | -43.75 | 0.920 | 0.153 | 6.54 | 61.47 | 0.676 | 0.543 | 72.88 | 6.63 | 47.38 | 0.845 | 0.285 | 81.28 |
| 5 | 5 | 9975 | 1.001 | 1.521 | 0.565 | 80.85 | -65.26 | 0.913 | 0.153 | 5.10 | 68.54 | 0.681 | 0.536 | 61.83 | 5.50 | 56.59 | 0.845 | 0.285 | 81.28 |
| 6 | 6 | 10813 | 1.306 | 4.450 | 0.330 | 80.69 | 66.11 | 0.932 | 0.131 | 11.53 | -16.00 | 0.773 | 0.403 | 73.46 | 11.89 | -28.51 | 0.864 | 0.254 | 75.77 |
| 6 | 6 | 10813 | 1.251 | 3.569 | 0.358 | 80.72 | 60.05 | 0.931 | 0.136 | 10.61 | 10.07 | 0.746 | 0.443 | 76.96 | 10.90 | -12.93 | 0.864 | 0.254 | 79.03 |
| 6 | 6 | 10813 | 1.200 | 2.859 | 0.388 | 80.76 | 43.70 | 0.928 | 0.140 | 9.69 | 20.44 | 0.757 | 0.467 | 80.97 | 10.07 | 13.29 | 0.864 | 0.254 | 82.78 |
| 6 | 6 | 10813 | 1.151 | 2.316 | 0.423 | 80.78 | 27.31 | 0.926 | 0.144 | 8.50 | 44.69 | 0.646 | 0.481 | 79.59 | 9.18 | 30.46 | 0.864 | 0.254 | 86.18 |
| 6 | 6 | 10813 | 1.100 | 1.937 | 0.453 | 80.81 | -43.75 | 0.923 | 0.148 | 7.53 | 61.47 | 0.656 | 0.461 | 77.65 | 8.28 | 47.38 | 0.864 | 0.254 | 90.18 |
| 6 | 6 | 10813 | 1.051 | 1.721 | 0.533 | 80.81 | -53.92 | 0.924 | 0.145 | 6.56 | 59.48 | 0.720 | 0.482 | 77.65 | 7.42 | 49.38 | 0.864 | 0.254 | 94.18 |

PERFORMANCE EVALUATION OF ICP RADIAL TURBINE

CLEARANCE = 0.015 IN.

TABLE B12

INPUT DATA

| RUN/PT | RPM | TORQUE COUNTS | PUVC IN.HG | P5P IN.HG | H1 IN.H2O | DPVC IN.HG | PATM IN.HG | HREF1 IN.HG | V4 MV | V5 MV | V20 MV | V21 MV | V22 MV | IPM DEG. F | ICJ DEG. F |
|--------|--------|------------------|---------------|--------------|--------------|---------------|---------------|----------------|----------|----------|-----------|-----------|-----------|---------------|---------------|
| 1 | 5790. | 178. | 9.10 | 5.83 | 23.53 | 3.295 | 30.16 | 0.0 | 1.841 | 1.759 | 1.163 | 1.250 | 1.422 | 79.0 | 32.0 |
| 1 | 7480. | 147. | 8.82 | 5.86 | 27.09 | 2.970 | 30.16 | 0.0 | 1.851 | 1.767 | 1.180 | 1.311 | 1.417 | 79.1 | 32.0 |
| 1 | 9030. | 118. | 8.50 | 5.89 | 33.01 | 2.659 | 30.16 | 0.0 | 1.848 | 1.772 | 1.199 | 1.378 | 1.457 | 79.2 | 32.0 |
| 1 | 10490. | 84. | 8.16 | 5.90 | 39.93 | 2.283 | 30.16 | 0.0 | 1.857 | 1.783 | 1.227 | 1.444 | 1.411 | 79.8 | 32.0 |
| 1 | 12050. | 54. | 7.73 | 5.91 | 47.79 | 1.869 | 30.16 | 0.0 | 1.869 | 1.788 | 1.243 | 1.496 | 1.820 | 79.8 | 32.0 |
| 1 | 13700. | 11. | 7.15 | 5.94 | 60.55 | 1.201 | 30.16 | 0.0 | 1.865 | 1.775 | 1.247 | 1.534 | 1.957 | 79.7 | 32.0 |
| 2 | 7190. | 266. | 13.43 | 8.79 | 35.28 | 4.671 | 30.16 | 0.0 | 1.896 | 1.836 | 1.264 | 1.326 | 1.390 | 78.0 | 32.0 |
| 2 | 8960. | 227. | 13.07 | 8.80 | 40.36 | 4.285 | 30.16 | 0.0 | 1.900 | 1.840 | 1.268 | 1.369 | 1.455 | 78.0 | 32.0 |
| 2 | 10500. | 190. | 12.65 | 8.81 | 47.34 | 3.940 | 30.16 | 0.0 | 1.908 | 1.840 | 1.283 | 1.421 | 1.571 | 77.9 | 32.0 |
| 2 | 11200. | 153. | 12.32 | 8.82 | 56.00 | 3.533 | 30.16 | 0.0 | 1.909 | 1.839 | 1.295 | 1.471 | 1.790 | 78.0 | 32.0 |
| 2 | 13440. | 119. | 11.91 | 8.83 | 12.60 | 3.103 | 30.16 | 3.81 | 1.911 | 1.840 | 1.310 | 1.544 | 1.948 | 78.0 | 32.0 |
| 2 | 14960. | 77. | 11.36 | 8.86 | 24.19 | 2.523 | 30.16 | 3.81 | 1.913 | 1.838 | 1.319 | 1.620 | 2.083 | 78.1 | 32.0 |
| 2 | 16720. | 15. | 10.54 | 8.91 | 21.96 | 1.612 | 30.16 | 3.81 | 1.914 | 1.835 | 1.333 | 1.733 | 2.210 | 78.1 | 32.0 |
| 3 | 8370. | 356. | 17.64 | 11.72 | 7.79 | 5.929 | 30.16 | 2.90 | 1.928 | 1.862 | 1.335 | 1.391 | 1.446 | 78.5 | 32.0 |
| 3 | 10460. | 300. | 17.17 | 11.73 | 15.54 | 5.444 | 30.16 | 2.90 | 1.929 | 1.864 | 1.319 | 1.397 | 1.551 | 78.6 | 32.0 |
| 3 | 12490. | 243. | 16.66 | 11.76 | 27.28 | 4.931 | 30.16 | 2.90 | 1.929 | 1.868 | 1.320 | 1.459 | 1.817 | 79.0 | 32.0 |
| 3 | 14600. | 182. | 16.03 | 11.80 | 27.21 | 4.230 | 30.16 | 4.32 | 1.908 | 1.861 | 1.329 | 1.552 | 2.017 | 79.0 | 32.0 |
| 3 | 16050. | 128. | 15.31 | 11.82 | 22.69 | 3.517 | 30.16 | 5.34 | 1.889 | 1.838 | 1.355 | 1.673 | 2.168 | 79.0 | 32.0 |
| 3 | 18050. | 60. | 14.49 | 11.89 | 20.46 | 2.637 | 30.16 | 6.92 | 1.864 | 1.817 | 1.358 | 1.762 | 2.272 | 78.5 | 32.0 |
| 4 | 9410. | 442. | 21.85 | 14.70 | 17.76 | 7.131 | 30.13 | 3.02 | 1.871 | 1.836 | 1.330 | 1.343 | 1.482 | 78.1 | 32.0 |
| 4 | 1090. | 392. | 21.54 | 14.74 | 12.93 | 6.765 | 30.13 | 3.83 | 1.864 | 1.838 | 1.321 | 1.322 | 1.619 | 78.0 | 32.0 |
| 4 | 13010. | 336. | 21.00 | 14.77 | 12.72 | 6.290 | 30.13 | 5.81 | 1.851 | 1.820 | 1.315 | 1.371 | 1.838 | 78.0 | 32.0 |
| 4 | 15000. | 272. | 20.40 | 14.79 | 14.93 | 5.589 | 30.13 | 5.70 | 1.838 | 1.796 | 1.331 | 1.529 | 1.984 | 78.5 | 32.0 |
| 4 | 17000. | 209. | 19.61 | 14.83 | 15.07 | 4.817 | 30.13 | 6.97 | 1.837 | 1.793 | 1.347 | 1.632 | 2.044 | 77.5 | 32.0 |
| 4 | 18100. | 165. | 19.11 | 14.87 | 10.86 | 4.277 | 30.13 | 8.08 | 1.836 | 1.793 | 1.360 | 1.702 | 2.174 | 77.2 | 32.0 |
| 5 | 10320. | 534. | 26.04 | 17.72 | 13.79 | 8.310 | 30.21 | 4.20 | 1.938 | 1.834 | 1.238 | 1.277 | 1.463 | 69.1 | 32.0 |
| 5 | 12040. | 477. | 25.63 | 17.75 | 10.23 | 7.902 | 30.21 | 5.00 | 1.972 | 1.873 | 1.285 | 1.354 | 1.652 | 71.0 | 32.0 |
| 5 | 13520. | 428. | 25.28 | 17.77 | 8.49 | 7.506 | 30.21 | 5.88 | 1.986 | 1.886 | 1.327 | 1.460 | 1.893 | 72.5 | 32.0 |
| 5 | 15060. | 372. | 24.77 | 17.80 | 10.91 | 6.957 | 30.21 | 6.63 | 1.980 | 1.891 | 1.357 | 1.570 | 2.011 | 73.5 | 32.0 |
| 5 | 16500. | 317. | 24.20 | 17.82 | 11.91 | 6.398 | 30.21 | 7.53 | 1.989 | 1.896 | 1.372 | 1.641 | 2.049 | 73.1 | 32.0 |
| 5 | 17980. | 266. | 23.70 | 17.83 | 11.45 | 5.839 | 30.21 | 8.75 | 1.986 | 1.895 | 1.400 | 1.779 | 2.256 | 73.1 | 32.0 |
| 6 | 12390. | 611. | 30.08 | 20.69 | 7.64 | 9.376 | 30.21 | 5.49 | 2.145 | 2.048 | 1.347 | 1.345 | 1.532 | 70.8 | 32.0 |
| 6 | 14020. | 571. | 29.80 | 20.72 | 8.86 | 9.094 | 30.21 | 5.87 | 2.145 | 2.054 | 1.355 | 1.357 | 1.701 | 70.0 | 32.0 |
| 6 | 15530. | 455. | 28.90 | 20.74 | 8.28 | 8.665 | 30.21 | 6.56 | 2.145 | 2.056 | 1.373 | 1.450 | 1.883 | 69.0 | 32.0 |
| 6 | 16980. | 396. | 28.29 | 20.78 | 8.18 | 8.133 | 30.21 | 7.62 | 2.136 | 2.052 | 1.393 | 1.550 | 2.010 | 69.5 | 32.0 |
| 6 | 18150. | 351. | 27.80 | 20.81 | 11.95 | 7.105 | 30.21 | 9.35 | 2.134 | 2.050 | 1.414 | 1.733 | 2.213 | 69.5 | 32.0 |

CLEARANCE = 0.015 IN.

OUTPUT DATA

TABLE B13

REDUCED TO STANDARD AIR IN ACCORDANCE WITH NASA METHOD.
TOTAL INLET PRESS. = 14.7 PSIA; TOTAL INLET TEMPERATURE
= 518.7 DEG.R.; GAMMA = 1.4; CP = 0.24 BTU/LBM-DEG.F.

| RUN/PT | PRESS RATIO | REF. SPEED RPM | REF. FLOW LB/SEC | HEAD COEFF | DEG. REACT | ANGLE ALPHA DEG | ANGLE BETA DEG | VEL COEFF GV | LOSS COEFF GV | NO BEARING LOSSES | | | | MAXIMUM BEARING LOSSES | | | | | |
|--------|----------------|----------------------|------------------------|---------------|---------------|-----------------------|----------------------|--------------------|---------------------|---------------------|-----------------------|--------------|------------------------|------------------------|---------------------|-----------------------|--------------|------------------------|----------------|
| | | | | | | | | | | REF MOM FT.LB | ANGLE ALF20 DEG | VEL COEFF | LOSS COEFF ROTOR | EFFIC- ENCY | REF MOM FT.LB | ANGLE ALF20 DEG | VEL COEFF | LOSS COEFF ROTOR | EFFIC- ENCY |
| 1 | 1.199 | 5605. | C.918 | 5.945 | 0.303 | 80.70 | 70.24 | 0.915 | 0.163 | 4.83 | -14.71 | C.651 | 0.576 | 63.22 | 5.12 | -37.91 | 0.924 | 0.322 | 67.09 |
| 1 | 1.199 | 7240. | C.872 | 3.571 | 0.347 | 80.70 | 59.22 | 0.913 | 0.166 | 3.99 | -45.22 | C.584 | 0.559 | 71.01 | 3.66 | -22.75 | 0.844 | 0.288 | 73.08 |
| 1 | 1.200 | 8734. | C.822 | 2.457 | 0.420 | 80.69 | 22.60 | 0.911 | 0.170 | 3.39 | 66.00 | C.535 | 0.713 | 72.76 | 3.39 | -6.85 | 0.857 | 0.265 | 73.11 |
| 1 | 1.199 | 10148. | C.762 | 1.819 | 0.506 | 80.68 | -47.34 | 0.904 | 0.176 | 2.79 | 79.64 | C.401 | 0.839 | 75.27 | 2.79 | 52.65 | 0.782 | 0.308 | 72.42 |
| 1 | 1.199 | 11355. | C.551 | 1.064 | 0.756 | 80.64 | -82.31 | 0.895 | 0.198 | 0.32 | 88.28 | C.360 | 0.871 | 53.79 | 0.86 | 61.66 | 0.823 | 0.323 | 72.43 |
| 2 | 1.295 | 6944. | 1.054 | 5.531 | 0.308 | 80.68 | 69.48 | 0.923 | 0.149 | 6.47 | 3.90 | C.598 | 0.642 | 64.06 | 6.92 | -26.39 | 0.757 | 0.430 | 67.55 |
| 2 | 1.299 | 8652. | 1.008 | 3.560 | 0.351 | 80.69 | 59.24 | 0.921 | 0.152 | 5.67 | 34.45 | C.640 | 0.591 | 73.13 | 6.09 | -6.69 | 0.837 | 0.330 | 78.60 |
| 2 | 1.298 | 10150. | 0.965 | 1.981 | 0.482 | 80.70 | 33.36 | 0.919 | 0.156 | 4.37 | 58.91 | C.594 | 0.647 | 75.26 | 5.32 | 42.44 | 0.822 | 0.323 | 82.51 |
| 2 | 1.298 | 11247. | 0.855 | 1.578 | 0.551 | 80.70 | -29.38 | 0.913 | 0.167 | 3.94 | 73.71 | C.565 | 0.688 | 68.38 | 3.44 | 53.41 | 0.849 | 0.378 | 76.15 |
| 2 | 1.298 | 16149. | 0.770 | 1.020 | 0.626 | 80.70 | -76.09 | 0.908 | 0.174 | 0.40 | -86.35 | C.422 | 0.751 | 15.78 | 0.90 | 82.86 | 0.826 | 0.374 | 65.15 |
| 3 | 1.398 | 8077. | 1.147 | 5.184 | 0.315 | 80.64 | 68.60 | 0.928 | 0.139 | 8.15 | -13.03 | C.693 | 0.520 | 67.96 | 8.52 | -32.05 | 0.823 | 0.372 | 71.07 |
| 3 | 1.398 | 10083. | 1.109 | 3.317 | 0.368 | 80.68 | 56.25 | 0.923 | 0.148 | 6.66 | 40.56 | C.637 | 0.594 | 74.35 | 7.25 | 30.49 | 0.793 | 0.373 | 78.44 |
| 3 | 1.398 | 12089. | 1.045 | 1.937 | 0.426 | 80.69 | -13.15 | 0.919 | 0.153 | 4.27 | 57.44 | C.615 | 0.621 | 73.17 | 6.47 | 51.46 | 0.826 | 0.378 | 81.24 |
| 3 | 1.398 | 15893. | C.878 | 1.337 | 0.613 | 80.70 | -73.14 | 0.915 | 0.163 | 2.98 | 74.20 | C.413 | 0.829 | 64.47 | 3.45 | 60.59 | 0.856 | 0.267 | 74.86 |
| 4 | 1.500 | 9087. | 1.215 | 4.902 | 0.319 | 80.59 | 67.75 | 0.932 | 0.132 | 9.51 | -14.00 | 0.723 | 0.478 | 70.16 | 9.89 | -30.36 | 0.836 | 0.301 | 72.97 |
| 4 | 1.500 | 10706. | 1.182 | 3.534 | 0.347 | 80.61 | 59.58 | 0.931 | 0.134 | 8.71 | 29.72 | C.668 | 0.554 | 74.94 | 8.59 | 1.45 | 0.800 | 0.359 | 78.52 |
| 4 | 1.500 | 12430. | 1.174 | 1.926 | 0.467 | 80.66 | -31.95 | 0.925 | 0.138 | 7.44 | 52.29 | C.638 | 0.593 | 77.87 | 7.59 | 27.67 | 0.798 | 0.363 | 82.44 |
| 4 | 1.500 | 16433. | 0.995 | 1.423 | 0.572 | 80.69 | -66.27 | 0.921 | 0.157 | 3.58 | 65.22 | C.723 | 0.477 | 73.99 | 6.49 | 50.58 | 0.862 | 0.197 | 81.02 |
| 5 | 1.600 | 9967. | 1.277 | 4.884 | 0.355 | 80.54 | 66.91 | 0.935 | 0.126 | 10.72 | -18.49 | C.765 | 0.413 | 72.38 | 11.09 | -31.39 | 0.866 | 0.250 | 74.87 |
| 5 | 1.600 | 11614. | 1.235 | 3.560 | 0.398 | 80.59 | 59.24 | 0.934 | 0.130 | 9.61 | 36.21 | C.745 | 0.444 | 73.70 | 10.01 | -18.07 | 0.859 | 0.262 | 80.87 |
| 5 | 1.600 | 13451. | 1.195 | 2.457 | 0.451 | 80.62 | 42.98 | 0.932 | 0.135 | 8.71 | 52.29 | C.728 | 0.470 | 80.30 | 9.78 | 13.45 | 0.849 | 0.280 | 82.77 |
| 5 | 1.600 | 15903. | 1.110 | 1.819 | 0.551 | 80.64 | -43.44 | 0.930 | 0.139 | 7.62 | 61.13 | C.684 | 0.532 | 77.90 | 7.62 | 32.72 | 0.835 | 0.303 | 82.68 |
| 5 | 1.600 | 17327. | 1.060 | 1.064 | 0.563 | 80.67 | -63.63 | 0.925 | 0.145 | 5.26 | 66.08 | C.691 | 0.522 | 74.09 | 5.26 | 54.71 | 0.832 | 0.308 | 79.71 |
| 6 | 1.700 | 10829. | 1.312 | 4.433 | 0.351 | 80.49 | 65.89 | 0.937 | 0.123 | 11.98 | -14.16 | C.767 | 0.411 | 73.73 | 11.98 | -27.16 | 0.858 | 0.265 | 76.06 |
| 6 | 1.701 | 11944. | 1.261 | 3.262 | 0.385 | 80.57 | 60.40 | 0.936 | 0.125 | 10.89 | 32.88 | C.752 | 0.437 | 73.23 | 11.01 | -12.57 | 0.843 | 0.279 | 82.19 |
| 6 | 1.700 | 14893. | 1.121 | 2.219 | 0.432 | 80.61 | 17.93 | 0.933 | 0.130 | 9.64 | 62.43 | C.726 | 0.473 | 79.11 | 10.01 | 17.35 | 0.833 | 0.306 | 84.68 |
| 6 | 1.700 | 16248. | 1.043 | 1.579 | 0.453 | 80.63 | -52.42 | 0.929 | 0.137 | 7.60 | 60.15 | C.712 | 0.493 | 77.86 | 7.60 | 40.58 | 0.826 | 0.318 | 83.27 |

APPENDIX C

PROGRAM NOSPD

Program NOSPD calculates the referred moments and referred flow rates for the stopped-rotor tests and is in essence a much simplified version of program RADIAL. The computational techniques used are the same in both programs and will not be repeated. Program NOSPD is listed in Table C1, and the input and output data are given in Table C2. Table B3 lists the torque calibration data used for each run. The items of input data defined in the preceding section apply to this program, except as noted below.

| <u>Card No.</u> | <u>FORTRAN</u> | <u>Description</u> |
|-----------------|--|---|
| 1 | NRUNS | Number of runs (clearances) to be processed |
| 2 | CLNC | |
| 3 | TCD | |
| 4 | NPTS | |
| 5 | V4, V5, TCJ, PATM, P5P, DPVC, TQ, TRM | |

TABLE C1

```

C PROGRAM NUSPD.
C CALCULATES REFERRED MOMENTS AND REFERRED FLOW RATES FOR
C STOPPED-ROTOR TESTS.
C
C DIMENSION V4(10),V5(10),TCJ(10),PATM(10),P5P(10),DPVC(10),PUVC(10)
C * ,TO(10),TRM(10),TCD(50)
C WRITE HEADING FOR OUTPUT.
C WRITE(6,1)
C 1 FORMAT(1H1,///,T38,'PERFORMANCE EVALUATION OF ICP RADIAL TURBINE',
C * //,T56,'TABLE',//,T47,'RESULTS OF ZERO-SPEED TESTS',//,T40,'INPUT
C * DATA',T97,'OUTPUT DATA',//,T99,'REF.',T109,'REF.',//,T15,'V4',T23,
C * ,V5',T31,'TCJ PATM P5P DPVC PUVC TORQUE TRM',T90
C * ,PRESS. MOMENT FLOW RATE',//,T5,'PT',T15,'MV DEG.F.
C * IN.HG IN.HG IN.HG COUNTS DEG.F RATIO FT.LB
C * LB/M/SEC.,/)
C WRITE(6,103)
C 103 FORMAT(12,-----)
C READ INPUT DATA.
C 2 FORMAT(14) NRUNS
C DO 3 N=1,NRUNS
C READ(5,4) CLNC
C 4 FORMAT(5,3)
C 5 READ(5,5) (TCD(I),I=1,5)
C 5 FORMAT(5F7.1)
C WRITE HEADING FOR RUN.
C WRITE(6,6) CLNC
C 6 FORMAT(//,T40,'RUN',T61,'CLEARANCE = ',F5.3,/)
C DO 7 K=1,NPTS
C READ(5,2) NPTS
C READ(5,8) V4(K),V5(K),TCJ(K),PATM(K),P5P(K),DPVC(K),PUVC(K),TO(K),
C * TRM(K)
C 8 FORMAT(9F8.4)
C PROCESS DATA POINT.
C GHG=13.63905-1.363030E-3*TRM(K)
C CF1=7C.438824*GHG/13.54
C CALL TEMP (V4(K),V5(K),TCJ(K),T4,T5)
C CALL FLOW (DPVC(K),PUVC(K),PATM(K),GHG,T4,WVC)
C CALL PRESS(T5,PATM(K),P5P(K),GHG,CF1,WVC,PR2,PTO)
C CALL EDC (T5,PR2,GAM,EXP,CP,THETA)
C CALL TORQ (TCD,TQ(K),TNET)
C CALL REFER (PTO,GHG,GAM,THETA,INET,WVC,WVCR,TNETR)
C CALL INPUT DATA AND RESULTS FOR THE DATA POINT.
C WRITE(6,10) K,V4(K),V5(K),TCJ(K),PATM(K),P5P(K),DPVC(K),PUVC(K),TO(K),TO

```

```

*(K),TRM(K),PR2,INEIR,WVCR
10 FORMAT(2X,I4,4X,2F8.3,3F8.2,F9.3,F8.2,F7.0,F7.1,6X,F7.3,F8.2,F10.3
*)
7 CONTINUE
IF(N.EQ.NRUNS) GO TO 100
GO TO 3
100 WRITE(6,101)
101 FORMAT(1H1)
3 CONTINUE
RETURN
END

```

```

SUBROUTINE TEMP (V4,V5,ICJ,T4,T5)
V=V4
J=1
100 T=ICJ+0.144+35.77*V-0.4518*V**2
IF(T-100.1102,102,101)
101 T=ICJ+1.252+34.86*V-0.1855*V**2
102 T=T+459.69
103 IF(J-1) 103,103,104
J=2
T4=T
V=V5
GO TO 100
104 T5=T
RETURN
END

```

```

SUBROUTINE FLOW(DPVC, FUV, PATM, GHG, T4, WVC)
DVC=DPVC*GHG/13.54
PVC=(PUVC+PATM)*GHG/13.54
A=1.+1.85E-5*(T4-532.)
Z=1.9+2.4E-3*(T4-560.)
Y=1.-.351*DVC/PVC
WVC=2.2854*A*Y*SQR(T(PVC*DVC/T4))
X=WVC*.8131/Z
WVC=(1.+CC1275/X)*WVC
RETURN
END

```

```

SUBROUTINE PRESS (T5, PATM, P5P, GHG, CF1, WVC, PR2, PTC)
A=T5-459.69
CP=.23943+3.4E-6*A+2.E-8*A**2
PS5=(PATM+P5P)*GHG/13.54
TT=T5
RHO=PS5*CF1/(TT*53.3448)
VO=WVC/(RHO*3.14159*6.25/144.)
TO=T5-(VO**2)/(2.*32.174*778.16*CP)
DTT=TT-TO
TT=TO
IF(ABS(DTT)-.01)>101, 101, 100
PTO=PS5+RHO*(VO**2)/(2.*32.174*CF1)
PR2=PTO/(PATM*GHG/13.54)
RETURN
END

```

100

101


```

SUBROUTINE EDC (T5,PR2,GAM,EXP,CP,THETA)
A=T5-459.69
GA=1.4018-2.E-5*A
EX=(GA-1.)/GA
DT=T5*(1.-1./PR2**EX)
AA=T5-459.69-DT/2.
AAA=ABS(AA-A)
IF(AAA-1.) 107,107,106
105
106 A=AA
GO TO 105
107 GAM=GA
EXP=EX
CP= 23943+3.4E-6*AA+2.E-8*AA**2
IF(GAM*T5)2050,2050,2051
2050 WRITE(6,2052) K,GAM,T5
2052 FORMAT(/,6X,I4,2F8.3)
2051 CONTINUE
THETA=(GAM/1.4)*(T5/518.7)
RETURN
END

```

```

SUBROUTINE TORQ (TCD,TQ,TNET)
DIMENSION TCD(5)
BFM=0.0
DO 100 I=1,5
IF(TCD(I)-TQ) 100,100,101
CONTINUE
100 IF(I.LT.5) GO TO 102
T=100.*(I-2)+100.*((TQ-TCD(I-1))/(TCD(I)-TCD(I-1)))
GO TO 103
101
102 AI=100.*(I-1)
T=AI+100.*((TQ-TCD(I))/(TCD(I+1)-TCD(I)))
103 TNET=T+BFM
RETURN
END

```

```

SUBROUTINE REFER (PTO,GHG,GAM,THETA,TNET,WVC,WVCR,TNETR)
DEL=(PTO*(.4891585*GHG/13.54)}/14.7
X=(GAM+1.)/(2.*(GAM-1.))
EPS=(.810/GAM)*((GAM+1.)/2.)**X
WVCR=WVC*(SQRT(THETA))*EPS/DEL
TNETR=TNET*EPS/DEL
RETURN
END

```

PERFORMANCE EVALUATION OF ICP RADIAL TURBINE

TABLE C2

RESULTS OF ZERO-SPEED TESTS

| PT | INPUT DATA | | | | | | OUTPUT DATA | | | | | |
|-------------------|------------|----------|---------------|---------------|--------------|---------------|---------------|------------------|--------------|-----------------|-------------------------|------------------------------|
| | V4 MV | V5 MV | ICJ DEG.F. | PATM IN.HG | P5P IN.HG | DPVC IN.HG | PUVC IN.HG | TORQUE COUNTS | IRM DEG.F | PRESS. RATIO | REF. MOMENT FT.LB | REF. FLOW RATE LBM/SEC |
| CLEARANCE = 0.081 | | | | | | | | | | | | |
| RUN 1 | | | | | | | | | | | | |
| 1 | 1.640 | 1.355 | 32.00 | 30.07 | 2.90 | 2.066 | 4.93 | 125. | 87.8 | 1.100 | 3.72 | 0.757 |
| 2 | 1.640 | 1.400 | 32.00 | 30.07 | 5.87 | 3.926 | 9.75 | 249. | 87.9 | 1.201 | 6.79 | 1.004 |
| 3 | 1.635 | 1.400 | 32.00 | 30.07 | 8.76 | 5.452 | 14.20 | 367. | 87.5 | 1.300 | 9.18 | 1.142 |
| 4 | 1.635 | 1.395 | 32.00 | 30.07 | 11.70 | 6.891 | 18.54 | 488. | 87.5 | 1.400 | 11.20 | 1.209 |
| 5 | 1.620 | 1.380 | 32.00 | 30.07 | 14.64 | 8.184 | 22.83 | 605. | 87.1 | 1.500 | 13.15 | 1.259 |
| 6 | 1.620 | 1.375 | 32.00 | 30.07 | 17.56 | 9.364 | 26.94 | 718. | 87.1 | 1.599 | 14.73 | 1.358 |
| 7 | 1.620 | 1.375 | 32.00 | 30.07 | 20.51 | 10.502 | 31.00 | 829. | 87.0 | 1.699 | 16.07 | 1.397 |
| CLEARANCE = 0.061 | | | | | | | | | | | | |
| RUN 2 | | | | | | | | | | | | |
| 1 | 1.719 | 1.626 | 32.00 | 30.10 | 2.91 | 2.043 | 4.94 | 126. | 76.0 | 1.100 | 3.62 | 0.756 |
| 2 | 1.762 | 1.679 | 32.00 | 30.10 | 5.82 | 3.348 | 9.63 | 250. | 75.2 | 1.199 | 6.70 | 0.936 |
| 3 | 1.816 | 1.738 | 32.00 | 30.10 | 8.81 | 5.429 | 14.23 | 374. | 75.0 | 1.302 | 9.18 | 1.143 |
| 4 | 1.823 | 1.759 | 32.00 | 30.10 | 11.70 | 6.830 | 18.64 | 492. | 75.0 | 1.401 | 11.35 | 1.240 |
| 5 | 1.834 | 1.774 | 32.00 | 30.10 | 14.64 | 8.083 | 22.85 | 608. | 75.0 | 1.502 | 13.14 | 1.306 |
| 6 | 1.847 | 1.784 | 32.00 | 30.10 | 17.60 | 9.265 | 26.91 | 724. | 75.0 | 1.600 | 14.79 | 1.357 |
| 7 | 1.851 | 1.783 | 32.00 | 30.10 | 20.53 | 10.371 | 30.95 | 835. | 75.0 | 1.699 | 16.14 | 1.394 |
| CLEARANCE = 0.041 | | | | | | | | | | | | |
| RUN 3 | | | | | | | | | | | | |
| 1 | 1.984 | 1.885 | 32.00 | 30.02 | 2.90 | 2.076 | 5.00 | 127. | 73.6 | 1.100 | 3.69 | 0.763 |
| 2 | 2.000 | 1.910 | 32.00 | 30.02 | 5.81 | 3.873 | 9.69 | 247. | 73.5 | 1.200 | 6.68 | 1.003 |
| 3 | 2.026 | 1.970 | 32.00 | 30.02 | 8.73 | 5.410 | 14.14 | 369. | 73.0 | 1.300 | 9.20 | 1.143 |
| 4 | 2.064 | 1.987 | 32.00 | 30.02 | 11.67 | 6.809 | 18.50 | 487. | 74.0 | 1.400 | 11.37 | 1.240 |
| 5 | 2.076 | 2.010 | 32.00 | 30.02 | 14.61 | 8.031 | 22.79 | 602. | 73.8 | 1.500 | 13.12 | 1.305 |
| 6 | 2.076 | 2.013 | 32.00 | 30.02 | 17.52 | 9.237 | 26.82 | 718. | 73.5 | 1.599 | 14.77 | 1.357 |
| 7 | | | 32.00 | 30.02 | 20.47 | 10.032 | 30.84 | 827. | 73.5 | 1.699 | 16.09 | 1.376 |
| CLEARANCE = 0.024 | | | | | | | | | | | | |
| RUN 4 | | | | | | | | | | | | |
| 1 | 1.973 | 1.853 | 32.00 | 30.04 | 2.90 | 2.063 | 4.96 | 129. | 77.2 | 1.100 | 3.70 | 0.760 |
| 2 | 1.985 | 1.884 | 32.00 | 30.04 | 5.91 | 3.876 | 9.66 | 253. | 77.8 | 1.203 | 6.77 | 1.007 |
| 3 | 1.996 | 1.899 | 32.00 | 30.04 | 8.72 | 5.448 | 14.19 | 372. | 77.9 | 1.398 | 9.21 | 1.147 |
| 4 | 2.005 | 1.910 | 32.00 | 30.04 | 11.63 | 6.844 | 18.50 | 486. | 77.3 | 1.500 | 11.34 | 1.213 |
| 5 | 2.005 | 1.920 | 32.00 | 30.04 | 14.53 | 8.141 | 22.82 | 606. | 77.5 | 1.599 | 13.15 | 1.362 |
| 6 | 2.005 | 1.921 | 32.00 | 30.04 | 17.43 | 9.315 | 26.90 | 720. | 77.0 | 1.697 | 14.08 | 1.400 |
| 7 | | | 32.00 | 30.04 | 20.43 | 10.415 | 30.96 | 829. | 76.6 | 1.699 | 16.08 | 1.400 |
| CLEARANCE = 0.015 | | | | | | | | | | | | |
| RUN 5 | | | | | | | | | | | | |
| 1 | 2.005 | 1.879 | 32.00 | 30.21 | 2.92 | 2.110 | 5.00 | 127. | 72.0 | 1.100 | 3.75 | 0.766 |
| 2 | 2.013 | 1.923 | 32.00 | 30.21 | 5.84 | 3.916 | 9.75 | 251. | 72.5 | 1.200 | 6.90 | 1.005 |
| 3 | 2.010 | 1.931 | 32.00 | 30.21 | 8.70 | 5.458 | 14.26 | 371. | 72.5 | 1.300 | 9.19 | 1.143 |
| 4 | 2.005 | 1.932 | 32.00 | 30.21 | 11.63 | 6.863 | 18.63 | 492. | 72.5 | 1.500 | 11.41 | 1.210 |
| 5 | 1.975 | 1.908 | 32.00 | 30.21 | 14.57 | 8.148 | 22.95 | 607. | 72.2 | 1.601 | 13.48 | 1.359 |
| 6 | 1.953 | 1.889 | 32.00 | 30.21 | 17.48 | 9.344 | 27.06 | 727. | 72.0 | 1.699 | 14.85 | 1.395 |
| 7 | 1.944 | 1.885 | 32.00 | 30.21 | 20.61 | 10.419 | 31.09 | 836. | 72.0 | 1.699 | 16.13 | 1.395 |

INITIAL DISTRIBUTION LIST

| | No. Copies |
|---|------------|
| 1. Defense Documentation Center Cameron Station Alexandria, Virginia 22314 | 20 |
| 2. Library Naval Postgraduate School Monterey, California 93940 | 2 |
| 3. Commander, Naval Air Systems Command Navy Department Washington, D. C. 20360 | 1 |
| 4. Mr. I. Silver Propulsion Administrator (Code 330) Research and Technology Naval Air Systems Command Navy Department Washington, D. C. 20360 | 1 |
| 5. Dr. F. I. Tanczos Technical Director (Code 033) Research and Technology Naval Air Systems Command Navy Department Washington, D. C. 20360 | 1 |
| 6. Commander, Naval Ship Systems Command Navy Department Washington, D. C. 20360 | 1 |
| 7. Office of Naval Research (Power Branch) Attn: Mr. J. K. Patton, Jr. Navy Department Washington, D. C. 20360 | 1 |
| 8. Superintendent Naval Academy Annapolis, Maryland 21402 | 1 |
| 9. Chairman Department of Engineering Naval Academy Annapolis, Maryland 21402 | 1 |
| 10. Chairman, Department of Aeronautics Naval Postgraduate School Monterey, California 93940 | 2 |

| | No. Copies |
|--|------------|
| 11. Professor R. D. Zucker Department of Aeronautics Naval Postgraduate School Monterey, California 93940 | 3 |
| 12. Professor M. H. Vavra Department of Aeronautics Naval Postgraduate School Monterey, California 93940 | 2 |
| 13. LT David D. Williams, USN 1637 77th Avenue, N. E. Bellevue, Washington, 98004 | 3 |
| 14. Dr. Allen E. Fuhs Chief Scientist (Code APX) AeroPropulsion Laboratory (AFSC) Wright Patterson Air Force Base, Ohio 45433 | 1 |
| 15. Dr. D. M. Dix Chief Engineer Northern Research and Engineering Corp. 219 Vassar St., Cambridge, Mass. 02139 | 1 |

Unclassified

Security Classification

DOCUMENT CONTROL DATA - R & D

Security classification of title, body of abstract and indexing annotation must be entered when the overall report is classified

| | | | |
|--|--|---|-----------------------|
| 1 ORIGINATING ACTIVITY (Corporate author) Naval Postgraduate School Monterey, California 93940 | | 2a. REPORT SECURITY CLASSIFICATION Unclassified | |
| | | 2b. GROUP None | |
| 3 REPORT TITLE Determination of Performance Parameters of a Dual Discharge Radial Turbine | | | |
| 4 DESCRIPTIVE NOTES (Type of report and, inclusive dates) None | | | |
| 5 AUTHOR(S) (First name, middle initial, last name) David Daniel Williams | | | |
| 6 REPORT DATE December 1968 | | 7a. TOTAL NO. OF PAGES 158 | 7b. NO. OF REFS 12 |
| 8a. CONTRACT OR GRANT NO. b. PROJECT NO N/A c. d. | | 9a. ORIGINATOR'S REPORT NUMBER(S) N/A 9b. OTHER REPORT NO(S) (Any other numbers that may be assigned this report) | |
| 10 DISTRIBUTION STATEMENT Distribution of this document is unlimited. | | | |
| 11. SUPPLEMENTARY NOTES None | | 12 SPONSORING MILITARY ACTIVITY Naval Postgraduate School Monterey, California 93940 | |

13 ABSTRACT

This study was conducted to establish the performance parameters of a radial inflow, dual discharge turbine and to determine the effect of variations in axial clearance on these parameters. The representative stream surface is taken at the outer discharge radius instead of at a computed mass-average discharge radius, as was done previously. This technique results in considerably simplified computations and in better correlation of the rotor loss parameters.

Tests were conducted at axial clearances from 0.015 to 0.081 inches and at total-to-static pressure ratios from 1.2 to 1.7 for each clearance. The test installation is located at the Turbo-Propulsion Laboratory of the Naval Postgraduate School, Monterey, California.

14

KEY WORDS

LINK A

LINK B

LINK C

ROLE

WT

ROLE

WT

ROLE

WT

RADIAL TURBINE

AXIAL CLEARANCE

PERFORMANCE PARAMETERS

DUDLEY KNOX LIBRARY
NAVAL POSTGRADUATE SCHOOL
MONTEREY CA 93943-5101

DUDLEY KNOX LIBRARY



3 2768 00305694 6